Variable Penetration Rate Cone Testing for Liquefaction Evaluation of Sands with Fines

Christopher P. Krage[1] and Jason T. DeJong[2]

U.S. Geological Survey Final Technical Report

Award No: *G12AP20013*
Term: *Jan. 2012 - Dec. 2013*

Principal Investigator:

Professor Jason T. DeJong
Department of Civil and Environmental Engineering
2001 Ghausi Hall
One Shields Ave
Davis, CA 95616

May 2014

[1] Graduate Student, University of California, Davis, Department of Civil and Environmental Engineering, 2001 Ghausi Hall, 1 Shields Ave, Davis, CA 95616. Email: cpkrage@ucdavis.edu

[2] Professor, University of California, Davis, Department of Civil and Environmental Engineering, 2001 Ghausi Hall, 1 Shields Ave, Davis, CA 95616. Phone: 530-754-8995, Email: jdejong@ucdavis.edu

ABSTRACT

Widely used in-situ based relationships for liquefaction potential evaluation (e.g. SPT N_{160}, CPT q_{c1N}) have significant implications; small shifts in the liquefaction potential curve result in either significant human and infrastructure risk or excessive conservatism and fiscal waste. While most current discussions/debates focus on relationships for clean sand, the uncertainty (and associated risk) increases significantly when fines are present. Review of *CRR*-q_{c1N} curves for 15% and 35% fines content levels reveals that the curves proposed by researchers vary widely. These trends are driven by case history databases, with no rigorous, systematic, physical framework to explain the observed trends.

Recent research from laboratory studies and numerical models of cone penetration in sand with fines indicates the drained and undrained q_{c1N} measurements to vary for different levels of fines content and in-situ state. At the standard cone penetration rate of 2 cm/s drained conditions do not exist with increasing fines content; excess pore pressures are generated and partially drained conditions exist. The use of a *CRR*-$q_{c1N_drained}$ relationship may reduce uncertainty in cone measurements inherent in partially drained penetration and better account for the presence of fines in liquefaction evaluation. Variable penetration rate cone testing provides a framework to quantify the effects of partial drainage on cone tip and pore pressure measurements. Controlled penetration rates from 0.002-20 cm/s are used to establish drained conditions to compare with standard rate cone soundings.

This study investigated the effect of fines content and drainage behavior on cone measurements in natural, liquefiable soil deposits. Investigation of this behavior provided insight as to the effect of fines content on *CRR*-q_{c1N} correlations. This study is also used to provide an initial reassessment of clean sand corrections currently used in practice; improved understanding of the linkage between fines content and tip resistance may reduce the risk and uncertainty in estimating the liquefaction potential of sands with fines. The use of variable penetration rate cone testing is shown to be a valuable tool for understanding the extent of this linkage. Several factors are shown to play a significant role in field tests, including: fines content, drainage condition, geologic depositional process, spatial variability, initial state, liquefaction history, and ground water level.

TABLE OF CONTENTS

ABSTRACT II
LIST OF TABLES V
LIST OF FIGURES VI
INTRODUCTION 1
BACKGROUND 2
CPT Based Liquefaction Evaluation 2
Intermediate Soils 4
Factors Affecting Drainage Conditions During Cone Penetration 5
Normalized Parameters for Comparison of Variable Rate Measurements 7
Effects of Penetration Rate on Cone Measurements 8
Previous Studies Using Variable Penetration Rate Cone Tests 9
TEST METHODS 11
Variable Penetration Rate CPT 11
PPT Filter Saturation 11
Site Layout 12
Field Sampling and Laboratory Characterization 12
ANALYSIS METHODS 13
Depth Offsets and Corrections 13
State Correlations 13
Increment Analysis 14
Consolidation/Dissipation Behavior 14
Normalized Velocity 14
TEST SITES 16
Granite Construction 123 16
Lenordini 51 17
River Park 18
Kornbloom B 18
RESULTS 20
Detailed Results from Kornbloom Site 20
Observations of Data from All Site 22
DISCUSSION 24

Variable Penetration Rate Cone Testing for Improved Characterization of Intermediate Soils 24
Effect on Estimates of Engineering Parameters..... 24
Variable Penetration Rate Cone Testing for Improved Prediction of Liquefaction Potential in Sands with Fines 25
CONCLUSIONS 27
ACKNOWLEDGEMENTS..... 28
REFERENCES 29
APPENDIX A - GRANITE CONSTRUCTION SUPPLEMENTARY FIGURES 77
APPENDIX B - LENORDINI FARM SUPPLEMENTARY FIGURES..... 82
APPENDIX C - RIVER PARK SUPPLEMENTARY FIGURES 87
APPENDIX D - KORNBLOOM SUPPLEMENTARY FIGURES..... 93

LIST OF TABLES

Table 1 - Summary of historic liquefaction sites evaluated in this study 32
Table 2 - Summary of Kornbloom samples obtained in the vicinity of the test location 33
Table 3 - Summary of variable rates performed within subintervals selected at Kornbloom 34
Table 4 - Summary of variable rate intervals for selected subintervals for all sites 35
Table 5 - CPT correlations for estimation of engineering parameters 36

LIST OF FIGURES

Figure 1 - Proposed *CRR*-q_{c1N} relationships by various researchers. 37

Figure 2 - Summary of case histories included in the Boulanger and Idriss (2014) CPT liquefaction database. 38

Figure 3 - Δq_{c1N} correction from Boulanger and Idriss (2014). 39

Figure 4 – Normalized velocity effects on normalized excess pore pressure and normalized penetration resistance for contractive clays 40

Figure 5 - Atterberg limits chart, showing representative values for each soil that exhibited cohesive, cohesionless, or intermediate behavior. 41

Figure 6 - Correlation between fines content and soil behavior type, I_c. 42

Figure 7 - Field decision chart for a 15 cm^2 cone. 43

Figure 8 - The state parameter as described visually using critical state soil mechanics. 44

Figure 9 - Influence of penetrometer velocity on dissipation behavior in centrifuge mixtures. 45

Figure 10 - Dissipation curves of normalized excess pore pressure with time. 46

Figure 11 – Variable penetration rate cone penetration tests in 75% sand, 25% kaolin mixture centrifuge test. 47

Figure 12 - Normalized drainage characteristic curve for variable penetration rates in a range of geo-materials. 48

Figure 13 - Saturation chamber developed for this study to ensure proper cone filter saturation. 49

Figure 14 - Example test layout used at each test site 50

Figure 15 - Disturbed Cone Sampler. 51

Figure 16- Aerial Photograph of Granite Construction 123 52

Figure 17 - Aerial photography of the Lenordini site 53

Figure 18 - Sand boils present at River Park immediately following the 1979 Imperial Valley earthquake and a geologic cross section of soil deposits. 54

Figure 19 - Map of the Kornbloom study area 55

Figure 20 - Summary of variable penetration rate cone tests at Kornbloom. 56

Figure 21 - Grain size distributions for the 6 Kornbloom samples obtained for this study. 57

Figure 22 - Summary of samples obtained at the Kornbloom site 58

Figure 23 - Dissipation results for Kornbloom Unit B. 59

Figure 24 - Selected intervals for rate analysis within Kornbloom Unit B. 60

Figure 25 - Interval summary for Kornbloom depth range of 2.53 to 3.33 m. 61

Figure 26 - Q/Q_{ref} behavior and drained to undrained normalization for Kornbloom Unit B. 62

Figure 27 - Pore pressure behavior for Kornbloom Unit B. 63

Figure 28 - Q/Q_{ref} behavior and drained to undrained normalization for the selected subintervals for each site..... 64

Figure 29 - Pore pressure behavior for all sites..... 65

Figure 30 - $Q_{drained}/Q_{ref}$ shown versus percent difference between mean values of q_t for the selected subinterval for two different standard penetration rate soundings..... 66

Figure 31 - Summary of mean, standard deviation and coefficient of variation (COV) values for each sensor measurement (q_t, f_s, u_2) and state estimation versus normalized velocity for selected subintervals for each site..... 67

Figure 32 - Trends of $Q_{drained}/Q_{ref}$ and fines content versus depth and $Q_{drained}/Q_{ref}$ versus depth below the ground water table..... 68

Figure 33 - Trends of $Q_{drained}/Q_{ref}$ vs. fines content, I_c, and in-situ state. 69

Figure 34 - Trends of friction angle estimates for different normalized velocities 70

Figure 35 - Trends of relative density estimates for different normalized velocities. 71

Figure 36 - Trends in state parameter estimates using Robertson (2010)..... 72

Figure 37 - Location of sites in Boulanger and Idriss (2014) triggering relationship..... 73

Figure 38 - Comparison between drained and clean sand corrections for selected subintervals..... 74

Figure 39 - Difference between Boulanger and Idriss (2014) correction and the Δqc1N,drained..... 76

Figure 40 - Empirical Δqc1N correction proposed by Boulanger and Idriss (2014) 75

INTRODUCTION

Increase in routine use of the Cone Penetration Test (*CPT*) as an in-situ geotechnical tool resulted in the adoption of the *CPT* as standard of practice for geotechnical site investigation (Mayne 2007). The *CPT* is a powerful tool due to simultaneous measurements (q_c, f_s, u_2, V_s), increased sampling frequency, and low cost. Disadvantages to the *CPT* are highlighted by the lack of a physical soil sample and the necessity to use correlations to estimate engineering parameters. Recent practical advances and continuing research seek to minimize these limitations (e.g. cone sampler, correlations studies, numerical models) and increase the benefits of using the *CPT*. The *CPT* is most effective and reliable when used to develop site specific correlations by pairing several *CPT* soundings with adjacent soil borings, preferably with associated sampling and laboratory characterization and testing. Coupling in this manner utilizes many of the benefits of the *CPT* while minimizing its drawbacks and uncertainties.

The earliest methods to evaluate liquefaction potential use *SPT* based correlations to predict liquefaction potential (Kishada 1966, Seed et al. 1984, 1985). Recent research effort to establish *CPT* based correlations drives the work performed in this study (Boulanger and Idriss 2014, Moss et al. 2006, Youd et al. 2001). While current discussions and debates focus on triggering relationships for clean sand, the uncertainty and associated risk of predicting liquefaction potential increases significantly when fines are present. Curves proposed by researchers vary widely for cases with 15% and greater than 35% fines content levels (Figure 1; Stark and Olson 1995, Suzuki 1997, Robertson and Wride 1998, Boulanger and Idriss 2014). These trends are driven primarily by case history databases, but understanding and a physical framework to explain the observed trends needs further development.

A potential justification for these empirical observations is the presence of fines in sand creating partially drained conditions during cone penetration at the standard penetration rate (Jaeger 2012). Increased fines content acts to reduce permeability in sandy soils, enabling the potential for pore pressure generation and partially drained penetration. Slowing the cone penetration rate in a sand can enable direct measurement of drained cone tip resistance and can control the drainage conditions around an advancing cone.

This thesis will focus on evaluating the drainage conditions present around an advancing cone and how drained, undrained, or partially drained behavior affects tip resistance measurements in natural deposits of sands with fines; this work will highlight the influence of fines on drainage condition and its influence on liquefaction evaluation. The following sections discuss in detail the effect of fines content on cone tip resistance, intermediate soils, factors affecting drainage conditions during cone penetration, the effect of penetration rate on cone measurement, and previous studies of variable penetration rate cone testing. A field test program is then described where a variable penetration rate cone system was utilized to examine the influence of cone drainage conditions on the tip resistance at four documented liquefaction sites. All sites showed evidence of surficial liquefaction during past California earthquake events with fines contents in liquefiable layers greater than 15% and up to 92%. Measurements from field tests using variable penetration rate cone testing are then used to evaluate penetration rate effects and reexamine CPT liquefaction triggering trends.

BACKGROUND

CPT Based Liquefaction Evaluation

Liquefaction is the phenomenon where development of excess pore pressure induced from cyclic loading results in loss of soil strength and results in flow like failure (Idriss and Boulanger, 2008). Liquefaction failure often results in significant consequences as evident in recent earthquakes (e.g. 2011 Christchurch, 2010 Darfield, 1999 Kocaeli, 1995 Kobe, 1989 Loma Prieta).

The liquefaction potential of sandy soil deposits have historically been evaluated using in-situ tests. The earliest methods use *SPT* based correlations to predict liquefaction potential (Kishada 1966, Seed et al. 1984, 1985), while recent research effort has been made to establish *CPT* based correlations. These researchers use empirical case history observations to predict the liquefaction potential of a site using CPT measurements (e.g. Boulanger and Idriss 2014, Moss et al. 2006, Robertson and Wride 1998, Youd et al. 2001). Youd et al. (2001) highlighted several different methods used to evaluate liquefaction potential (including *SPT*, *CPT*, shear wave velocity (V_s), and Becker penetration test (*BPT*) for gravelly soils). All procedures identify potentially liquefiable sites by comparing site specific measurements to empirical observations of liquefied and non liquefied sites. *CPT* based procedures do this by evaluating normalized cone resistance (q_{c1N}) and level of earthquake shaking (CSR) against empirical *CRR*-q_{c1N} trends.

The trends used to identify potentially liquefiable sites are developed from observations of empirical case histories (liquefied and non-liquefied cases) and strong motion recordings (Figure 2). Empirically derived resistance ratios (*CRR*, black line in Figure 2) are used to determine the factor of safety against liquefaction failure using normalized tip resistance (q_{c1N} or corrected tip resistance q_{c1Ncs}, X-axis) and earthquake shaking (*CSR*, Y-axis) (Idriss and Boulanger 2008, Boulanger and Idriss 2014).

These in-situ based relationships used for liquefaction potential evaluation (e.g. *SPT* $(N_1)_{60}$, *CPT* q_{c1N}) have significant implications; small shifts in the liquefaction potential curve result in either significant human and infrastructure risk or excessive conservatism and fiscal waste. While current discussions/debates focus on relationships for clean sand, the uncertainty and associated risk increases significantly when fines are present. Review of *CRR*-q_{c1N} curves for 15% and 35% fines content levels (Figure 1) reveals that the curves proposed by researchers vary widely (Stark and Olson 1995, Suzuki 1997, Robertson and Wride 1998, Boulanger and Idriss 2014). For example, compare the suite of curves for sand with a fines content of about 35% (recognizing that the Robertson and Wride method uses soil behavior type I_c as a proxy for fines content where an I_c value of 2.59 is assumed to be comparable to a fines content of 35%) and notice that q_{c1N} can range from 10 to 17 for small values of CSR (CSR = 0.10) and from 24 to 106 for higher values of CSR (CSR=0.50).

Empirical observations show a dependence on fines content (cases with higher fines content are more resistant to liquefaction than clean sands at the same q_{c1N}). Because of this, cases with fines are corrected to a clean sand equivalent ($q_{c1N,cs}$) in order to assess liquefaction potential. Boulanger and Idriss (2014) suggest applying a correction term to (Δq_{c1N}) to account for the influence of fines on q_{c1N} relative to the baseline clean sand relationship (Figure 3).

Though empirical observations show a clear dependence on fines content and normalized tip resistance, further understanding of the governing mechanisms within a fundamental framework to appropriately explain these observations is lacking. Equations 1-5 present the Boulanger and Idriss (2014) approach for the empirical corrections:

$$q_{c1N} = C_N \frac{q_c}{P_a} \tag{1}$$

$$C_N = \left(\frac{P_a}{\sigma'_v}\right)^m \leq 1.7 \tag{2}$$

$$m = 1.338 - 0.249\left(q_{c1Ncs}\right)^{0.264} \tag{3}$$

$$q_{c1Ncs} = q_{c1N} + \Delta q_{c1N} \tag{4}$$

$$\Delta q_{c1N} = \left(11.9 + \frac{q_{c1N}}{14.6}\right)\exp\left(1.63 - \frac{9.7}{FC+2} - \left(\frac{15.7}{FC+2}\right)^2\right) \tag{5}$$

where q_c is the measured tip resistance (note that the correct cone tip resistance for unequal area effects, $q_t = q_c + u_2(1-\alpha)$ where α is the cone area ratio as per Lunne et al. (1997) should be used whenever possible), C_N is the overburden correction factor, P_a is atmospheric pressure (101.3 kPa), σ'_v is the vertical effective stress, q_{c1N} is the overburden corrected normalized tip resistance, and q_{c1Ncs} is the clean sand corrected normalized tip resistance. Note that Eq. 1 (and therefore 2, 3, 4, and 5) requires iteration to determine q_{c1N} and q_{c1Ncs}. Also note that the correction factor Δq_{c1N} requires both fines content (*FC*) and tip resistance (q_{c1N}) as inputs. This correction accounts for the varying liquefaction resistance in sands with fines and results in one unique *CRR*-q_{c1Ncs} trend. As an example, a site with *FC* of 85% and q_{c1N} of 29 can have a Δq_{c1N} of 61; a nearly 200% increase over the uncorrected tip resistance.

A potential justification for the varying liquefaction resistance in sands with fines is the presence of fines can create partially drained conditions during cone penetration at the standard penetration rate. Jaeger (2012) showed that *CPT* penetration at the standard rate of 2.0 +/- 0.5 cm/s (ASTM D5778) can lead to partially drained conditions and associated cone tip measurements with increasing fines content. Other numerical and experimental studies, such as those summarized in Figure 4 (consisting primarily of clays and silty clays) have shown that varying the penetration rate can control the drainage conditions around an advancing cone. If partial drainage in sands with fines does alter cone measurements, and the difference between partially drained and drained penetration is similar to Δq_{c1N} corrections, then drained tip resistances may be able to establish a unique location for *CRR*-q_{c1N} curves with fines content. Slowing the cone penetration rate in a sand with fines can enable direct measurement of drained cone tip resistance and can validate this potential physical explanation.

Intermediate Soils

Sands with high fines content and other intermediate soils, such as those discussed above and which occur naturally (e.g., sandy clays, silty clays, clayey silt, and silty sands) are frequently encountered on project sites worldwide and violate assumptions inherent in the geotechnical engineering profession's standard of practice for characterization of sands (e.g., drained response and use of effective stress parameters) and clays (e.g., undrained response and use of undrained shear strength). Behavior of intermediate soils (including sands with fines) can be transitional between sands and clays or can exhibit unique behavior that differs from both sands and clays. As a result a given intermediate soil may simultaneously exhibit properties like a sand, while other properties may be more similar to a clay; some properties are "sand-like" while others are "clay-like". Many researchers, including Idriss and Boulanger (2008) and Bray and Sancio (2006), have recognized the complicated nature of these materials, and therefore recommend laboratory testing to compliment in-situ testing in order to better understand soil behavior and cyclic strengths. Intermediate soils in the transitional zone between sands and clays have been highlighted by Idriss and Boulanger (2008) and typically have a plasticity index of 4 to 7 (Figure 5), though other studies show this range could be wider (e.g. Dahl 2011). For these soils, practitioners and researchers are faced with a dilemma when encountering intermediate soils on a project: should they be characterized as "sand-like" and therefore apply correction factors to obtain equivalent clean sand values (q_{c1Ncs})?

Though quantifying index properties from laboratory tests on samples best identifies most intermediate soils, correlations using in-situ test data can also be used. Researchers have proposed correlations based on trends observed using soil behavior charts, where the CPT measurements (q_c, friction ratio (R_f), and u_2) are used to provide an initial estimate of the most likely soil present based on cone penetration behavior. In the Q_t-F_r chart the series of contours that are used differentiate between soil types can be approximated using the I_c index (Been and Jefferies 1992, Robertson and Wride 1998). In general, $I_c < 2.05$ correspond to clean sand, $I_c > 2.95$ corresponds to clay and silty clay, with a gradual transition between the two occurring in between. For practical purposes Robertson and Wride (1998) suggest I_c values less than 2.6 to represent "sand-like" behavior and I_c values greater than 2.6 to represent "clay-like" behavior. Intermediate soils, including the sands with high fines content investigated herein, often have I_c values near this cutoff value (Ku et al., 2012), making it difficult to determine whether "sand-like" or "clay-like" behavior governs. In addition, Boulanger and Idriss (2014) recommend using I_c as a proxy for fines content when a paired CPT and boring data do not exist (based on the work by Suzuki et al. 1998). Though this relationship has significant scatter (Figure 6), the apparent fines content from an I_c correlation can be used to estimate FC for the Δq_{c1N} correction (Eq. 5) as previously discussed.

The transition between "sand-like" and "clay-like" behavior also encompass a transition in drainage from drained penetration to undrained penetration due to a change in the soil's permeability as the fines content increases. This is significant, since drainage conditions can influence the magnitude of measured tip resistance. In "sand-like" soils, drained conditions typically control, resulting in drained soil strength being mobilized and often used in design. In "clay-like" soils, undrained conditions control, resulting in the undrained strength being mobilized during cone penetration and being used in design of geosystems. Intermediate soils often have partially drained behavior between the two above cases, and therefore the engineer is

forced to make decisions regarding drainage conditions both in characterization of the material and in how the material will perform during geosystem loading.

Factors Affecting Drainage Conditions During Cone Penetration

Drainage conditions during cone penetration are dependent on the relative influence of pore pressure generation and dissipation, which occur simultaneously during penetration. Pore pressure generation is primarily dependent on the rate of cone penetration (v) while the rate of dissipation is dependent on the soil's permeability (k), horizontal consolidation coefficient (c_h), and rigidity (I_R) (Teh and Houlsby 1991). Standard rate cone penetration in clean sands occurs without generation of excess pore pressure while standard rate cone penetration in clays results in full development of excess pore pressure. When pore pressure generation conditions dominate (e.g. relatively low soil permeability at the standard cone penetration rate) the cone measures undrained soil response (e.g. clays) while a drained response is measured when pore pressure dissipation occurs rapidly (e.g. relatively high permeability in sands).

Excess pore pressure (Δu) generation and dissipation depends on soil type, stress history, penetration mechanism, and pore pressure sensor location (tip u_1, cone shoulder u_2, cone shaft u_3). Early theoretical solutions for cone dissipation behavior are based on monotonically decreasing Δu with time (e.g. Teh and Houlsby 1991). Observations of non-traditional pore pressure dissipation behavior (i.e. when Δu does not monotonically decrease with time) led to the development of theoretical models to explain the change in dissipation shape and can be explained through the work of Burns and Mayne (1998). They separated the components which contribute to the generation of excess pore pressure as follows:

$$u_2 = u_0 + \Delta u_{oct} + \Delta u_{shear} \tag{6}$$

where u_2 is the pressure measured at the cone shoulder, u_0 is the pressure due to hydrostatic conditions ($u_0 = \gamma_{water}$*depth), $\Delta u_{2,oct}$ is the octahedral mean stress, and $\Delta u_{2,shear}$ is the octahedral shear stress. It follows that excess pore pressure is due to a combination of mean and shear components:

$$\Delta u = (u_2 - u_0) = \Delta u_{oct} + \Delta u_{shear} \tag{7}$$

When mean stress dominates (as in highly contractive soils), excess pore pressure is expected to a large, positive quantity. When the mean stress is on the same order as the shear stress component, the influence of the shear component can result in negative Δu_2 values. This framework is useful to understand the influence of penetration mechanisms, soil type, and stress history on Δu_2 generation. The presence of negative Δu pressures does tend to occur in silty soil deposits and mine tailings, and can be better understood with the framework described by Eq. 7 (e.g. Finke et al., 2001). Though separation of components $\Delta u_{2,shear}$ and $\Delta u_{2,oct}$ is not practical for field dissipation tests it is a useful exercise for describing and creating a better understanding of the mechanisms behind Δu_2 generation.

Methods to estimate the horizontal consolidation coefficient using pore pressure dissipation tests are proposed in literature (e.g. Teh and Houlsby 1991, DeJong and Randolph

2012). The Teh and Houlsby method was developed for fully undrained dissipation tests in clays while DeJong and Randolph modified the solution to consider intermediate soils and effects of partial drainage during cone penetration. During cone dissipation tests the pore pressure dissipates primarily in the radial direction due to depositional layering and differences in horizontal and vertical soil fabric (Baligh and Levadoux 1986) suggesting that the consolidation coefficient determined from piezocone dissipation is more representative of the horizontal rather than vertical drainage conditions.

This drainage behavior can be characterized using pore pressure dissipation tests, extracting the time to 50% dissipation of Δu, t_{50}. Consolidation behavior can then be determined from dissipation tests using Teh and Houlsby's (1991) analytical solution for pore pressure dissipation:

$$c_h = \frac{a^2 T_{50} \sqrt{I_R}}{t_{50}} \tag{8}$$

where c_h is the horizontal consolidation coefficient, T_{50} is the analytical time factor for 50% dissipation (T_{50} = 0.247), a is the functional cone radius (4.37/2 for a 15 cm^2 cone), I_R is the soil rigidity, and t_{50} is the time for 50% dissipation of excess pore pressure from a dissipation test. Teh and Houlsby's solution is valid for undrained penetration. DeJong and Randolph (2012) modified Teh and Houlsby's solution to account for partially drained penetration (when t_{50} is between 10 and 50 s). This results in the following practical form to estimate t_{50} under partially drained conditions:

$$t_{50} = d^2 T_{50} (2^{1/b} - 1) \frac{V_{50}}{vd} \tag{9}$$

where d is the cone diameter, T_{50} is the analytical time factor (0.61), b is a fitting coefficient (Value), V_{50} is the normalized velocity corresponding to 50% dissipation of undrained excess pore pressure, and v is the penetration rate (20 mm/s). Radial consolidation can be practically estimated in partially drained conditions when using the following iterative practical form:

$$t_{50} = \frac{\sqrt{I_R}}{c_h} \left[78 + 0.25 c_h^{1.2} \right] \tag{10}$$

for V_{50} of 3, b of .75, d of 3.43 cm, and ν of 20 mm/s. Note that c_h obtained from this iteration must be multiplied by 1.5 for a 15 cm^2 cone (solution is for a 10 cm^2 cone).

Assigning a rigidity index (I_R) is difficult in silty soils since I_R is the ratio of tangent modulus (G) to undrained shear strength (s_u). While undrained strengths can be obtained in the field using fast penetration rates (V > 30), obtaining a laboratory s_u and N_{kt} factor ($N_{kt} = (q_t - \sigma'_{vo}) / s_u$) for site specific correlation requires undisturbed sampling and high quality lab testing. Estimation of consolidation behavior requires knowledge of I_R, since rigidity is shown to influence stress conditions around the advancing cone (Teh and Houlsby, 1991). Therefore when I_R cannot be determined using laboratory tests, it can be practically estimated for intermediate soils when considering soil properties and cone measurements (q_c, f_s, V_s, PI, OCR)

and using chart solutions (Keaveny 1985). This provides the best estimate of I_R possible given the available data.

The normalized velocity term (Finnie and Randolph 1994) can be used to capture the relative influence of the pore pressure generation and dissipation mechanisms:

$$V = \frac{vd}{c_h} \tag{11}$$

where v = penetration velocity (typically 2.0 cm/sec), d = cone diameter (3.43 cm or 4.37 cm), and c_h = horizontal consolidation coefficient. Randolph (2004) showed that drained conditions occur at normalized velocities less than about 0.1-0.3, while undrained conditions occur at values larger than 30-100. DeJong and Randolph (2012) suggest drained conditions occur for V < 0.3 and undrained conditions for V > 30. This framework can be practically incorporated into a field decision chart to quickly determine the drainage conditions at varying rates and soil drainage characteristics (Figure 7).

Normalized Parameters for Comparison of Variable Rate Measurements

Trends in normalized velocity can be captured using normalized parameters for comparison of variable penetration rate cone measurements. Observations in the database of variable penetration rate tests on clays and silty clays compiled by DeJong and Randolph (2012) compiled a database led to use of the following functional equations to capture penetration rate effects:

$$\frac{\Delta u_2}{\Delta u_{2,ref}} \approx 1 - \frac{1}{1 + (V / V_{50})^{c}} \tag{12}$$

$$\frac{Q}{Q_{ref}} \approx 1 + \left(\frac{Q_{drained} / Q_{ref} - 1}{1 + (V / V_{50})^{c}} \right) \tag{13}$$

where V is the normalized velocity, V_{50} is the normalized velocity corresponding to the penetration rate at which 50% dissipation of the excess pore pressure for undrained penetration occurs, and c is the maximum rate of change in $\Delta u_2/\Delta u_{2ref}$ and Q/Q_{ref} and controls how quickly excess pore pressure dissipates with penetration rate. $Q_{drained}/Q_{ref}$ is the normalized drained cone resistance where Q_{ref} is the normalized tip resistance for the undrained penetration case (V > 30). Note the normalized tip resistance is calculated as $Q = (q_t - \sigma_{vo}) / \sigma'_{vo}$.

The keys to this functional form are V_{50}, c, and $Q_{drained}/Q_{ref}$. DeJong and Randolph (2012) recommend using V_{50} and c values of 3 and 1 when site specific data is unavailable. Estimation of $Q_{drained}/Q_{ref}$ is more difficult and is difficult without site specific data.

Schneider et al. (2007) suggested evaluating drainage response to penetration rate by normalizing excess pore pressure by effective overburden stress and using the pore pressure parameter, B_q:

$$\frac{\Delta u_2}{\Delta u_{2,ref}} = \frac{u_2 - u_0}{u_{2,undrained} - u_0} \tag{14}$$

$$\frac{\Delta u_2}{\sigma'_{vo}} = \frac{u_2 - u_0}{\sigma'_{vo}} \tag{15}$$

$$B_q = \frac{u_2 - u_0}{q_t - \sigma_{vo}} \tag{16}$$

Schnaid et al. (2010) suggested that penetration rate effects can be normalized by the difference between drained and undrained tip resistance (whereas DeJong and Randolph (2012) suggested a ratio of drained to undrained tip resistance):

$$U = \frac{q_t - q_{t,undrained}}{q_{t,drained} - q_{t,undrained}} \tag{17}$$

where a U value of 1 signifies drained conditions and U of 0 signifies undrained conditions. This framework captures the transition between drained and undrained penetration but normalizes the effect of tip resistance. This framework is useful for comparing for soils that may exhibit penetration rate effects but have different values of $Q_{drained}/Q_{ref}$.

Effects of Penetration Rate on Cone Measurements

Prior to discussing specific trends, the effect of penetration rate on cone measurements can be conceptually understood using the state parameter. The state parameter is defined as the difference between the in situ void ratio, e_0, and the critical state void ratio, e_{cs}, at a specific (average or vertical) effective stress level (Figure 8, Jefferies and Been 2006, Jaeger 2012). This state parameter framework provides a useful context from which the volume change tendencies (dilative or contractive) of a given soil can be explored and explained. If the soil has a large positive state (state > 0.20; signifying very loose conditions) then the soil is expected to respond in a manner consistent with being highly contractive. In drained cone penetration, no excess pore pressure would develop, but the drained tip resistance would be relatively low since the soil is contractive. In undrained cone penetration large positive excess pore pressures would be generated, which reduces the effective stress in the soil, and hence reduces the cone tip resistance relative to the drained tip resistance. If the state is highly negative (state < -0.20; dense conditions) then the soil is expected to respond in a dilative manner. In drained cone penetration, this would again result in no development of excess pore pressures. However, the magnitude of the drained tip resistance would be much higher than for the loose (state > 0.20) condition. In undrained cone penetration negative excess pore pressures would develop, increasing the effective stress, and making the undrained tip resistance higher than the drained tip resistance. If the state is small (signifying a near critical state initial condition) then the soil is expected to be less sensitive to pore pressure generation and the difference in penetration resistance between drained and undrained conditions will be minimal.

Centrifuge studies show that varying the penetration rate (pore pressure generation) can have an effect on cone measurements (Figure 6, Chung et al. 2006, Kim et al. 2008, Oliveria et

al. 2010, Jaeger et al. 2010, DeJong et al. 2012). As expected, penetration rate reduction in soils with positive states generate less excess pore pressure, more consolidation around the cone, and larger cone tip resistances. In these soils the magnitude of penetration resistance is the smallest under fully undrained penetration and the largest under fully drained penetration.

The presence increasing fines content in a liquefiable layer would decrease the permeability of the soil layer, thereby affecting the drainage conditions (decreasing c_h) and increasing normalized velocity. This would result in the transition from fully drained to partially drained behavior (shift to the right in Figure 6). Large positive states (e.g. state > 0.20), which is typical for sand susceptible to liquefaction, then this transition from fully drained to partially drained would result in a smaller measured tip resistance. This effect is similar in consequence to fines content correction; drained resistance is larger than partially drained tip resistance in contractive soils and clean sand equivalent tip resistance ($q_{c1N\text{-}CS}$) is larger than uncorrected values (q_{c1N}) in sands with fines.

Recent research from laboratory studies and numerical models of cone penetration in sand with fines indicates the drained and undrained q_{c1N} measurement to vary for different levels of fines content and in-situ state (Jaeger 2012). Using a state based framework, Jaeger (2012) showed that trends of drained and undrained penetration in sands with fines matched well with empirical fines content observations. However, at the standard cone penetration rate of 2 cm/s drained conditions do not exist with increasing fines content; excess pore pressures are generated and partial drainage conditions exist. Use of a $CRR\text{-}q_{c1N_drained}$ relationship would reduce uncertainty in cone measurements inherent in partially drained penetration and better account for the presence of fines.

Previous Studies Using Variable Penetration Rate Cone Tests

Previous research shows that partial drainage is present in many intermediate soils and can significantly affect measured tip resistance (Schneider et al. 2007, Schnaid et al. 2010, Jaeger et al. 2010, Jaeger 2012, Wahl 2012, DeJong and Randolph 2012). Though many studies focus on laboratory, centrifuge, or numerical responses to drained, undrained and partially drained behavior, relatively few field trials exist (e.g. Schnaid et al. 2010, Wahl 2012).

Schneider et al. (2007) used centrifuge tests to show that varying penetration rate is sensitive to the soil type, mineralogy, and stress history. Variable penetration rate cone tests were performed in different mixtures of lightly and heavily over-consolidated kaolin (clay) and lightly and over-consolidated mixtures of 95% silica flour and 5% bentonite (silt). For the normally consolidated kaolin, the magnitude of Δu_2 generation decreases monotonically with decreasing penetration rate (Figure X). When normalizing by the $\Delta u_{2,initial}$, it appears that Δu_2 is dominated by $\Delta u_{2,oct}$ at the fast penetration rates and the effect of $\Delta u_{2,shear}$ becomes more pronounced decreasing penetration rate (Eq. 7; Figure 9).

They showed that for the silty, silica flour bentonite mixture, decreasing the penetration rate will also lead to less generation of Δu_2 (decrease in both $\Delta u_{2,shear}$ and $\Delta u_{2,oct}$; Figure 9). Both cases show the transition between undrained, partially drained, and fully drained penetration. Observations of the different mixtures indicate that silty soils can exhibit non-standard dissipation behavior ($\Delta u_2 < 0$) and have a significant $\Delta u_{2,shear}$ component while Δu_2 in clayey

soils tends to decrease monotonically. Silva et al. (2006) modeled penetration velocity in kaolin mixtures to show that pore pressure generation decreases with decreasing penetration velocity (Figure 10) agreeing well with the observations from Schneider et al. (2007).

Jaeger et al. (2010) examined the relationship between penetration velocity, tip resistance, and pore pressure for mixtures of 75% sand and 25% kaolin (Figure 11). He showed that decreasing penetration velocity leads to an increase in q_t and a correlated decrease in u_2. This effect was shown to occur in partially drained and fully drained conditions (V < .1), signifying undrained conditions for V > 20. The maximum ratio from drained to undrained cone tip resistance was about 17, which is substantially higher than was found in earlier studies. This has been attributed to the soil preparation method creating a meta-stable structure that produced a very low undrained penetration resistance (affecting the denominator in the ratio, Q_{ref}). Nonetheless, the results agree well with previous findings that indicate the drained resistance is higher than the undrained resistance for loose, contractive soils.

Schnaid et al. (2010) showed that the normalized velocity framework is applicable to a range of geomaterials from intermediate soils to mine tailings (Figure 12). Cone and field vane tests performed at variable rates in deposits of mine tailings in northern Brazil show undrained, partially drained and fully drained penetration using the functional form presented in Eq. 17. For all materials the measured drained penetration resistance at slower rates was larger than the undrained penetration resistance. Consistently, the excess pore pressure during undrained penetration was positive, indicating loose, contractive soils.

Variable penetration rate cone tests can be used to control the drainage conditions around an advancing cone (drained, partially drained, undrained). Previous studies have shown penetration rate influences Δu_2 generation in a variety of soil deposits and results in a difference in tip resistance. Furthermore, application of variable penetration rate cone tests in natural soil deposits is limited and needs further study.

TEST METHODS

The purpose of this study is to verify the hypothesis that the presence of fines in liquefiable soils can be accounted for by using a drained cone test (faster/slower) rather than the standard 2 cm/s rate. Use of variable penetration rate cone testing as discussed in DeJong et al. (2012) is an effective tool to study the effects of drainage conditions on cone measurements. Details of tests methods are discussed in detail in the following section.

Variable Penetration Rate CPT

This study builds on previous studies (Wahl 2012, Jaeger 2012, DeJong et al. 2012) by using a modified 12 ton Hogentogler rig (shared by NEES@UCLA). The rig was modified through the addition of a pair of computer controlled hydraulic servo-valves to accurately control penetration rate. Use of closed loop computer control allows for accurate control of penetration rate from 0.001 to 20 cm/s. Additionally, a small volume (0-3 lpm) and large volume (0-140 lpm) hydraulic servo valves are used in parallel to increase precision in control of penetration rate. Specific details of the rig modifications can be found in Wahl (2012).

An ELC15 CFP seismic cone from A.P. van den Berg was used for all studies herein. The tip load cell has a nominal range of 50 MPa, a maximum range of 100 MPa, and accuracy to 50 kPa. The sleeve friction load cell has a nominal range of 750 kPa, a maximum range of 1.5 MPa, and accuracy to 5 kPa. The pore pressure transducer has a nominal range of 1 MPa, a maximum range of 2 MPa, and accuracy to 5 kPa. Pore pressure was measured in the u_2 position (behind the shoulder of the cone tip). This results in a cone application class of Class 2 Type TE2 for soil type B (ISSMGE 1999).

Seismic tests were performed only on standard rate tests, typically during rod breaks (e.g. 1 m intervals) as per ASTM D5778. Dissipation tests were also performed during standard soundings at various depths following standard guidelines. Depth for dissipation tests were typically targeted using piezocone information from a prior cone sounding and information from historic CPT soundings.

PPT Filter Saturation

Adequate pore pressure transducer (PPT) saturation is essential for studying the drainage behavior around an advancing cone. A loss of, or decrease in, the cone's PPT saturation would result in erroneous u_2 measurements. This occurs through the collapse of air bubbles present if the saturation fluid and the PPT cavity is not carefully deaired, resulting in an underestimation of pressure. Adequate saturation of the filter element is necessary to combat this potential problem. Lunne et al. (1997) further discusses the effects of poor filter saturation and provides guidance on how to evaluate good PPT filter saturation.

Saturation must be conducted carefully in order to avoid introducing air into the cone's pore pressure element. The level of vacuum applied to de-air saturation fluid, the type of saturation fluid and the depth to groundwater are important to understand in order to ensure proper filter saturation. In this study 200 cSt. pure silicon oil is used for pore pressure saturation and a vacuum saturation chamber was specifically designed to provide adequate saturation of the

filter element (Figure 13). Vacuum (>29 in Hg) is applied to first de-air the saturation fluid and the PPT cavity. This is applied separately in the two chambers in Figure X. Once the saturation fluid and PPT cavity are properly de-aired (~1 hr for saturation and ~5 minutes for PPT chambers) valves are opened to allow the saturation fluid to fill the reservoir and saturate the cone (note that saturation fluid only needs to be deaired upon initial entry to the system). Once the filter element is submerged in the de-aired fluid, valves are closed and vacuum (>29 in Hg) is applied only to the saturation chamber until full saturation is attained (typically ~45 minutes). At this level of vacuum pressure, small air bubbles "boil" out of the fluid, thereby de-airing the fluid; the same was true of the PPT cavity. Vacuum is then released and the cone is covered with a prophylactic in order to maintain saturation during subsequent handling and preparation. If the ground water level is low enough (> 2m), then the hole is pre-pushed using an oversized conical probe and backfilled with water. This minimizes the amount of dry soil for the cone to penetrate through, thereby reducing the risk of filter de-saturation.

Site Layout

The test layout implemented at each site investigated consisted of six cone tests (Figure 14). Typically, three standard 2 cm/s cone profiles, performed in the far corners of the triangular arrangement, were used to match the site conditions with the historic borings and to evaluate horizontal and vertical spatial variability across the soil volume being investigated. Once the three standard tests were performed, three variable penetration rate soundings were performed within the triangle created by the first three soundings. Discrete disturbed samples were then retrieved from the center of the testing triangle for laboratory characterization and determination of fines content. On two occasions, the presence of spatial variability required that the test layout be altered to minimize variability between soundings.

Field Sampling and Laboratory Characterization

A conical disturbed sampler on loan from the USGS (Figure 15) was used to obtain small samples (approximate dimensions of 1” D x 8” long), adequate for general laboratory characterization. Samples were taken from a sampling location within the general test grid (Figure 14) at targeted depths (either corresponding critical layer or dissipation tests). Laboratory characterization tests were performed according to ASTM standards for Atterberg limits, sieve analysis, and hydrometer tests.

ANALYSIS METHODS

This section presents data processing methods, selection criteria for increment analysis, a methodology to compare between adjacent soundings, and a range of CPT-based correlations used. Sites were methodically processed according to Lunne et al. (1997) to include: pore pressure adjusted tip resistance (q_t), sleeve friction (f_s), friction ratio (R_f), pore pressure (u_2), SBT index (I_c), depth, and penetration rate. Estimates of overburden were derived from historic water contents for each site. The SBT index (I_c) was determined according to Robertson (2012).

Depth Offsets and Corrections

Lack of uniformity between closely spaced soundings sometimes required vertical offsets to align similar geologic units. Geologic deposition is rarely uniform in alluvial environments (i.e. meandering river depositional environment; Nichols 2009) and sometimes depth offsets between soundings are necessary to align specific geologic features (i.e. steep drop off in q_c) within an interval. This was to ensure comparisons made between soundings would be within the same geologic unit. Applied offsets are listed for each interval summary; note that offsets are applied uniquely to each layer due to the variability of the depositional process. Offsets never exceeded 28 cm (~11 in), and were typically less than 10 cm.

Field measurements in this study were performed at a sampling frequency of 10 Hz (or 1 data point every 2 mm for standard rate) and was adjusted based on the penetration velocity to acquire data points every 2 mm. Note that most of the historic CPT soundings supplied CPT data every 5 cm. The cone data acquired from field tests was processed and interpolated to allow for comparison at similar depths using linear interpolation between adjacent sample points.

The measurement of tip resistance, sleeve friction, and pore pressure is ascribed to the depth of the cone tip since the cone measurements should be representative of the soil at that reported depth. This requires the application of an offset for the geometric differences between the q_c, f_s, and u_2 sensor locations. Centroid corrected depths based on cone geometry are used to shift pore pressure and sleeve friction measurements to the centroid of tip resistance (located 2/3^{rds} between the cone tip and shoulder). This correction is important for comparing thin soil layers and/or measurements between small depth increments.

State Correlations

The significance of penetration rate effects depends on the variation between cone measurements from partially drained penetration and those obtained during drained or undrained penetration. As discussed above, strongly contractive (ξ>0) or strongly dilative (ξ<0) soils are expected to show significant effects while soils that are closer to critical state (ξ=0) are expected to show smaller effects (Jaeger 2012). The potential change in cone measurements due to changes in penetration rate (e.g. from drained to undrained penetration) for a given soil could be estimated if the state can be estimated or is known. Accurately determining a soil's state requires extensive laboratory tests, though empirical methods to estimate state exist (Schnaid and Yu 2007, Robertson 2010). The Robertson (2010) state estimation method, where Robertson instead uses ψ to represent the state parameter, is shown below and used in this study:

$$\xi = 0.56 - 0.33\log(Q_{tn,cs}) \quad (18)$$

where $Q_{tn,cs}$ is the equivalent clean sand normalized cone resistance. $Q_{tn,cs}$ is derived from a K_c correction factor based on fines content, mineralogy, and plasticity and from soil behavior type I_c correlations.

Increment Analysis

Depth increments were carefully selected to compare between different penetration rates. These increments must meet the following criteria:

- Soundings must avoid rod breaks
- Soundings match characteristic behavior of historic sounding
- Be contained within the identified liquefiable layer

Small depth increments were chosen for comparison since aligning depth increments from multiple tests can be problematic due to the presence of lateral variability and pauses in penetration (i.e. rod breaks and dissipation tests). These increments were targeted based on critical layers from liquefaction triggering databases (Boulanger and Idriss, 2014).

Comparison between all adjacent soundings from each site was performed through use of a Mathcad™ routine. Soundings were binned by depth range and individual offsets were applied if necessary (described above). Bins by depth range were determined to avoid rod breaks within similar geologic units.

Consolidation/Dissipation Behavior

Drainage behavior is characterized using pore pressure dissipation tests as described in the preceding section. The time to 50% dissipation of excess pore pressure (Δu), t_{50} is then extracted from dissipation tests with known hydrostatic (u_0) conditions to determine consolidation behavior using the Teh and Houlsby's (1991) analytical solution for pore pressure dissipation (Eq. 8). Teh and Houlsby's solution is only valid for undrained penetration therefore DeJong and Randolph (2012) modified their solution to account for partially drained penetration (when t_{50} is between 10 and 50 s). The resulted in the practical forms (Eqs. 9 and 10) which can then be used to estimate t_{50} under partially drained conditions.

Estimation of consolidation behavior requires knowledge of I_R, since rigidity is shown to influence stress conditions around the advancing cone (Teh and Houlsby, 1991). Therefore when I_R cannot be determined using laboratory tests (as in this study), it can be practically estimated for intermediate soils when considering soil properties and cone measurements (q_c, f_s, V_s, PI, OCR) and using chart solutions (Keaveny 1985). This provides the best estimate of I_R possible given the available data.

Normalized Velocity

Normalized velocity is computed using the functional form developed by Finnie and Randolph (1994) shown in Eq. 11. Normalized velocity trends are compared using normalized

tip resistance ratio (Eq. 13). When undrained penetration rates are unavailable, an alternate condition for Q_{ref} must be defined if appropriate. If another reference condition cannot be established, then the normalized tip resistance ratio (Eq. 13) is not useful. Therefore selected intervals for comparison of penetration rate effects must have accurate undrained penetration tests to use the DeJong and Randolph (2012) framework (Eq. 13). Other normalizations schemes for tip resistance and pore pressure are used as described in the background section on normalized parameters (Eqs. 12, 13, 14, 15, 16, and 17).

Summary of Analysis Methodology

The analysis methodology used in this study is listed below in sequential order to provide transparency and clarity. All steps have been described above and are applied to each individual test site.

Processing Steps:

1. Select Site
    a. Compile all available in-situ data (*CPT*, *SPT*, interpreted stratigraphy, V_s, dissipation tests)
    b. Compile all dissipation tests
    c. Determine t_{50} for each test
    d. Determine average response for layer of interest (a representative t_{50})
    e. Using all available information (q_c, f_s, V_s, *PI*, *OCR*), make an estimate for I_R
    f. Combine steps *d* and *e* to determine average c_h for layer of interest (using DeJong and Randolph, 2012)
2. Lab tests
    a. Compile all available historic and current lab test data (γ, ω_c, *LL*, *PL*, *PI*, *FC*, C_u, C_c, D_{10}, etc)
    b. Distinguish between historic and study tests
3. Interval selection
    a. Look for uniform layers with consistent behavior
    b. Similarities in q_t profiles
    c. Similar thicknesses
    d. Any depth offsets if necessary
    e. Assign t_{50}, I_R, c_h to each interval
    f. Determine Q/Q_{ref}, $\Delta u_2/\Delta u_{2ref}$, $\Delta u/\sigma'_{vo}$, and V
    g. Combine for average response of layer of interest
    h. Show the individual response for each interval within layer of interest
4. Compile and summarize
5. Repeat all steps for other sites

TEST SITES

Field implementation of variable penetration rate cone testing was used to evaluate the effects of partial drainage in sands with fines. Potential sites were identified in this study using information from the original site investigations provided by post earthquake reconnaissance teams. Following preliminary identification, sites were selected for implementation of variable penetration rate cone testing after considering the following criteria:

- Site is located in or near California
- Site contains a layer of loose liquefiable material known to have liquefied during a previous earthquake event
- Loose material has a fines content from 5 to 50%
- Loose material is anticipated to be relatively uniform
- Critical layer is present in liquefaction triggering database
- Site access
- Ability to test within 5' of original boring
- Presence of both CPT and SPT borings during earthquake reconnaissance

Four tests sites were identified from sites present in present in the CPT liquefaction databases (Boulanger and Idriss 2014) using the above criteria. These sites are summarized in Table 1, which includes the earthquake event(s), magnitude, presence of liquefaction, identified depth and thickness of critical layer (Factor of Safety against liquefaction < 1), groundwater estimation, soil type, and fines content. Of the sites chosen in this study, two are located in the Santa Cruz/Monterey region and two are located within the Imperial Valley region of California. The four sites were tested during two separate field campaigns. Variable penetration rate cone tests were performed at Granite Construction 123 and Lenordini 51 in August 2012. Studies at River Park A and Kornbloom B were completed March/April 2013.

An in-depth description of each site, including historic information and site geology/stratigraphy is presented below. Soil characterization from disturbed samples obtained at each site is included and used to compare with the adjacent, historic SPT borings.

Granite Construction 123

Granite Construction 123 (referred to as Granite or GRN herein) is a historic liquefaction site located near Watsonville, CA, just south of the Pajaro River. The site experienced ground shaking and earthquake induced liquefaction during the 1989 Loma Prieta Earthquake, with $CSR_{M=7.5,\sigma=1}$ estimate of 0.238 according to Boulanger and Idriss (2014). Site liquefaction is evident by the presence of sand boils across the site. The site was used as a storage yard for the Granite Construction company and bordered the Pajaro River to the north. Post earthquake reconnaissance teams from the USGS performed several CPTs and SPTs in the Watsonville/Pajaro region, including 4 CPT and 2 SPTs within the Granite site (Bennett and Tinsley 1995). Only one of these CPTs (Granite 123) has a corresponding SPT boring and was therefore selected for this study. Groundwater elevation during this study is around 6 m depth and is controlled by the nearby Pajaro River. Figure 16 shows an aerial photograph of the site just 3 days after the main event.

Holzer et al. (1994) reported on the geologic depositional processes for the nearby Miller farm site (1 km upstream of Granite 123, similar perpendicular distance from the existing river). Two units of Holocene flood-plain deposits are described: an older, silty clay unit and a younger, predominately sand unit consisting of heterogeneous channel and point bar deposits. Lateral spreading in the case of nearby sites (Miller and Farris Farms) is constrained to the younger flood-plain deposits (Holzer et al. 1994). The significant heterogeneity of young flood-plain depositional processes is consistent with the limited and spread out observations of sand boils at the Granite site.

Initial reconnaissance reports describe a 1 m thick liquefiable layer at a depth of 7-8 meters. The average cone tip resistance (q_{cN}) for this layer is 44 (4.4 MPa) (Boulanger and Idriss, 2014). The original fines content is listed as 18%, resulting in a Δq_{c1N} adjustment of 25.

Variable penetration rate cone testing began on 8/22/12 and finished on 8/24/12. 9 cone tests were performed at the site and one series of disturbed samples were obtained in the three day period. Multiple tests were necessary for this site due to the encountered spatial variability within the critical layer. The results from standard CPTs showed substantially different cone profile signatures for soundings 2, 4, and 5 when compared with 1, 3, and 6. Further analysis of the profile shows that soundings 1, 3, and 6 best agree with the historic profile, therefore the variable penetration rate sequence was performed within the triangular grid bounded by 1, 3 and 6.

Lenordini 51

Lenordini 51 (referred to as Lenordini or LEN herein) is a historic liquefaction site located near Salinas, CA, just north of the Salinas River. The site experienced significant ground shaking and earthquake induced liquefaction during the 1989 Loma Prieta Earthquake with $CSR_{M=7.5,\sigma=1}$ estimate of 0.187 according to Boulanger and Idriss (2014). Site liquefaction is evident by the widespread presence of sand boils across the site (as evident in aerial photographs in Figure 17). The site is an active artichoke and strawberry farm with Highway 101 to the east. Post earthquake reconnaissance teams from the USGS performed several CPTs and SPTs within the Lenordini Family Farm, including 4 CPT and 2 SPTs (Bennett and Tinsley 1995). Groundwater elevation during this study is around 1.4 m depth and is controlled by the nearby Salinas River and farming irrigation.

Sand boils at the Lenordini Farm were concentrated near an abandoned meandering river channel (Figure 15, Tinsley, personal communication 2012). The silty sand and sandy silt units comprising the upper 7 m (including the historic liquefied interval) at Lenordini 51 are likely due to similar heterogeneous channel and point bar deposits as observed at the Granite, Miller and Farris sites.

Initial reconnaissance reports describe a 2 m thick liquefiable layer at a depth of 3.7-5.7 meters. The average cone tip resistance (q_{cN}) for this layer is 45 (4.5 MPa) (Boulanger and Idriss, 2014). The original fines content is listed as 10%, resulting in a Δq_{c1N} adjustment of 6.6.

Variable penetration rate cone testing began on 8/28/12 and finished on 8/29/12. 6 cone tests were performed at the site and one series of disturbed samples were obtained in a two day period.

River Park

River Park (referred to as River Park or RVP herein) is a historic liquefaction site located in Brawley, CA. The site experienced significant ground shaking and earthquake induced liquefaction during the 1979 Imperial Valley earthquake with a CSR estimate of 0.17 according to Moss et al. (2004) (note that this site was not included in the Boulanger and Idriss 2014 database). The site experienced significant shaking during 2 additional events. Site liquefaction is evident by the widespread presence of sand boils across the site (Figure 18a). The site is located within the pasture grounds/parking lot of the Brawley Rodeo grounds. Post earthquake reconnaissance teams from the USGS performed several CPTs and SPTs within the pasture region (Youd and Bennett 1983). Additionally, the site was selected for reevaluation using a piezocone probe (Moss et al. 2004). Groundwater elevation at the site is around 1.5 m depth and controlled by the nearby New River. The site consists of 2-3m of surficial silt, overlying approximately 1 m of clay, beneath which is a thick sand layer which densifies with depth (Figure 18b). Unit A (brown silt) and the upper part of Unit C (gray sand) are believed to have liquefied during the event (Youd and Bennett 1983).

The geologic setting at River park consists of 3 distinct units with a variety of depositional processes (Bennett et al. 1981). The surficial silt layer (Unit A) is a result of higher energy flood-plain processes, the middle clay layer (Unit B) is a result of lower energy, higher flood level environments, and the lower sand layer (Unit C) is a massive point bar deposit (Bennett et al. 1981, Youd and Bennett 1983). The spatial uniformity of these units suggest very distinct depositional periods.

Initial reconnaissance reports describe a 1.5 m thick liquefiable layer at a depth of 0.5-2 meters. The cone tip resistance (q_{cN}) for this layer is 39.9 (3.99 MPa) as shown in Moss et al. (2004). The original fines content is listed as 80%, resulting in a Δq_{c1N} adjustment of 64.

Variable penetration rate cone testing began on 3/23/13 and finished on 4/21/13. A total of 10 cone tests were performed at the site and one series of disturbed samples were obtained within one two day (3/23-24) and one single day (4/21) period. The testing hiatus was due to equipment failure of the CPT truck hydraulic drive. Additionally, this site was selected for further study of sample disturbance in shallow, low plasticity silty and clayey soils (to be addressed in a separate publication).

Kornbloom B

Kornbloom B (referred to as Kornbloom or KRN herein) is a historic liquefaction site located near Calipatria, CA. The site experienced significant ground shaking and earthquake induced liquefaction during the 1981 Westmoreland Earthquake with $CSR_{M=7.5,\sigma=1}$ estimate of 0.195 according to Boulanger and Idriss (2014). Additionally, the site experienced significant shaking during the 1979 Imperial Valley and 1987 Superstition Hills earthquake, but did not liquefy during these events. Site liquefaction during the 1981 event is evident by the widespread presence of sand boils across the site (Figure 19a, Bennett et al. 1984). The site is agricultural farmland near the south east edge of the Salton Sea. Post earthquake reconnaissance teams from the USGS (and Purdue University, Stanford University, and University of Texas) performed several CPTs and SPTs adjacent to the canal, including 6 CPT and 3 SPTs (Bennett et al. 1984). Groundwater elevation at the site during this study is around 0.4 m depth and is controlled by

agricultural irrigation. The site consists of 1.5 m of silty clay (Unit A) overlying 4 m of silt and sandy silt (Unit B) overlying more silty clay and sandy silt deposits (Units C-F) (Figure 19b). The sandy silt that comprises Unit B is known to have liquefied during the event by matching sand boil ejecta with samples obtained from this unit (Bennett et al. 1984).

The geology at Kornbloom consists of alternating sequences of low and medium energy flood-plain, deltaic, and lacustrine deposition. The spatial uniformity and low penetration resistance of Unit B suggests a low energy fluvial deposition (Bennett et al. 1984). The Kornbloom study site currently located less than 2 km from the southeast portion of the Salton Sea and approximately 1 km away from an existing river channel.

Initial reconnaissance reports describe a 2.6 m thick liquefiable layer at a depth of 2.7-5.3 meters. The average cone tip resistance (q_{cN}) for this layer is 21.4 (2.14 MPa) (Boulanger and Idriss, 2014). The original fines content is listed as 92%, resulting in a Δq_{c1N} adjustment of 61.3.

Variable penetration rate cone testing began on 4/22/13 and finished on 4/23/13. A total of 7 cone tests were performed at the site and one series of disturbed samples were obtained within a two day period.

RESULTS

A series of cone tests were performed at each test site. The results will be discussed for the Kornbloom site as described in the analysis methods section. First, the Kornbloom site will be presented in detail, then final results from each site will be summarized, and finally site specific and general observations will be made. All the figures described in the detailed description for the Kornbloom site are included in Appendices A-D for each test site.

Detailed Results from Kornbloom Site

The layer of interest (Unit B) at Kornbloom is a thick silt layer (1.5-6 m). The loose, liquefiable layer is identified from previous studies. All available information for each site is compiled to evaluate site stratigraphy (Figure 20). This includes *CPT* and V_s measurements from this study and historic *SPT* and stratigraphic interpretation. The primary depth interval of interest, between 2.7 and 5.3 m, contains an average q_c value of 2.1 MPa and SPT N values of 8. Soil samples obtained using the disturbed sampler shows grain size distributions for the 6 samples obtained in this study from Kornbloom (Figure 21). All samples across the Kornbloom site are shown in Figure 22, revealing that the layer of interest is primarily composed of silt. Table 2 summarizes the information obtained from Kornbloom soil samples. As evident, the fines content ranged from 62 to 95%, the PI from 0 to 2, with USCS soil classification of ML for Unit B.

The range of penetration rates required in order to obtain drained cone measurements were determined based on the soil's c_h. Consolidation characteristics for the silt layer based on 4 dissipation tests (Figure 23) indicated a c_h value in the rage of 5.0 cm^2/s. This value is consistent with typical properties for silty soils. As evident in the dissipation plots in Figure 23, the excess pore pressures were initially negative, and dissipation to hydrostatic conditions required less than 2 minutes, indicating partial drainage with t_{50} values ranging between 15 and 20 seconds (mean value of 16 seconds).

Interpretation using the DeJong and Randolph (2012) modified Teh and Houlsby (1991) framework and assuming a representative I_R value of 240, resulted in a c_h range from 1.8 to 5.5 cm^2/s. As mentioned above, determination of the I_R value in sandy/silty materials is complicated, and therefore a representative 'typical' value was used. I_R can be estimated using correlations from soil index properties (e.g. Keaveny 1985) which are based on 8 tests on clay, mostly with OCR < 1.3 and PI > 30. Estimating I_R for Kornbloom requires extrapolation beyond the limits of this database. Unit B has a representative q_c of 2 MPa, f_s of 10 kPa, V_s of 118 m/s, *PI* of 0-5, and an *OCR* estimate of 10-15. Therefore a value of 250 is a reasonable approximation for I_R. Practically the I_R value could range from 100 to 500, which would result in a shift of c_h from about 1.2 to 7.0 cm^2/s; this variation is relatively insignificant and less than one order of magnitude. The median c_h value of 5.0 cm^2/s was used for calculations of normalized velocity using Eq. 7, recognizing that a shift in c_h did not change the observed trends, since c_h was unique for Unit B.

Based on the estimated c_h value, drained cone penetration is expected to occur at a rate of about 0.034 cm/s or slower, with faster rates creating partially drained conditions. This is evident in Figure 20, where trends for rates of 0.02 cm/s follow the hydrostatic line. Drained,

undrained, and partially drained penetration velocities can be easily determined from Figure 7 with a known c_h.

Two intervals were selected within Unit B to quantify rate effects (Figure 24). These intervals were chosen to avoid the effects of rod breaks and to compare penetration rate effects on cone measurements. The depth interval from 2.53 to 3.33 m is further summarized in Figure 25 as an interval summary sheet (additional Kornbloom intervals are summarized in Appendix A). The interval summary sheet shows the trends of velocity, q_c, f_s, and u_2 measurements versus depth, the cumulative distributions for q_c, f_s, and u_2 for the selected depth bin, and the average value of q_c, f_s, and u_2 for the selected depth bin plotted versus penetration velocity. Finally, average excess pore pressure and state are shown vs. velocity. The selection of the depth interval and calculations are performed according to the methods described in the analysis methods section.

Average and cumulative q_t, f_s, and u_2 measurements are compared for four different penetration rates (0.02, 0.2, 2.0, and 20 cm/s). Cumulative frequency plots summarize the range of values within a given interval (Figure 25). Narrow curves reflect uniformity in measurements while wide curves reflect a larger standard deviation in the measurement. This effect is most evident for the u_2 measurement, comparing drained penetration (0.02 cm/s, brown) to undrained penetration (20 cm/s, red). The narrow band of u_2 values for the drained penetration rate is similar to the 4 kPa increase in hydrostatic pressure (u_0) while the u_2 measurements for undrained penetration vary widely for the depth interval. Similar results are observed in q_t cumulative frequency plots where similar, but offset shapes are observed. The lowest q_t observed for this interval at different penetration rates (i.e. cumulative frequency of 0) ranges from 0.45 to 1.45 MPa while the largest q_t observed ranges from 1 to 2.45 MPa (cumulative frequency of 1). The average q_t values for different penetration rates within this interval range from 0.7 to 1.7 MPa. This shows that use of only average values to quantify penetration rate effect may detract from variability in sensor measurements and soil conditions. The clearest indication of the presence of a penetration rate effect is similarly shaped, but offset, cumulative frequency distributions. This indicates similar variability for measurements at each penetration rate, but the offset shows the influence of penetration rate on cone measurements. Nonetheless, average values for depth intervals can be used as long as variability in the measurements are understood.

A clear dependence on penetration rate is shown for Unit B where $Q_{drained}/Q_{ref}$ is 2.38 (Figure 26) with dashed lines representing the fits from Eq. 13 and 17. This agrees well with experimental results from previous studies, indicating drained to undrained ratios of 1.3-15 for contractive, normally consolidated clays. Additionally, this reflects a 1.4-1.5x increase of drained penetration vs. partially drained penetration at the standard penetration rate (v=2 cm/s, V= 1.8). The effect is less agreeable for excess pore pressure conditions, though the 20 cm/s sounding offsets the trend significantly. Significant scatter exists in the $\Delta u_2/\Delta u_{2ref}$ normalization (Eq. 14; Figure 27a), due in part to the dilative behavior observed at the site ($\Delta u < 0$). Drainage response is shown more clearly using B_q and $\Delta u_2/\sigma'_{vo}$ (Eqs. 15 and 16; Figure 27c and 27d) as recommended by Schneider et al. (2007). Though excess pore pressures are negative, the range of B_q and $\Delta u_2/\sigma'_{vo}$ tends to converge with decreasing penetration rate. Results from the Kornbloom intervals are summarized in Table 3.

Kornbloom's state parameter value is close to or equal to zero, providing some explanation for observed magnitude of the penetration resistance and scatter in pore pressure trends with normalized velocity. An average state of 0.005 is estimated for Kornbloom using Eq. 18 and standard 2 cm/s penetration tests results. It is expected that soils with relatively large absolute values of state (either highly contractive or dilative) would show significant penetration rate effects and volume change tendencies. The small state present at Kornbloom suggests soil conditions that are close to critical (and therefore stress is less influenced by changes in strain).

Overall the observations and trends within the Kornbloom variable penetration rate cone data are consistent with those observed by other researchers. The q_t value measured at the slower penetration velocity (0.02 cm/s) is 1.37 times larger than the q_t value measured at conventional rate of 2 cm/s. The relative uniformity in geologic features between soundings due to the low energy fluvial depositional processes provide clarity in the observed trends.

Observations of Data from All Site

Combination and integration of data from all sites, following the detailed analysis procedures as detailed above for Kornbloom, reveal similar trends but with increased scatter due to higher spatial variability (Figure 28 and 29, Table 4). This is evident in the variation between the three standard rate cone penetration soundings performed at each location, and most clearly presented in the depth interval summaries in Figure 25 (Appendix A-D for all sites). The increased variations at sites Granite and Lenordini are attributable to the geologic depositional process, which consisted of higher energy, alluvial processes than the deposits present at Kornbloom and River Park (Youd and Bennett 1981, Bennett et al. 1984). Thick, low energy flood-plain, deltaic, and lacustrine deposits present at Kornbloom Unit B resulted in a uniformly distributed silt unit (Bennett et al. 1984). Additionally, the proximity of Kornbloom to the Salton Sea is unique, while the other 3 sites were predominately fluvial deposits. The flood-plain deposits observed at River Park (Unit A and C) are likely sourced from higher energy than the depositional processes at Kornbloom Unit B (Bennett et al. 1981). River Park Unit A is a higher energy flood plain deposit while Unit C is a massive point bar deposit.

Normalization of penetration rate effects using $Q_{drained}/Q_{ref}$ (Eq. 13) and U (Eq. 17) (Figure 28) show that the magnitude of the penetration rate effect varies for each site but follows the trends observed by previous researchers. Higher q_t values at Granite and Lenordini are attributed to differences in geologic deposition compared to Kornbloom and River Park.

Measureable penetration rate effects are expected when the percent difference between standard rate soundings is less than 20% (Figure 30). Attempts to resolve spatial variability using absolute difference, percent difference and coefficient of variation between standard 2 cm/s soundings are made. Kornbloom has an absolute difference of 132 kPa, percent difference of 8.7%, and COV of 29-31%. Lenordini has an absolute difference of 337 kPa, percent difference of 19%, and COV of 12-28%. Granite has an absolute difference of 1006 kPa, percent difference of 17.6% and COV of 15-29%. River Park has an absolute difference of 298 kPa, percent difference of 59.6% and COV of 11-28%. Measured q_t COV for the selected intervals ranges between 12-31%, which is within the range for cone measurements as shown by Baecher and Christian (2003).

This analysis is expanded to all penetration rates as shown in Figure 31. The magnitude of the mean q_t for the selected intervals varies for each site but tends to increase with decreasing normalized velocity. COV also tends to decrease with decreasing normalized velocity where the range of q_t COV for drained penetration is 10-18% while the range for undrained penetration is 14-43%. Mean, standard deviations, and COV for f_s follow similar trends as q_t where the range of COV for drained penetration is 5-21% while the range for undrained penetration is 10-68%. Trends in u_2 show that the mean value tends to increase with decreasing penetration rate. The scatter in standard deviation for u_2 is large and there are no discernible trends for COV. The state parameter tends to converge to a value of -0.02 to -0.07 for drained conditions while the range is larger for undrained conditions.

Trends in B_q and $\Delta u_2/\sigma'_{vo}$ show the values tend to converge with decreasing normalized velocity and Δu_2 tends to be more positive under drained conditions while $\Delta u_2/\Delta u_{2ref}$ does not do well to capture penetration rate drainage effects. The u_2 trends for Kornbloom (Figure 25) show a decrease in cumulative frequency width (smaller σ) with decreasing penetration velocity, which is consistent with observations from other sites (Appendix A-D). This is expected since decreasing penetration rate should results in more drained conditions. u_2 values are also influenced by spatial variability and smearing of soil around the u_2 sensor location.

DISCUSSION

Variable Penetration Rate Cone Testing for Improved Characterization of Intermediate Soils

Tip resistance is influenced by penetration rate for sands with fines and can be evaluated using the normalized framework as discussed. The 4 sites tested herein are significant since partial drainage, not drained penetration, occurs at the standard penetration rate of 2 cm/s. Penetration rate effects are binned by various index parameters to discover trends in the data.

Many of the field sites showed pore pressures (u_2) below hydrostatic (u_0) conditions ($\Delta u < 0$). In contractive soils such as those researched previously by others (e.g. clays, silty clays, clayey silts) the normalized excess pore pressure ($\Delta u/\Delta u_{ref}$) will follow a similar but opposite trend as normalized tip resistance (Q/Q_{ref}) with respect to normalized velocity; as the excess pore pressure increases with normalized velocity, the tip resistance decreases. This is not what is observed at the sites tested herein. In Kornbloom, for example, the tip resistance increases as the normalized velocities decreased, while the excess pore pressure tends to be more negative at higher normalized velocities and near zero at low normalized velocities (Figure 28 and 29). This trend was also observed by Schneider et al. (2007) when investigating the loose silica flour bentonite mixture. In the context of Burns and Mayne (1998) this would suggest that for soils with increasing sand and silt content, the $\Delta u_{2,shear}$ component generates a more significant response than the $\Delta u_{2,oct}$ component, resulting in overall negative values of Δu_2.

Trends in $Q_{drained}/Q_{ref}$ and Δu_2 suggest dependence on the depth below ground water table but not the depth below ground surface (Figure 32). While there is not a clear mechanistic justification for the dependence of Δu_2 generated on depth below ground water table, it is plausible that the excess pore pressure field is not fully developed immediately below the ground water table and additional preferential drainage conditions may exist (e.g. vertical drainage along cone shaft). River Park is the only site where the variable rate interval was selected just below the ground water table. This site had the smallest hydrostatic ground water conditions (Figure 32) and happens to correspond to the smallest and most variable penetration rate effects. Kornbloom, on the other hand, had the clearest $Q_{drained}/Q_{ref}$ trend and the highest u_0 (smallest depth below ground water table) over the zone of interest.

All sites that were tested had surficial observations of liquefaction during at least one previous event. It is possible that loose deposits will gradually densify, approaching critical state upon shaking, and thereby decreasing the potential for significant penetration rate effects. River Park and Kornbloom were both subjected to several additional events with no surface manifestation of liquefaction.

$Q_{drained}/Q_{ref}$ is shown versus fines content, soil behavior type and in-situ state in Figure 33. The only discernible trend seems to be increasing $Q_{drained}/Q_{ref}$ with decreasing I_c. Given the range of values and the limited number of data points, no clear trends exist.

Effect on Estimates of Engineering Parameters

Given the influence in penetration rate observed in penetration resistance and pore pressure, the next question is: how might the effects of partial drainage during penetration at 2

cm/s influence correlations used to estimate soil properties? Sand based correlations are typically developed based on data in clean sands, which are inherently based on drained cone tip resistances. In practice, however, these correlations are frequency used for all "sand-like" soils, typically those with I_c < 2.6. As evident in all 4 soils investigated in this study (I_c ranging from 2.25 to 2.57) cone resistance is not fully drained at the standard penetration rate. The effect of partial drainage on estimations of engineering parameters was investigated using several widely used CPT correlations as provided in Table 5.

Friction angle from drained penetration is 1.5^o to 2° larger for drained penetration than for standard rate penetration for Kornbloom and Lenordini (Figure 34). The Mayne (2007) correlation for friction angle is only a function of tip resistance and is therefore very sensitive to penetration rate effects. Friction angle estimates for Granite for drained and standard rate penetration are similar, due to the presence of greater spatial variability at the site. Friction angle estimates for River Park are even less discernible, due to the aforementioned reasons.

Relative density from drained penetration ranges from 1.04 to 1.52 times greater than for standard rate penetration for Granite, Lenordini, and Kornbloom (Figure 35). The Jamiolkowski et al. (2001) correlation is only a function of tip resistance and is therefore sensitive to differences between drained and partially drained penetration resistance. Note that this correlation for D_R is only recommended for soils with less than 15% fines through it is routinely used in practice for all sand-like soils.

Empirical estimates of the state parameter range from -0.09 to 0.03 (Figure 36) revealing that estimation of the state parameter is sensitive to penetration rate. The state behavior for each site is unique, so the comparison of state trends between the sites is of little practical value.

Overall, the estimated friction angle and relative density tend to increase while the estimated state parameter tends to decrease with the transition from partially drained to fully drained penetration.

Variable Penetration Rate Cone Testing for Improved Prediction of Liquefaction Potential in Sands with Fines

Application of Δq_{c1N} results in the shift of q_{c1N} points to the right to values of q_{c1Ncs}. The difference between standard rate and drained penetration ($\Delta q_{c1N,drained}$) is compared in a similar manner by applying $\Delta q_{c1N,drained}$ to q_{c1N}, resulting in drained tip resistances, $q_{c1N,drained}$. The liquefaction potential for the subintervals previously discussed will be evaluated only for those subintervals in order to be consistent with the discrete samples obtained in this study and the observations made in the preceding sections. Because of this, the observations from these specific subintervals will not necessarily match the observations or trends of the entire historically identified depth interval (Table 1).

The location of the original historic intervals and the subintervals studied herein are shown together in Figure 37 and q_{c1Ncs} and $q_{c1N,drained}$ are compared in CSR-q_{c1N} space (Figure 38). q_{c1N}, Δq_{c1N} and q_{c1Ncs} are determined for the selected subintervals using Eqs. 1-5. It is acknowledged that $CSR_{M=7.5,\sigma'vo=1}$ will change slightly for each site, since σ_{vo}, σ'_{vo} and r_d will change slightly. This effect is negligible for the comparisons performed herein, therefore the

original $CSR_{M=7.5,\sigma'vo=1}$ values will be used. The empirically based fines content correction tends to be larger in magnitude than the difference between drained and partially drained penetration. Trends in percent increase in q_{c1N} for the selected subintervals for are shown for both correction methods (Figure 39).

The fines content of the subintervals is generally consistent with the values reported in literature with one exception; Lenordini has a reported fines content for the liquefied interval of 26%, while the subinterval evaluated herein has a fines content of 63%. The historic fines content is meant to be a representative fines content while the samples obtained from this study were specifically targeted based on observations of q_t and u_2 trends with penetration velocity.

The correction for partially drained to fully drained tip resistance ranges from 2.5 to 11 (excluding the River Park outlier) for each subinterval, while Δq_{c1N} values for each subinterval range from 25 to 60 (Figure 38). Comparison between q_{c1Ncs} and $q_{c1Ndrained}$ (Figure 40) shows that the difference between drained and partially drained penetration does not fully account for the Δq_{c1N} correction term.

CONCLUSIONS

The study shows that use of variable penetration rate cone testing is a valuable tool to understand the extent of which cone tip resistance is affected partial drainage and how fines content can influence penetration resistance. The results from a field study were used to explore the hypothesis, evaluate drainage conditions around an advancing cone, and provide an initial reassessment of the clean sand equivalent corrections currently used in practice. Several factors were shown to influence field cone penetration tests in sands with fines.

1. Normalized velocity trends present in previous studies are observed in natural soil deposits. The range of $Q_{drained}/Q_{ref}$ at the four sites tested was at the low end of previously recorded values. Review of previous studies show $Q_{drained}/Q_{ref}$ depends on soil mineralogy, in-situ state, and stress history.
2. Spatial variability is difficult to quantify and can limit the effectiveness of comparing closely spaced cone soundings. A proper understanding of the mechanism of geologic deposition and the associated uncertainty provides added confidence to stratigraphic interpretation. The variability present in penetration rate effects at the Granite site are attributed to variability in fluvial deposition, while the uniformity in Kornbloom trends is attributed to the low energy flood-plain, deltaic, and lacustrine depositional processes.
3. The relatively small magnitude of penetration rate effect may be due to small state as the overall tendency of volume change is minimal due to the in-situ condition being close to the critical state line. All four sites have small estimates of in-situ state parameter (ranging from -0.02 to -0.08).
4. Non-standard pore pressure dissipation test measurements and $\Delta u_2 < 0$ have not been widely observed in previous studies (which are mostly based dissipation tests in clayey soils) and therefore differ from previous plots of the normalized velocity framework and complicate fundamental understanding of drainage behavior. Improved understanding of the components of excess pore pressure generation (Eq. 6 and 7) is useful for interpretation of drainage conditions in silty soils. The presence of $t_{50} < 50$ seconds signify partially drained conditions during penetration at the standard rate.
5. Estimates of soil engineering properties tend to be sensitive to penetration rate. Overall, the estimated friction angle and relative density tend to increase while the estimated state parameter tends to decrease with the transition from partially drained to fully drained penetration.
6. Penetration rate effect is observable at some sites, but does not account for the magnitude of Δq_{c1N} adjustments present in liquefaction evaluation. The difference between drained and partially drained penetration was shown to be not as significant as Δq_{c1N}. Where decreasing penetration rate can eliminate partial drainage caused by increasing fines content, Δq_{c1N} accounts for both fines content and q_{c1N}. However, the effects of partial drainage on measured cone resistance cannot fully account for the empirical fines content correction factors in sands with fines.
7. Variable penetration rate cone tests are useful for proper understanding of drainage conditions around an advancing cone. They can be used to compare drained, partially drained, and undrained penetration resistances in order to evaluate the significance of penetration rate effects.

ACKNOWLEDGEMENTS

This work would not have been possible without assistance from USGS researchers Drs. John Tinsley, Mike Bennett and Tom Holzer. We would like to thank the landowners for their willingness to allow me to test on their land: Mr. Nick Nichols, Mr. Mike Miller, Mr. Carson Kalin, Mrs. Yazmin Arellano and Mr. Shayne Ferber. A special thanks to colleagues at the UCD GCM and SIL labs for their assistance in this research. And to Mr. Bob Nigbor and the NEES@UCLA team for their generosity in sharing equipment used in this study. Finally this research was performed through support from the United States Geological Survey under grant #G12AP20013.

REFERENCES

ASTM D422-63 (1998) "Standard test method for particle-size analysis of soils."

ASTM D4318-00 (2000) "Standard test method for liquid limit, plastic limit, and plasticity index of soils."

ASTM D5778-07 (2007) "Standard test method for performing electronic friction cone and piezocone penetration testing of soils."

Baecher, G.B. and Christian, J.T. (2005) Reliability and statistics in geotechnical engineering. John Wiley & Sons.

Baligh, M.M., and Levadoux, J.N. (1986). "Consolidation after undrained piezocone penetration II: interpretation." *J. of Geotech. Eng*., 112 (7): 727-745.

Been, K. and Jefferies, M.G. (1992). "Towards systematic CPT interpretation." *Proc. of the Wroth memorial symposium*, London: Thomas Telford, pp. 121-134.

Bennett, M. J., Youd, T. L., Harp, E. L., and Wieczorek, G. F. (1981). "Subsurface investigation of liquefaction, Imperial Valley earthquake, California, October, 15, 1979." *U.S. Geological Survey*: Open File Report 81-502. 87 pp.

Bennett, M.J., McLaughlin, P.V., Sarmiento, J.S., and Youd, T.L. (1984). "Geotechnical investigation of liquefaction sites, Imperial Valley, California." *U.S. Geological Survey*, Open File Report 84-252: 111 pp.

Bennett, M. and Tinsley, J.C. (1995). "Geotechnical data from surface and subsurface samples outside of and within liquefaction-related ground failures caused by the October 17, 1989, Loma Prieta earthquake, Santa Cruz and Monterey counties, California." *U.S. Geological Survey*, Open-File Report 95-663, 360 pp.

Bierschwale, J.G., and Stokoe, K.H. (1984). "Analytical evaluation of liquefaction potential of sands subjected to the 1981 Westmoreland earthquake." *Geotechnical Engineering Report GR 84*, 15.

Boulanger, R. W., and Idriss, I. M. (2004). "State normalization of penetration resistance and the effect of overburden stress on liquefaction resistance." *Proc., 11th International Conference on Soil Dynamics and Earthquake Engineering, and 3rd International Conference on Earthquake Geotechnical Engineering*, D. Doolin et al., eds., Stallion Press., Vol. 2, pp. 484-491.

Boulanger, R.W., and Idriss, I.M. (2014). "CPT and SPT based liquefaction triggering procedures." *CGM Report 14-01*, University of California, Davis.

Bray, J.D, and Sancio, R.B. (2006) "Assessment of the liquefaction susceptibility of fine-grained soils." *J. Geotech and Geoenviron. Eng*. 132 (9): 1165-1177.

Burns, S.E. and Mayne, P.W. (1998) "Monotonic and dilatory pore pressure decay during piezocone tests in clay." *Canadian Geotechnical Journal*. 35:1063-1073.

Chung, S.F., Randolph, M.F., and Schneider, J.A. (2006). "Effect of penetration rate on penetrometer resistance in clay." *J. of Geotech. and Geoenviron. Eng*., 132 (9): 1188-1196.

Dahl, K.R. (2011). "Evaluation of seismic behavior of intermediate and fine grained soils." *PhD. Thesis*, Dept. of Civil Engineering, University of California, Davis, Davis, CA, 1120 p.

DeJong, J.T., Jaeger, R.A., Boulanger, R.W., Randolph, M.F., and Wahl, D.A.J. (2012). "Variable penetration rate cone testing for characterization of intermediate soils." *Geotechnical and Geophysical Site Characterization 4*. Vol. 1,Taylor and Francis, London: 25-42.

DeJong, J.T., and Randolph, M.F. (2012) "Influence of partial consolidation during cone penetration on estimated soil behavior type and pore pressure dissipation measurements." *J. of Geotech. and Geoenviron. Eng*., 138 (7): 1-13.

Finke, K.A., Mayne, P.W., Klopp, R.A. (2001) "Piezocone penetration testing in Atlantic piedmont residuum." *J. of Geotech. And Geoenviron. Eng.*, 127 (1): 48-54.

Finnie, I.M.S., and Randolph, M.F. (1994). "Punch-through and liquefaction induced failure of shallow foundations on calcareous sediments." *Proc. 7th Int. Conf. on Behavior of Offshore Structures, Boston*, pp. 217-230.

Holzer, T.L., Tinsley, J.C., Bennett, M.J., and Mueller, C.S. (1994). "Observed and predicted ground deformation - Miller Farm lateral spread, Watsonville, California." *Proc., 5th US—Japan Workshop on Earthquake Resistant Design of Lifeline Facilities and Countermeasures for Soil Liquefaction*, Technical Rep. No. NCEER-94, Vol. 26: pp. 79-99.

Idriss, I.M. and Boulanger, R.W. (2008) *Soil liquefaction during earthquakes*. Earthquake Engineering Research Institute.

ISSMGE International Society for Soil Mechanics and Geotechnical Engineering (1999). "International reference test procedure for the cone penetration test (CPT) and the cone penetration test with pore pressure (CPTU): Report of the ISSMGE Technical Committee 16 on Ground Property Characterisation from In-Situ Testing." In F.B.J. Barends et al. (eds), *Geotechnical engineering for transportation infrastructure: Proceedings of the twelfth european conference on soil mechanics and geotechnical engineering, Amsterdam, Netherlands, 7–10 June 1999, Vol. 3*: 2195–2222. Rotterdam: A.A. Balkema.

Jaeger, R.A., DeJong, J.T., Boulanger, R.W., Low, H.E., and Randolph, M.F. (2010). "Variable penetration rate CPT in an intermediate soil." *Proc., 2nd Int. Symp. Cone Penetration Testing*.

Jaeger, R. A. (2012). "Numerical and experimental study on cone penetration in sands and intermediate soils." *PhD. Thesis*, Dept. of Civil Engineering, University of California, Davis, Davis, CA, 268 p.

Jamiolkowski, M., D.C.F. LoPresti, and M. Manassero, "Evaluation of Relative Density and Shear Strength of Sands from Cone Penetration Test and Flat Dilatometer Test", *Soil Behavior and Soft Ground Construction (GSP 119)*, ASCE, Reston, Virginia, 2001, pp. 201-238.

Jefferies, M., and Been, K. (2006). Soil *liquefaction: a critical state approach*. CRC press.

Kim, K., Prezzi, M., Salgado, R, and Lee, W. (2008). "Effect of penetration rate on cone penetration resistance in saturated clayey soils." *J. of Geotech. and Geoenviron. Eng.*, 134 (8): 1142-1153.

Keaveny, J.M. (1985). "In-situ determination of drained and undrained soil strength using the cone penetration test." *PhD. Dissertation*, University of California, Berkeley, Berkeley, CA.

Kishida, H. (1966). "Damage to reinforced concrete buildings in Niigata City with Special reference to foundation engineering." *Soils and Foundations*, Japanese Society of Soil Mechanics and Foundation Engineering, 6(1),71–86.

Ku, C.S., Ou, C.Y., Juang, C.H. (2010). "Reliability of CPT Ic as an index for mechanical behavior classification of soils." *Geotechinque*, 60 (11): 861-875.

Lunne, T., Robertson, P. K., and Powell, J. J. M. (1997). *Cone penetration testing in geotechnical practice.* Blackie Academic and Professional, Melbourne, Australia.

Mayne, P. W. (2007). "Cone penetration testing state-of-practice." *NCHPR Project 20-05*, Topic 37–14.

Moss, R. E. S., Seed, R. B., Kayen, R. E., Stewart, J. P., Der Kiureghian, A., and Cetin, K. O. (2006). "CPT-based probabilistic and deterministic assessment of in situ seismic soil liquefaction potential." *J. Geotechnical and Geoenvironmental Eng.*, ASCE 132(8), 1032–051.

Nichols, G. (2009) *Sedimentology and stratigraphy*. John Wiley & Sons.

Oliveria, J.R.M., Almeida, M.S., Motta, H.P., and Almeida, M.C. (2010). "Influence of penetration rate on penetrometer resistance." *J. of Geotech. and Geoenviron. Eng.*, 137 (7)

Randolph, M. F. (2004). "Characterisation of soft sediments for offshore applications." *Proc., Int. Conf. on Geotechnical and Geophysical Site Characterization, ISC-2*, Millpress, The Netherlands, 209–232.

Robertson, P.K. (2009). "Interpretation of cone penetration tests – a unified approach." *Canadian Geotechnical Journal*, 46: 1337-1355.

Robertson, P.K. (2010). "Estimating in-situ state parameter and friction angle in sandy soils from CPT." *Proceedings of the 2nd International Symposium on Cone Penetration Testing*, Vol. 10, pp. 2-43.

Robertson, P.K. (2012) "The James K. Mitchell Lecture: Interpretation of in-situ tests - some insights." *Geotechnical and Geophysical Site Characterization 4*. Vol. 1,Taylor and Francis, London: 25-42.

Robertson, P. K., and Wride, C. E. (1998). "Evaluating cyclic liquefaction potential using the cone penetration test." *Canadian Geotechnical J.* 35(3), 442–59.

Schnaid, F., & Yu, H. S. (2007). "Interpretation of the seismic cone test in granular soils." *Geotechnique*, 57 (3): 265-272.

Schnaid, F., Bedin, J., and Costa Filho, L. M. (2010). "Drainage characterization of tailings from in situ test." *Proc., 2nd Int. Symp. Cone Penetration Testing*.

Schneider, J.A., Lehane, B.M., and Schnaid, F. (2007) "Velocity effects on piezocone measurements in normally and over consolidated clays." *Int. J. of Physical Modelling in Geotechnics*, 7(2): 23-34

Seed, H. B., Tokimatsu, K., Harder, L. F. Jr., and Chung, R. (1984). "The influence of SPT procedures in soil liquefaction resistance evaluations." *Earthquake Engineering Research Center*, University of California, Berkeley, Report No. UCB/EERC-84/15, 50 pp.

Seed, H. B., Tokimatsu, K., Harder, L. F. Jr., and Chung, R. (1985). "Influence of SPT procedures in soil liquefaction resistance evaluations." *Journal of Geotechnical Engineering*, ASCE, 111(12), 1425-1445.

Silva, M. F., White, D. J., and Bolton, M. D. (2006). "An analytical study of the effect of penetration rate on piezocone tests in clay." *Int. J. Numer.Anal. Methods Geomech*., 30(6), 501–527.

Stark, T. D., and Olson, S. M. (1995). "Liquefaction resistance using CPT and field case histories." *J. Geotechnical Eng.*, ASCE 121(12), 856–69.

Suzuki, Y., Koyamada, K., and Tokimatsu, K. (1997). "Prediction of liquefaction resistance based on CPT tip resistance and sleeve friction." in *Proceedings, 14th International Conference on Soil Mechanics and Foundation Engineering*, Hamburg, Germany, Vol. 1, pp. 603–06.

Suzuki Y., Sanematsu, T., and Tokimatsu, K. (1998). "Correlation between SPT and seismic CPT." In: Robertson PK, Mayne PW (eds.), in *Proceedings, Conference on Geotechnical Site Characterization*, Balkema, Rotterdam, pp. 1375–380.

Teh, C.I. and Houlsby, G.T. (1991) "An analytical study of cone penetration test in clay." *Geotechnique*, 41 (1): 17-34.

Tinsley, J.C. (2012) Personal Communication.

Toprak, S., Holzer, T. L., Bennett, M. J., Tinsley, J. C. (1999). "CPT- and SPT-based probabilistic assessment of liquefaction potential." *Proceedings of Seventh US Japan Workshop on Earthquake Resistant Design of Lifeline Facilities and Counter-measures Against Liquefaction*. T. D. O'Rourke, J. P. Bardet, and M. Hamada, eds., Report MCEER-99-0019, MCEER, NY.

Wahl, D.A.J. (2012). "Implementation of variable rate cone penetration testing: an experimental field study." *M.Sc. Thesis*, Dept. of Civil Engineering, UC Davis, Davis, CA, 147 p.

Youd, T. L., Idriss, I. M., Andrus, R. D., Arango, I., Castro, G., Christian, J. T., Dobry, R., Finn, W. D. L., Harder, L. F., Hynes, M. E., Ishihara, K., Koester, J. P., Liao, S. S. C., Marcuson, W. F., Martin, G. R., Mitchell, J. K., Moriwaki, Y., Power, M. S., Robertson, P. K., Seed, R. B., and Stokoe, K. H. (2001). "Liquefaction resistance of soils: summary report from the 1996 NCEER and 1998 NCEER/NSF workshops on evaluation of liquefaction resistance of soils." *J. Geotechnical and Geoenvironmental Eng., ASCE* 127(10), 817–33.

Youd, T. L., and Bennett, M. J. (1983). "Liquefaction sites, Imperial Valley, California." *Journal of the Geotechnical Engineering Division, ASCE*, 109(3), 440-457.

Table 1 - Summary of historic liquefaction sites evaluated in this study

Site	Earthquake	M_w	Liquefied?	Crit. depth range	GWT	USCS	% Fines	Reference
Leonardini51	1989 Loma Prieta, USA	6.93	Yes	3.1–3.7	1.80	SM	36	Bennett and Tinsley (1995); Toprak et al. (1999)
GraniteConst123	1989 Loma Prieta, USA	6.93	Yes	7.2–7.8	5.00	SP/SM	18	Bennett and Tinsley (1995); Toprak et al. (1999)
River Park A	1979 Imperial Valley, USA	6.53	Yes	0.5-2.5	0.30	ML	80	Bennett et al (1981); Youd & Bennett (1983); Moss et al (2004)
River Park A	1981 Westmorland , USA	5.90	No	0.5-2.5	0.30	ML	80	Bennett et al (1981); Youd & Bennett (1983); Moss et al (2004)
River Park A	1987 Superstition Hills, USA	6.54	No	0.5-2.5	0.30	ML	80	Bennett et al (1981); Youd & Bennett (1983); Moss et al (2004)
KornbloomB	1979 Imperial Valley, USA	6.53	No	2.6–5.2	2.74	ML	92	Bennett et al. (1984); Bierschwale and Stokoe (1984)
KornbloomB	1981 Westmorland , USA	5.90	Yes	2.6–5.2	2.74	ML	92	Bennett et al. (1984); Bierschwale and Stokoe (1984)
KornbloomB	1987 M=6.5 Superstition Hills	6.54	No	2.6–5.2	2.74	ML	92	Bennett et al. (1984); Bierschwale and Stokoe (1984)

Table 2 - Summary of Kornbloom samples obtained in the vicinity of the test location

Sounding	Mid Depth [m]	w_n [%]	w_l [%]	PI	% Sand	% Silt	% Clay	D_{50}	C_u	FC [%]	SPT N	Description	USCS
TK4a	0.7	24			24	58	18	0.04	43	76	12	Sandy silt	ML
TK4a	1.4				18	65	17	0.04		82		sandy silt	
TK4a	1.6	26			12	65	23	0.02		88	4	clayey silt	CL
TK4a	2.2				26	68	6	0.05	3.3	74	7	sandy silt	ML
TK4a	3.0	28			38	53	9	0.06	9	62	3	Sandy silt	ML
TK4a	3.7	30			4	83	13	0.03	11	96	9	silt	ML
TK4a	4.5	29			17	74	9	0.05	8.7	83	8	Sandy silt	ML
TK4a	5.3				11	83	6	0.05	2.6	89	12	Clayey silt	ML
TK4a	5.9	33			10	60	30	0.03		90		silty clay	CH
TK4a	6.2	36			5	28	67	0		95	3		
This Study	2.2	22	23		36	56	8	0.07	3.3	64		Sandy Silt	ML
This Study	2.6	32	26	2	5	80	15	0.04		95		Sandy Silt	ML
This Study	3.0	30	25	1	4	86	10	0.04	31	96		Sandy Silt	ML
This Study	4.5	25			19	74	7	0.06	13	81		Silt with Sand	ML
This Study	7.1	26	26	5	13	77	10	0.04	24	83			CL-ML
This Study	10.1	22			51	45	4	0.08	1.8	49		Silty Sand	SM

Note: This study is adjacent to sounding TK4a from Bennett et al. (1984)

Table 3 - Summary of variable rates performed within subintervals selected at Kornbloom

Test	Int.	Rate (cm/s)	Depth range (m)		q_{c1}	σ'_{vo}	σ_{vo}	Δu_2	$\Delta u_2/\Delta u_{2ref}$	Q	Q/Q_{ref}	Bq	C_N	q_{c1N}	$\Delta u_2/\sigma'_{vo}$	V_s (m/s)	I_R	t_{50} (s)	c_h (cm^2/s)	V
KRN01	1	2.03	2.53	3.33	11.8	32.5	56.1	-56.3	7.9	40	1.8	-0.050	1.70	20.0	-1.73	108	240	16	5	1.8E+0
KRN03	1	2.01	2.53	3.33	10.8	32.5	56.1	-34.0	4.8	32	1.7	-0.033	1.70	18.4	-1.05	108	240	16	5	1.8E+0
KRN04	1	0.24	2.53	3.33	17.8	32.5	56.1	-36.4	5.1	54	2.8	-0.021	1.70	30.3	-1.12	108	240	16	5	2.1E-1
KRN05	1	20.45	2.53	3.33	6.7	32.5	56.1	-7.1	1.0	19	1.0	-0.011	1.70	11.4	-0.22	108	240	16	5	1.8E+1
KRN06	1	0.02	2.53	3.33	16.4	32.5	56.1	-15.8	2.2	49	2.6	-0.010	1.70	27.8	-0.49	108	240	16	5	2.1E-2
KRN01	2	2.02	3.53	4.33	19.6	41.7	75.1	-78.9	1.5	45	1.6	-0.041	1.70	33.3	-1.89	125	240	16	5	1.8E+0
KRN03	2	2.01	3.53	4.33	17.9	41.7	75.1	-81.9	1.6	42	1.4	-0.047	1.70	30.4	-1.96	125	240	16	5	1.8E+0
KRN04	2	0.25	3.53	4.33	26.1	41.7	75.1	-84.8	1.6	62	2.1	-0.033	1.70	44.4	-2.03	125	240	16	5	2.1E-1
KRN05	2	20.46	3.53	4.33	12.7	41.7	75.1	-51.8	1.0	29	1.0	-0.043	1.70	21.5	-1.24	125	240	16	5	1.8E+1
KRN06	2	0.03	3.53	4.33	23.9	41.7	75.1	-19.5	0.4	56	1.9	-0.008	1.70	40.7	-0.47	125	240	16	5	2.2E-2

Table 4 - Summary of variable rate intervals for selected subintervals for all sites

Test	Int.	Rate (cm/s)	Depth range (m)		q_{c1}	σ'_{vo}	σ_{vo}	Δu_2	$\Delta u_2/\Delta u_{2ref}$	Q	Q/Q_{ref}	Bq	C_N	q_{c1N}	$\Delta u_2/\sigma'_{vo}$	V_s (m/s)	I_R	t_{50} (s)	c_h (cm^2/s)	V
KRN01/3	1/2	2.02	2.53	4.33	15.0	37.1	65.6	-62.8	3.9	39	1.6	-0.043	1.70	25.5	-1.7	116.5	240	16	5	1.8E+00
KRN04	1/2	0.24	2.53	4.33	22.0	37.1	65.6	-60.6	3.4	58	2.5	-0.027	1.70	37.4	-1.6	116.5	240	16	5	2.1E-01
KRN05	1/2	20.46	2.53	4.33	9.7	37.1	65.6	-29.4	1.0	24	1.0	-0.027	1.70	16.5	-0.7	116.5	240	16	5	1.8E+01
KRN06	1/2	0.02	2.53	4.33	20.1	37.1	65.6	-17.7	1.3	53	2.3	-0.009	1.70	34.2	-0.5	116.5	240	16	5	2.2E-02
LEN02/3	3	2.07	3.83	4.08	17.5	51.1	76.4	-48.2	0.8	33	1.1	-0.028	1.65	29.0	-0.9		240	6	7	1.3E+00
LEN04	3	0.20	3.83	4.08	23.6	51.1	76.4	-47.3	0.8	45	1.5	-0.020	1.60	37.8	-0.9		240	6	7	1.3E-01
LEN05	3	20.39	3.83	4.08	16.1	51.1	76.4	-59.7	1.0	30	1.0	-0.038	1.66	26.8	-1.2		240	6	7	1.3E+01
LEN06	3	0.02	3.83	4.08	25.1	51.1	76.4	-17.4	0.3	48	1.6	-0.007	1.59	39.9	-0.3		240	6	7	1.3E-02
GRN01/6	4	2.04	7.88	8.28	56.5	139.4	155.5	-18.1	0.4	40	1.7	-0.003	0.81	45.8	-0.1		240	10	6	1.5E+00
GRN07	4	0.02	7.88	8.28	59.4	139.4	155.5	-4.6	0.1	42	1.8	-0.001	0.81	48.3	0.0		240	10	6	1.5E-02
GRN08	4	0.21	7.88	8.28	39.4	139.4	155.5	-8.2	0.2	27	1.2	-0.002	0.79	31.3	-0.1		240	10	6	1.5E-01
GRN09	4	20.49	7.88	8.28	34.4	139.4	155.5	-40.4	1.0	24	1.0	-0.012	0.79	27.1	-0.3		240	10	6	1.5E+01
RVP03/10	5	1.96	1.5	1.98	6.4	28.6	31.8	-18.0	1.1	22	1.3	-0.031	1.70	10.9	-0.6		240	15	4.9	1.8E+00
RVP04/09	5	0.25	1.5	1.98	6.0	28.6	31.8	-39.2	2.3	20	1.2	-0.067	1.70	10.2	-1.4		240	15	4.9	2.2E-01
RVP05	5	0.02	1.5	1.98	4.0	28.6	31.8	-8.2	0.5	13	0.8	-0.022	1.70	6.8	-0.3		240	15	4.9	2.1E-02
RVP06/08	5	20.20	1.5	1.98	5.1	28.6	31.8	-16.9	1.0	17	1.0	-0.035	1.70	8.7	-0.6		240	15	4.9	1.8E+01
KRN01/3	1/2	2.02	2.53	4.33	15.0	37.1	65.6	-62.8	3.9	39	1.6	-0.043	1.70	25.5	-1.7		240	16	5	1.8E+00

Table 5 - CPT correlations for estimation of engineering parameters

Property Estimated	**Correlation Used**	**Reference**
SBT type	$I_c = [(3.47 - logQ_{t1})^2 + (logF_r + 1.22)^2]^{0.5}$	Robertson (2012)
State	$\xi = 0.56 - 0.33\log(Q_{tn,cs})$	Robertson (2010)
Friction Angle	$\varphi'(\text{deg}) = 17.6 + 11 * \log\left(\frac{q_t}{\sqrt{\sigma'_{vo} * \sigma_{atm}}}\right)$	Mayne (2007)
Relative Density	$D_R = 100\left[0.268 * \ln\left(\frac{q_t / \sigma_{atm}}{\sqrt{\sigma'_{vo} * \sigma_{atm}}}\right) - 0.675\right]$	Jamiolkowski et al. (2001)

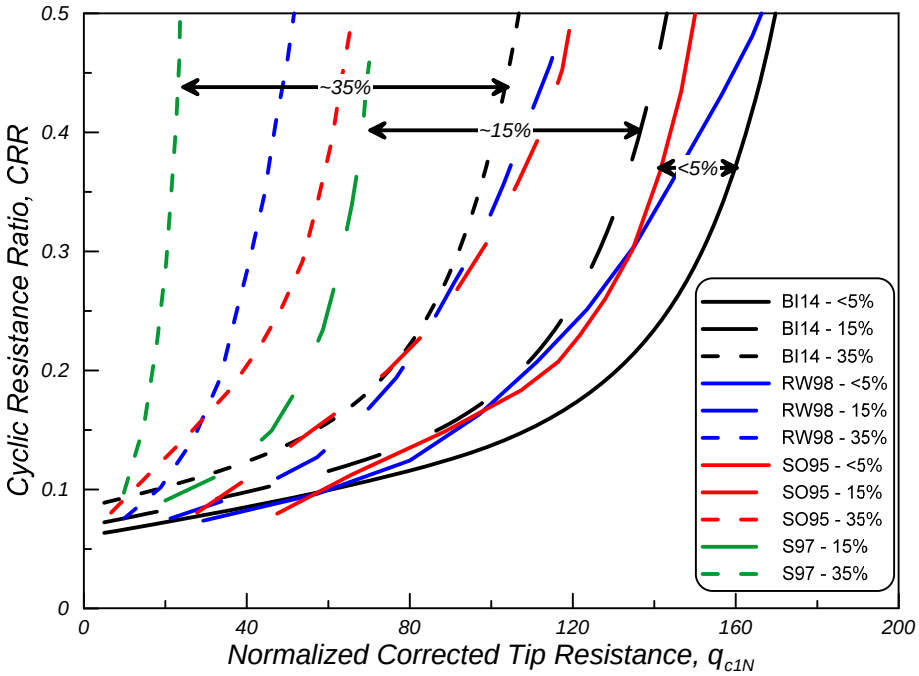

Figure 1 - Proposed *CRR*-q_{c1N} relationships by various researchers (BI14 - Boulanger and Idriss 2014, RW98 - Robertson and Wride 1998, SO95 - Stark and Olson 1995, S97 - Suzuki 1997).

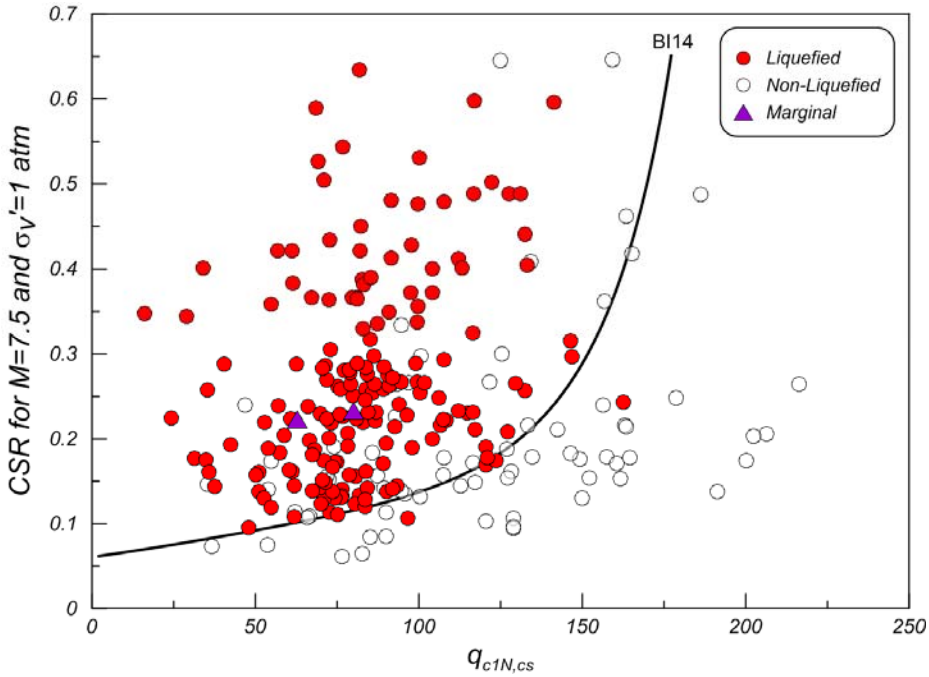

Figure 2 - Summary of case histories included in the Boulanger and Idriss (2014) CPT liquefaction database. Note that the curve and data points are clean sand equivalent tip resistances q_{c1Ncs}.

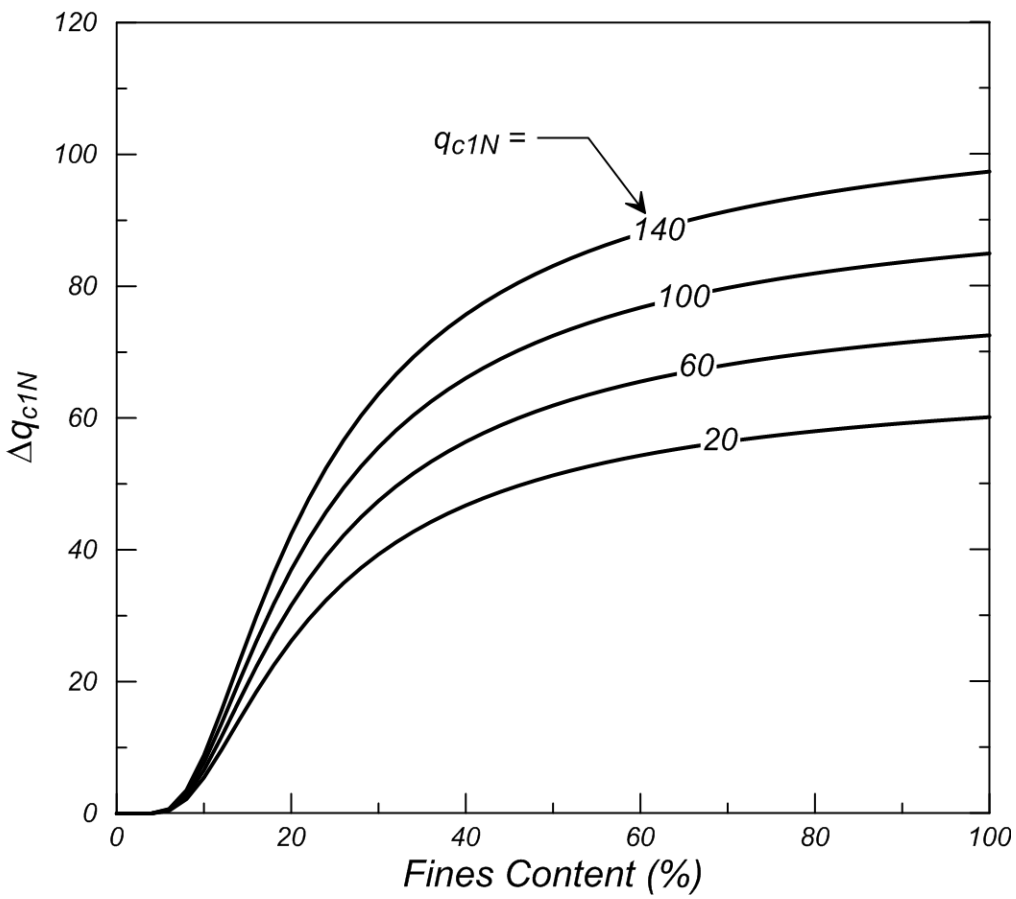

Figure 3 - Δq_{c1N} correction from Boulanger and Idriss (2014).

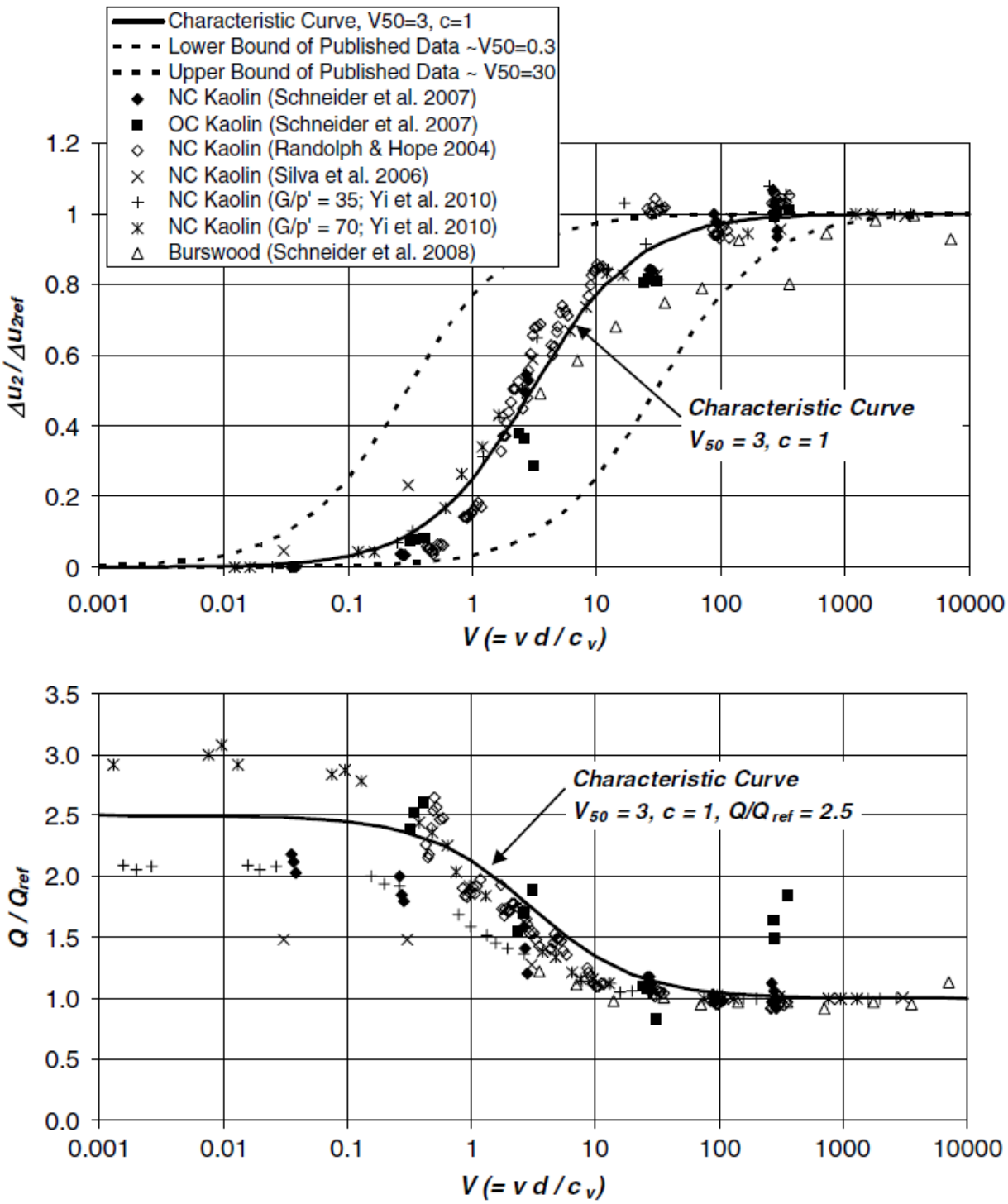

Figure 4 – Normalized velocity effects (a) normalized excess pore pressure and (b) normalized penetration resistance for contractive clays (after DeJong et al. 2012).

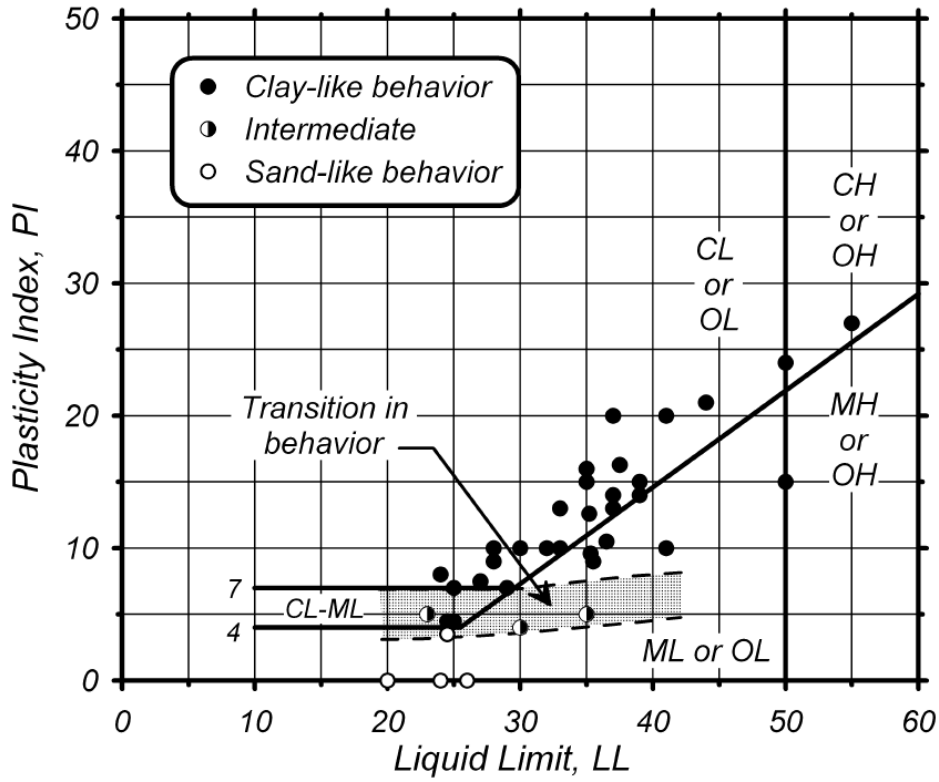

Figure 5 - Atterberg limits chart, showing representative values for each soil that exhibited cohesive, cohesionless, or intermediate behavior (from Idriss and Boulanger 2008).

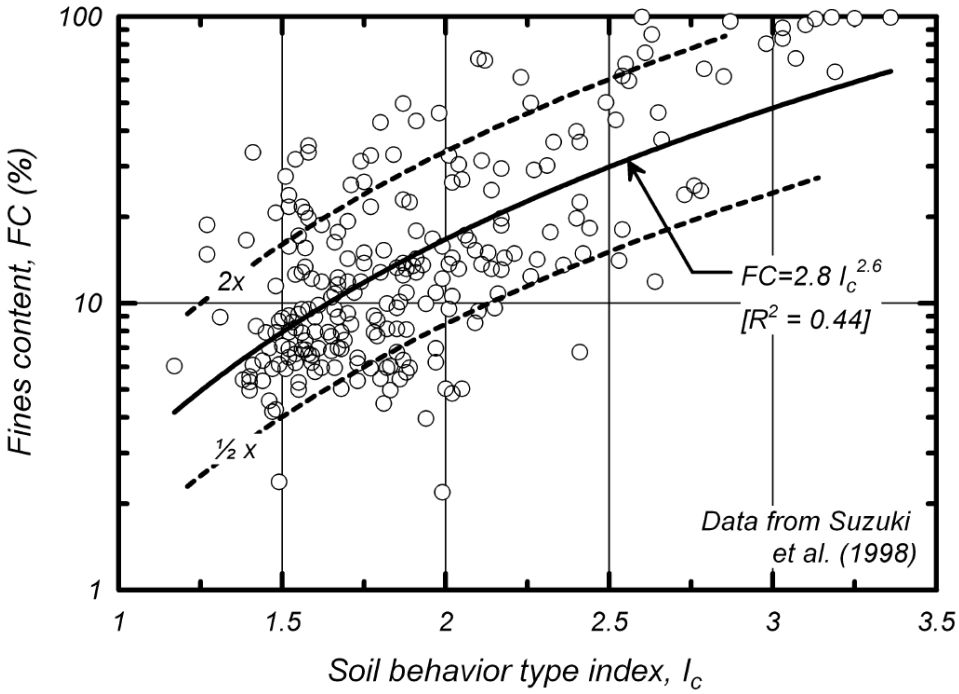

Figure 6 - Correlation between fines content and soil behavior type, I_c (data from Suzuki et al. 1998, reprinted in Idriss and Boulanger 2008).

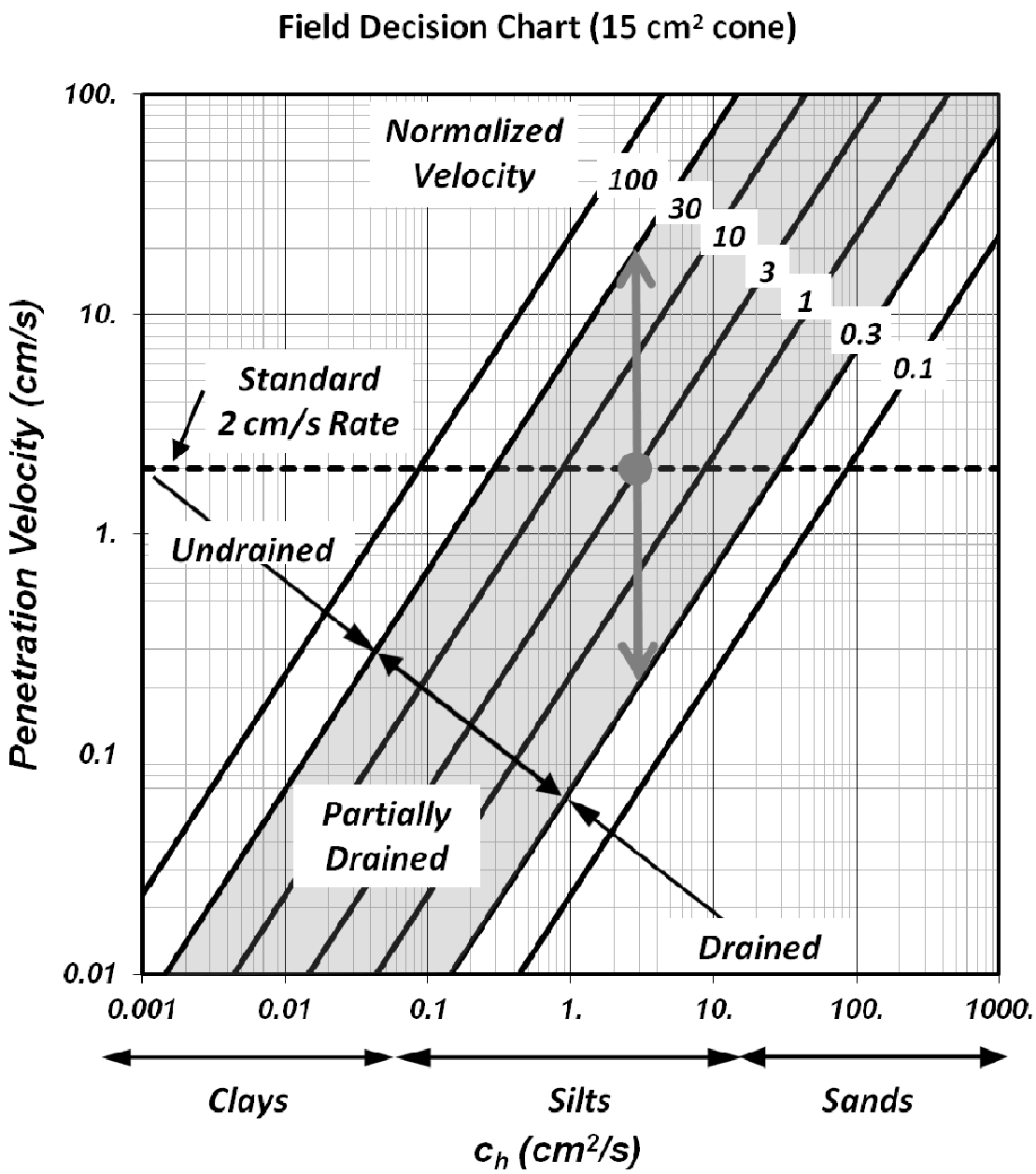

Figure 7 - Field decision chart for a 15 cm^2 cone. The gray line shows the range of penetration rates that capture partially drained behavior for a silt with c_h of 3 cm^2/s (from DeJong et al. 2012).

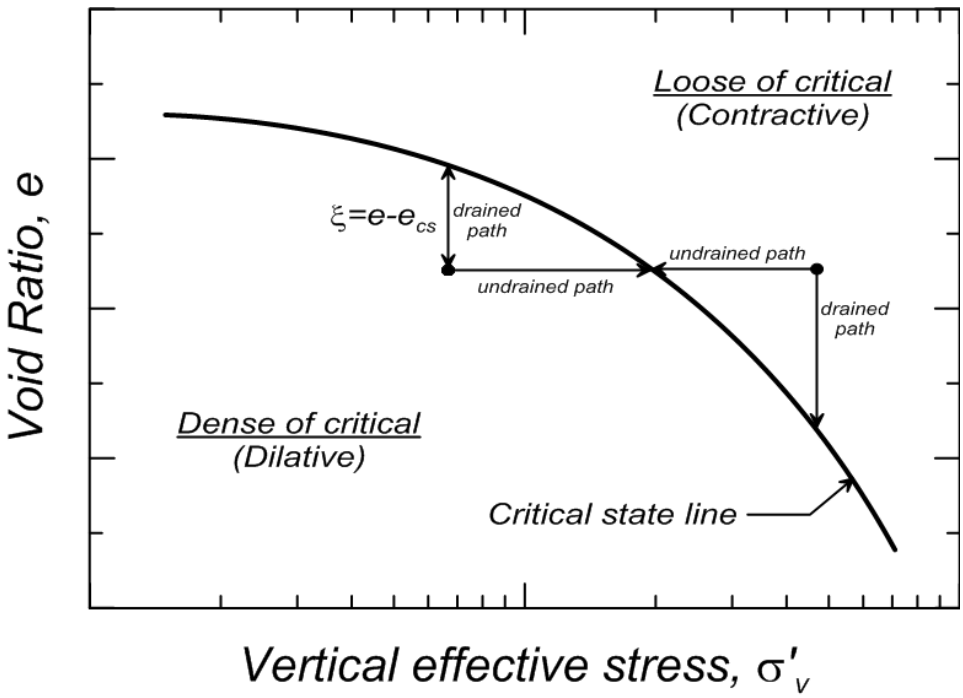

Figure 8 - The state parameter as described visually using critical state soil mechanics (after Idriss and Boulanger 2008).

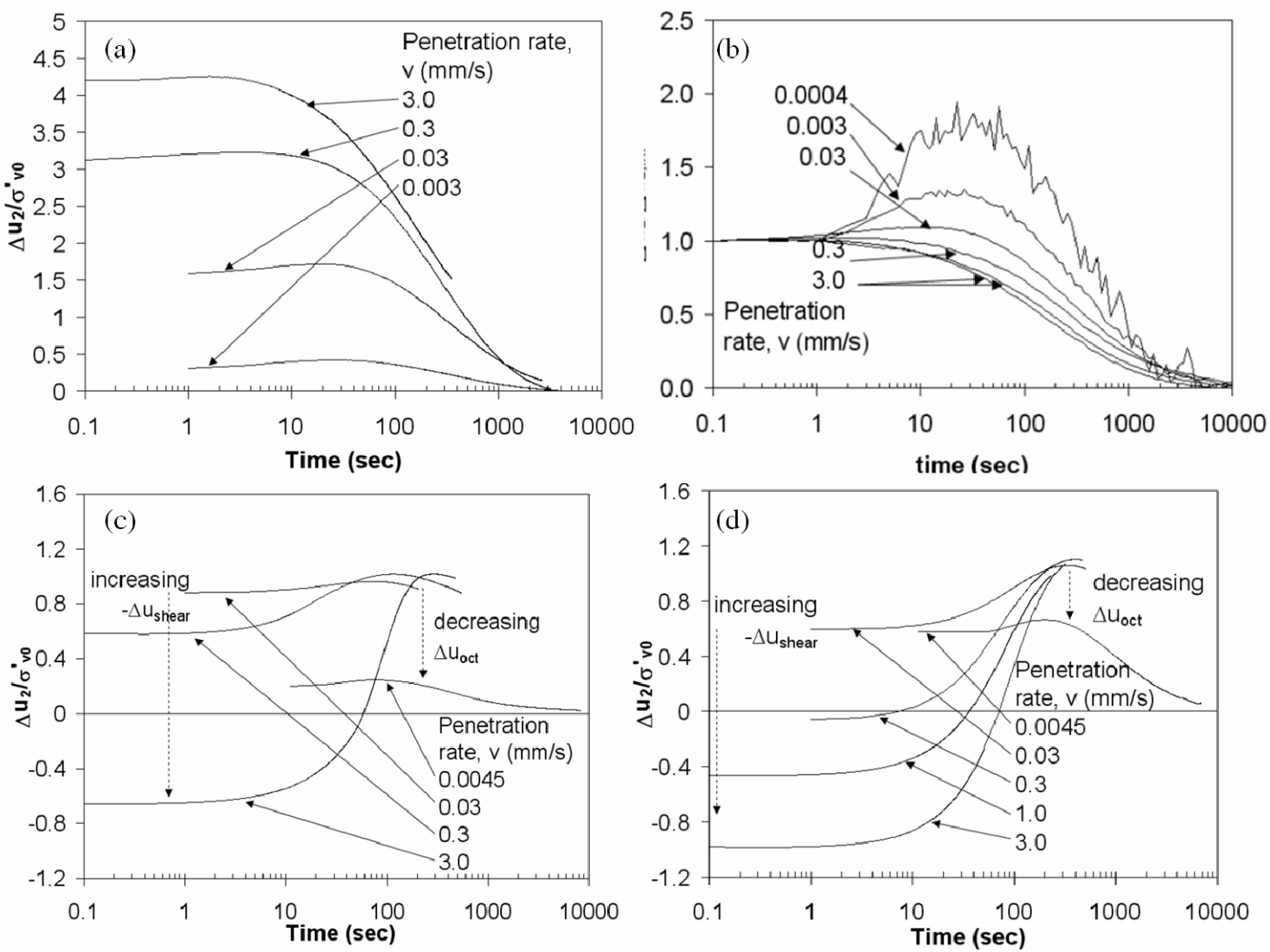

Figure 9 - Influence of penetrometer velocity on dissipation behavior in centrifuge mixtures of (a) normally consolidated kaolin clay, (b) NC kaolin normalized by $\Delta u_{2,initial}$, (c) lightly overconsolidated silica flour and bentonite, and (d) highly overconsolidated (right) (from Schneider et al. 2007).

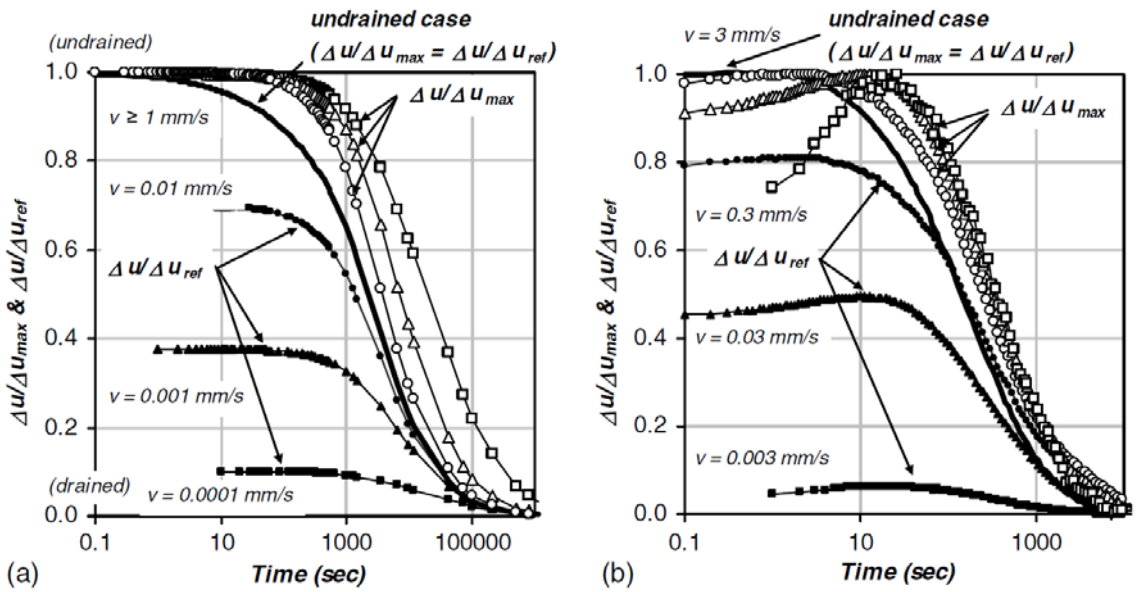

Figure 10 - Dissipation curves of normalized excess pore pressure with time: (a) numerical results from cavity expansion analysis for NC kaolin (data from Silva et al. 2006); (b) experimental data for NC kaolin (data from Schneider et al. 2007) reprinted in DeJong and Randolph (2012).

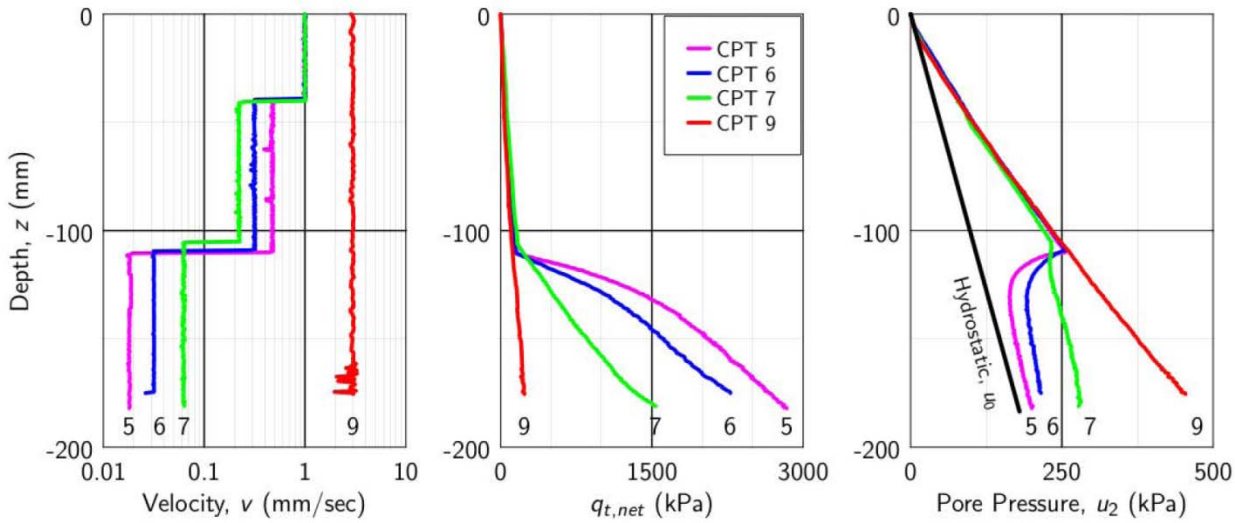

Figure 11 – Variable penetration rate cone penetration tests in 75% sand, 25% kaolin mixture centrifuge test (from Jaeger et al. 2010).

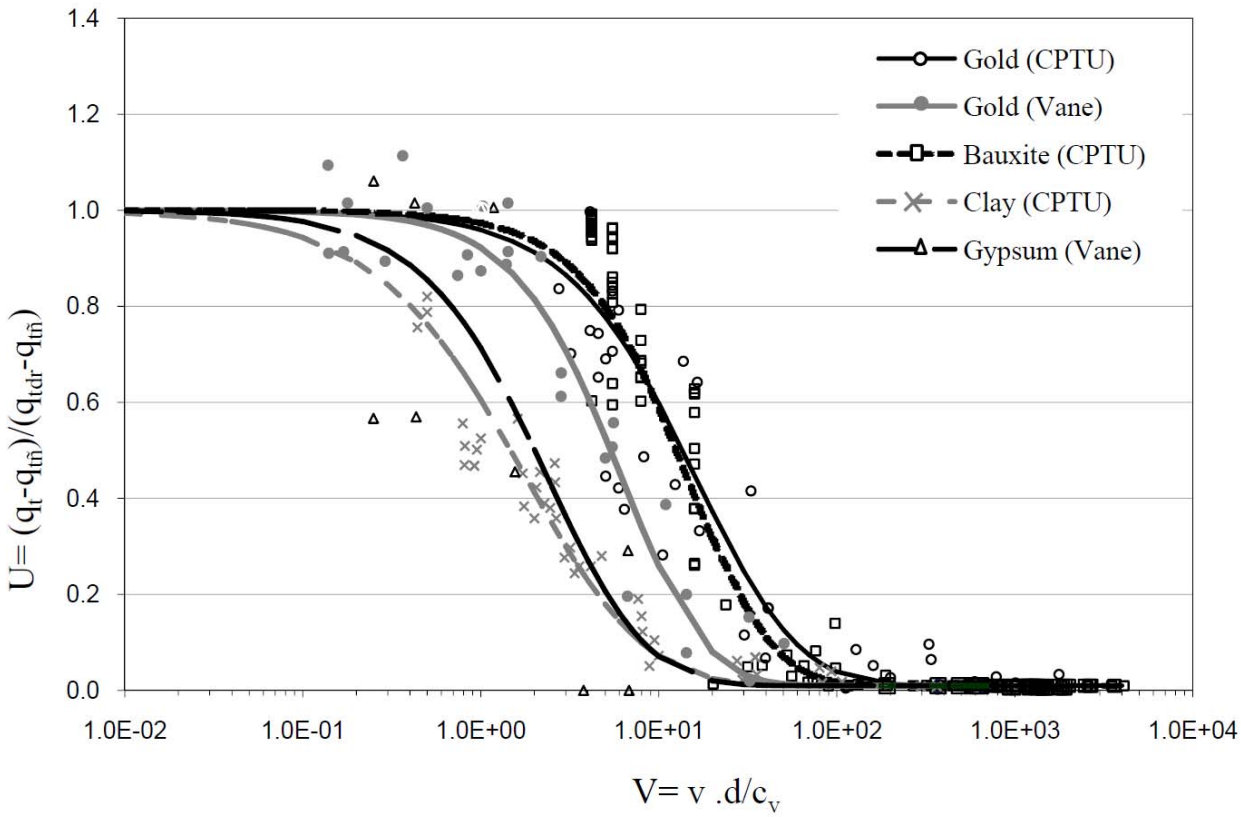

Figure 12 - Normalized drainage characteristic curve for variable penetration rates in a range of geo-materials (from Schnaid et al. 2010).

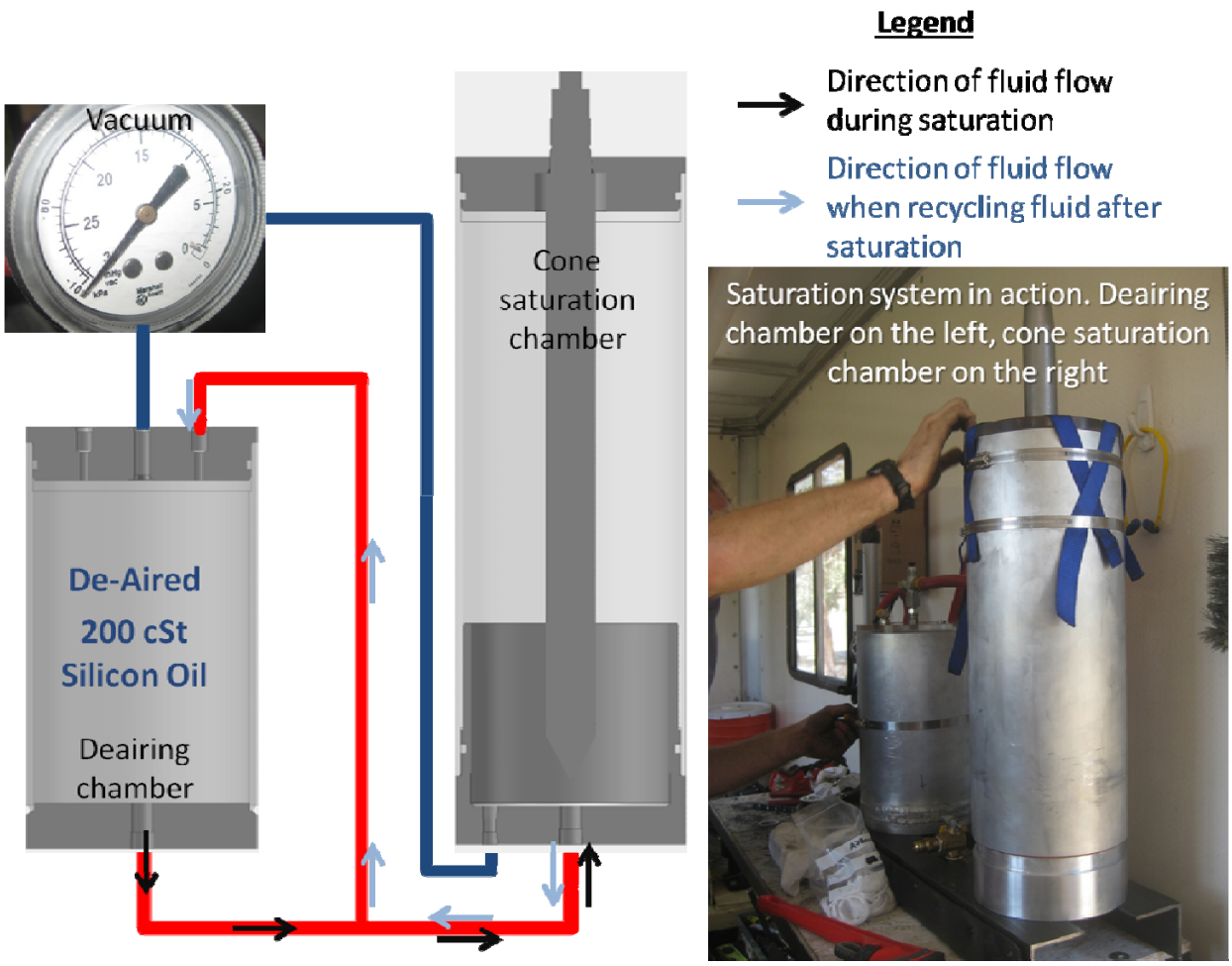

Figure 13 - Saturation chamber developed for this study to ensure proper cone filter saturation.

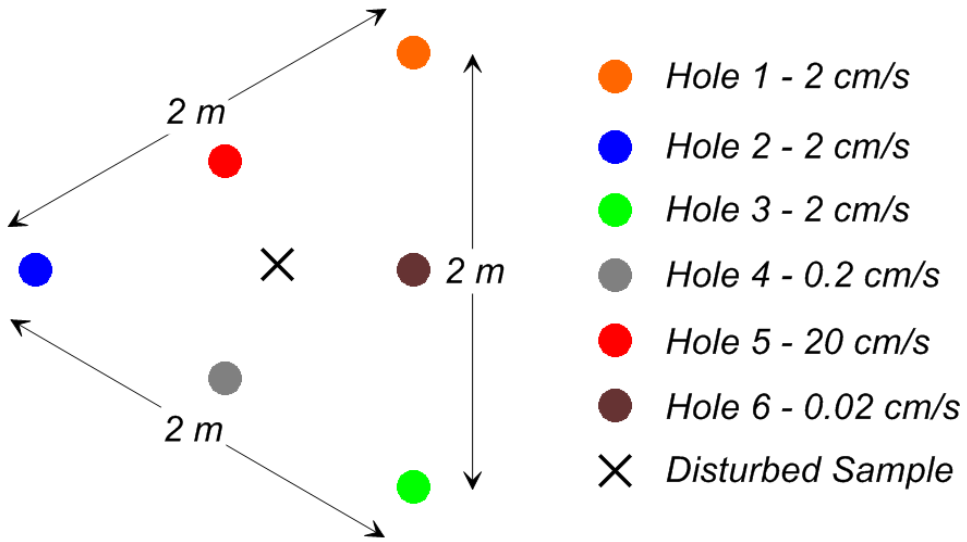

Figure 14 - Example test layout used at each test site.

Figure 15 - Disturbed Cone Sampler on loan from USGS. The sampler is pushed like a typical cone, however upon reaching the target sampling depth, the sampler is stopped and then the tip is retracted 10 inches. Sleeve friction holds the body of the cone in place while ball bearings are used to engage a locking mechanism, revealing a cylindrical cavity within the sampler. The sampler is then pushed an additional 10 inches to fill the cavity with soil.

Figure 16- Aerial Photograph of Granite Construction 123 taken on 10/20/1989, only 3 days after the main event. Note that the building just north of 124 has since been demolished. Sand boils are present throughout the region and boring 123 is located immediately upon sand boil ejecta (image from the USGS).

Figure 17 - Aerial photography of the Lenordini site (with boring 51 highlighted) taken on 10/20/1989, only 3 days after the main event. Variable rate tests were performed along the farm access road at this location (image from the USGS).

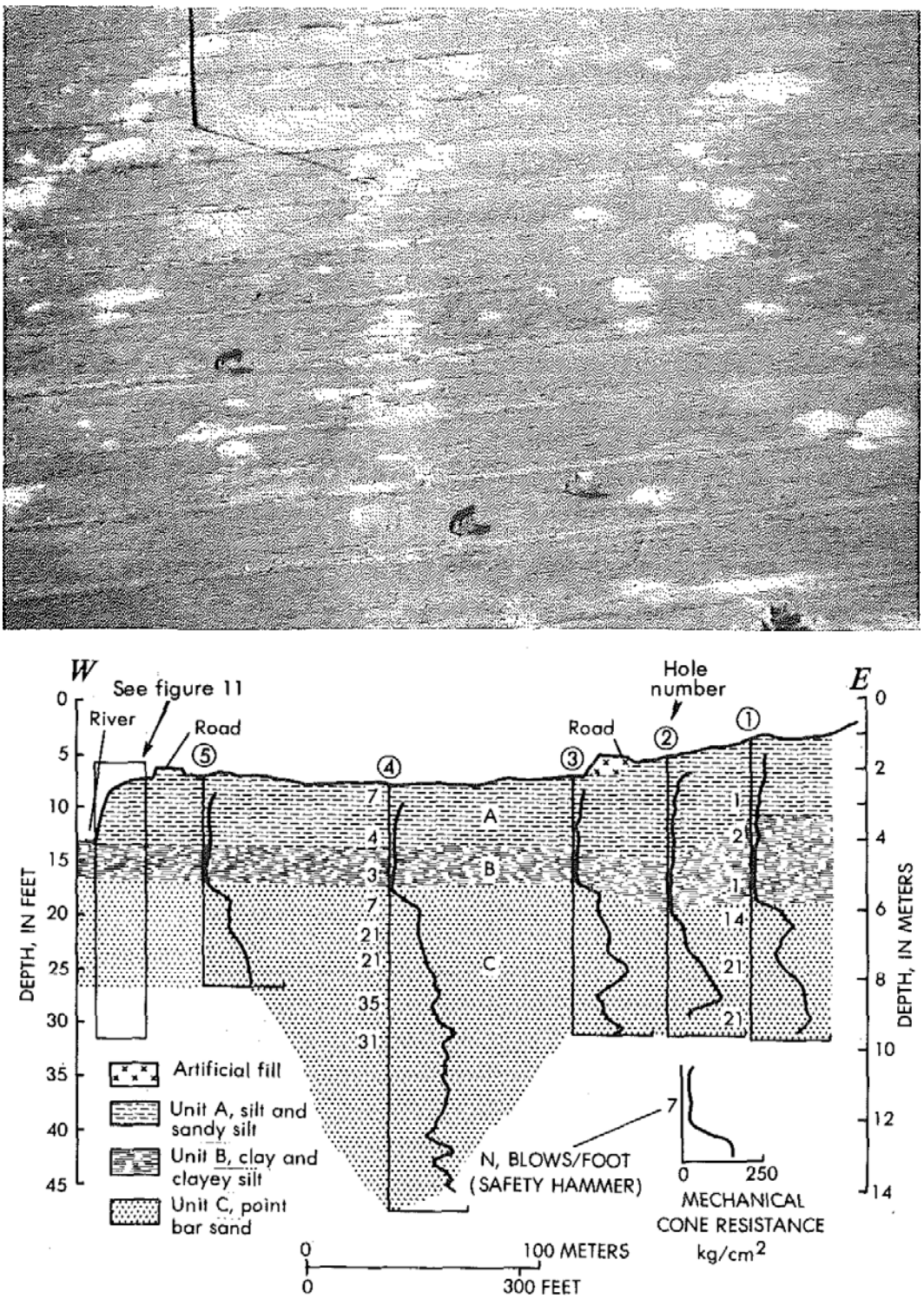

Figure 18 - Sand boils present at River Park immediately following the 1979 Imperial Valley earthquake (top) and a geologic cross section of soil deposits. Note that the Unit A and the top of Unit C are believed to have liquefied during the same event (from Youd and Bennett 1981). Tests performed in this study near CPT-5.

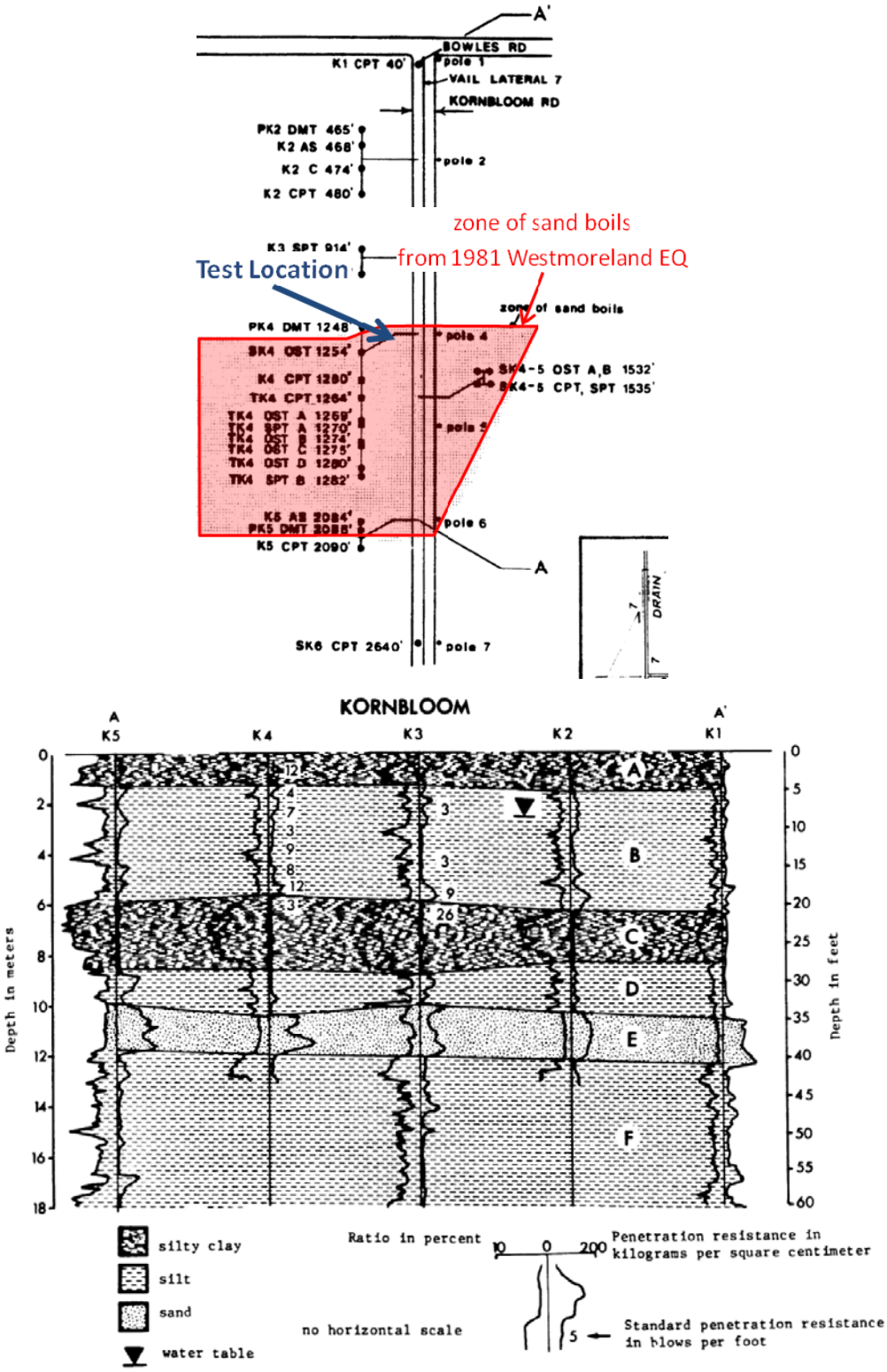

Figure 19 - Map of the Kornbloom study area (top). Note the widespread presence of sand boils from the 1981 Westmoreland event. Kornbloom geologic cross section (below). Note that Unit B is believed to have liquefied during the 1981 Westmoreland earthquake (from Bennett et al. 1984).

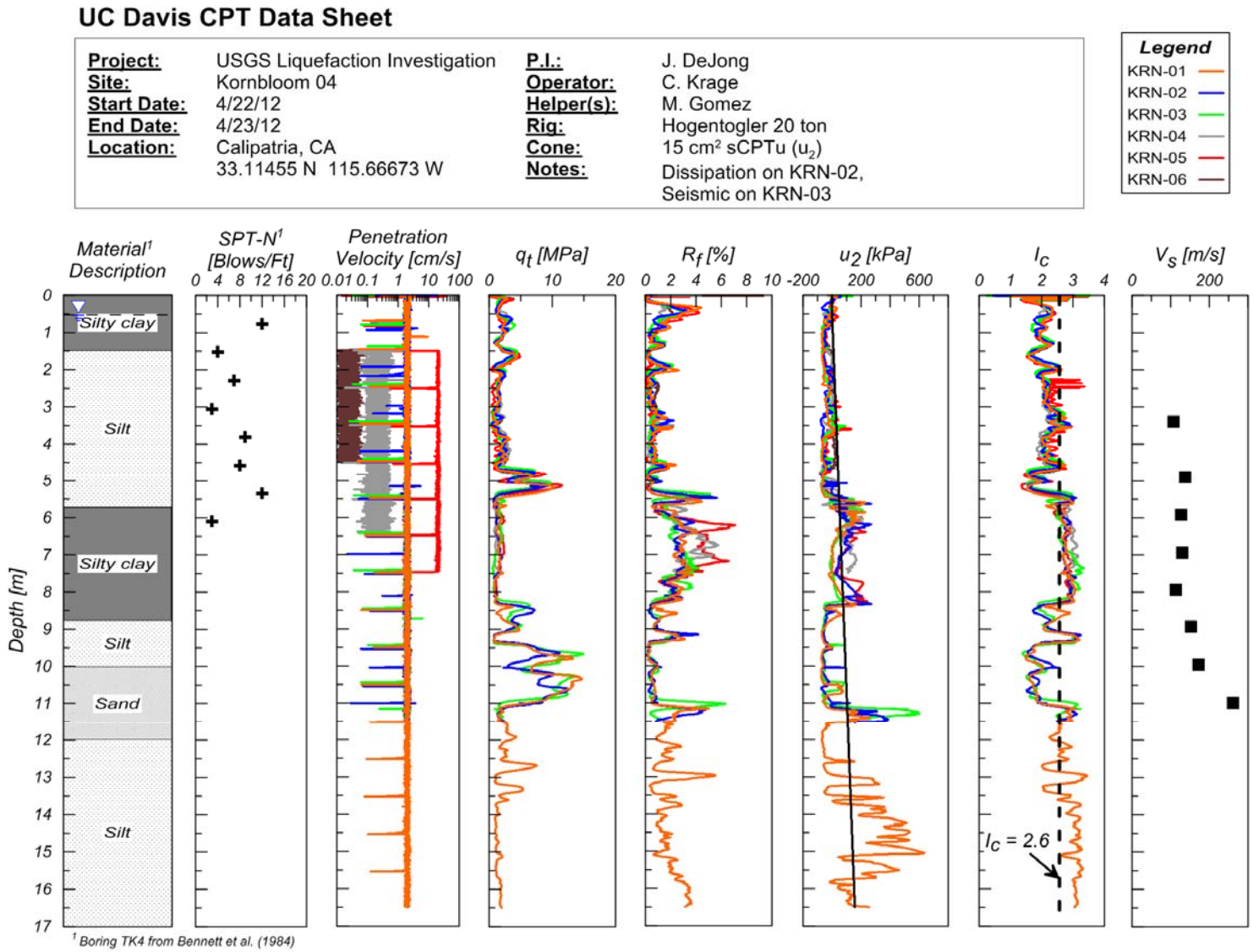

Figure 20 - Summary of variable penetration rate cone tests at Kornbloom.

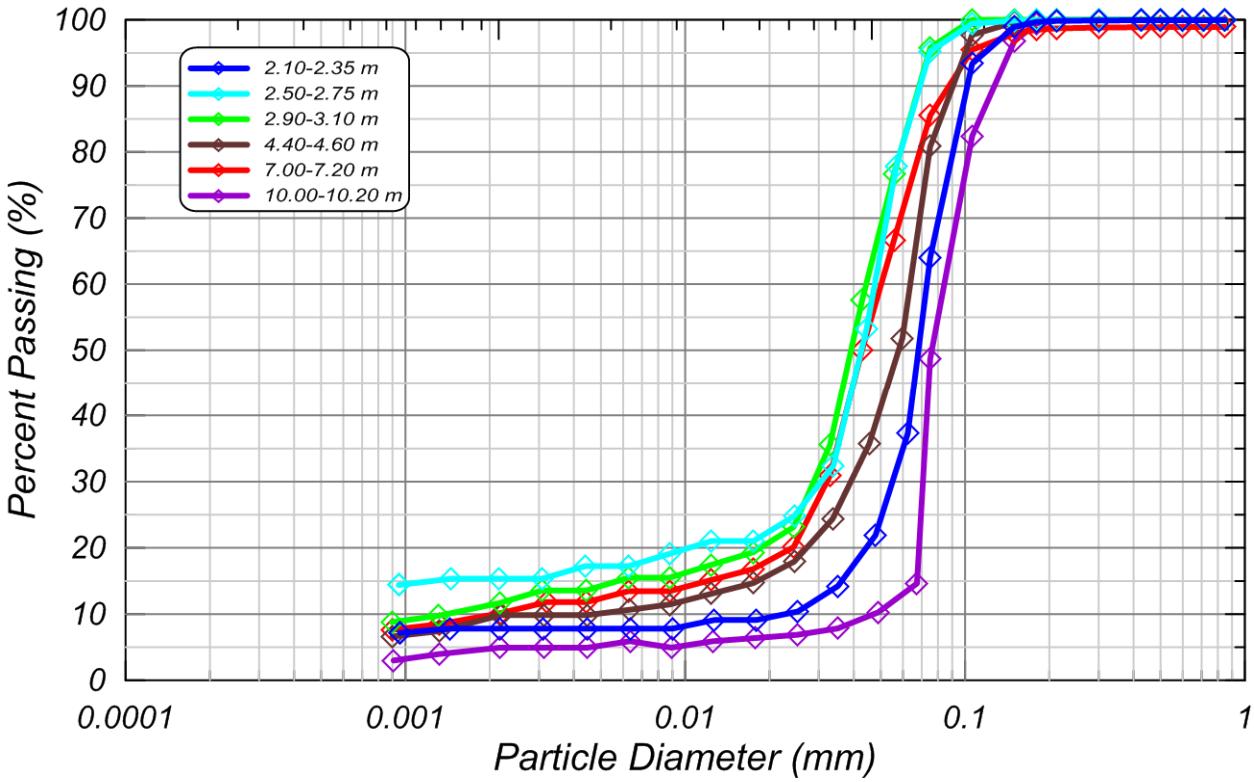

Figure 21 - Grain size distributions for the 6 Kornbloom samples obtained for this study. Depth intervals are shown in the figure legend.

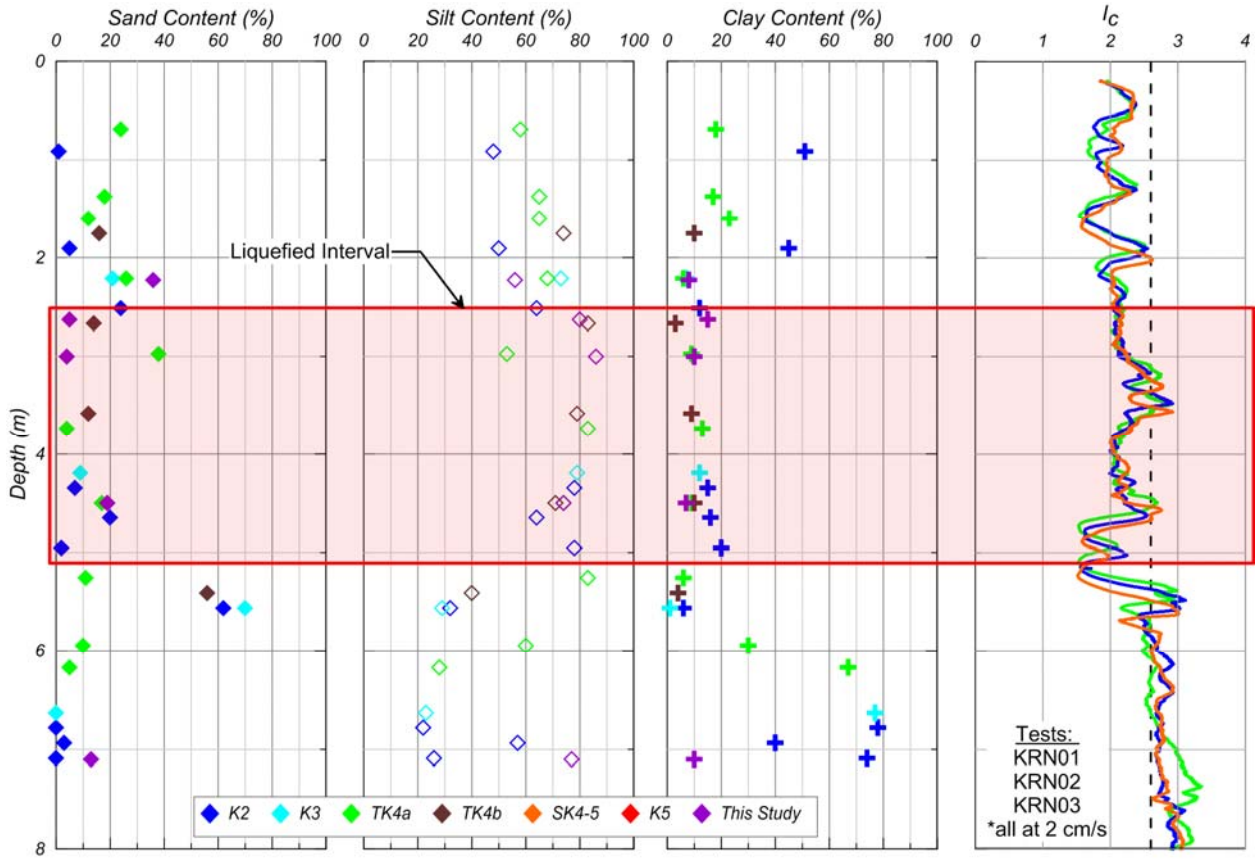

Figure 22 - Summary of samples obtained at the Kornbloom site (data from Bennett et al. 1984 and this study).

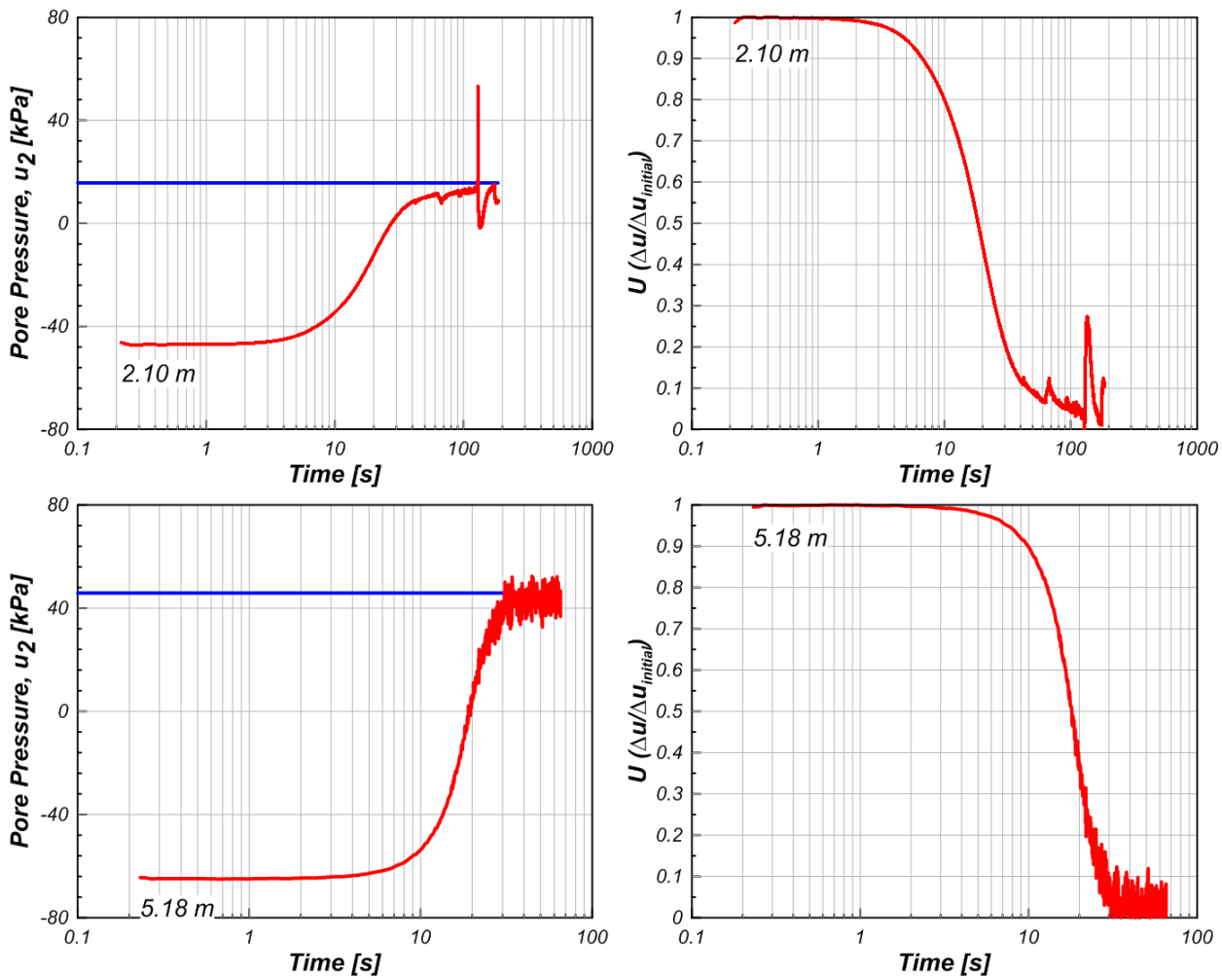

Figure 23 - Dissipation results for Kornbloom Unit B.

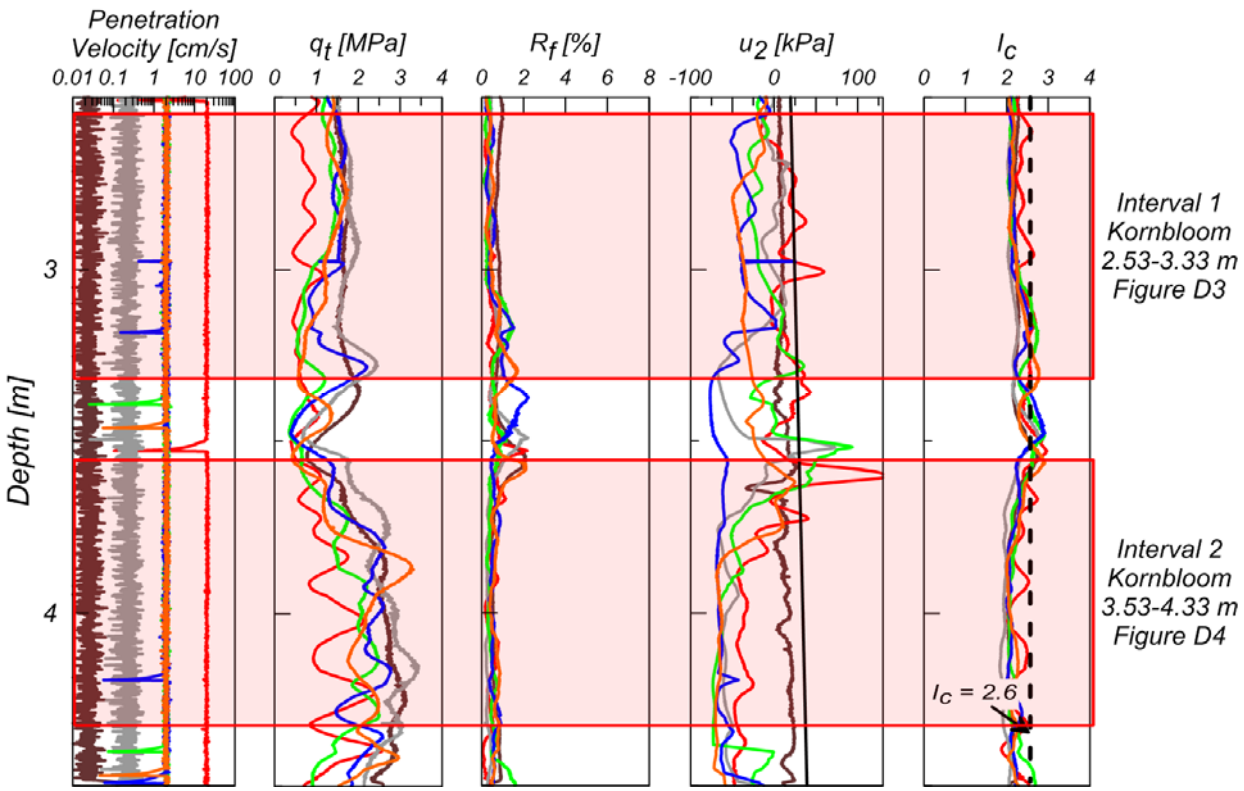

Figure 24 - Selected intervals for rate analysis within Kornbloom Unit B.

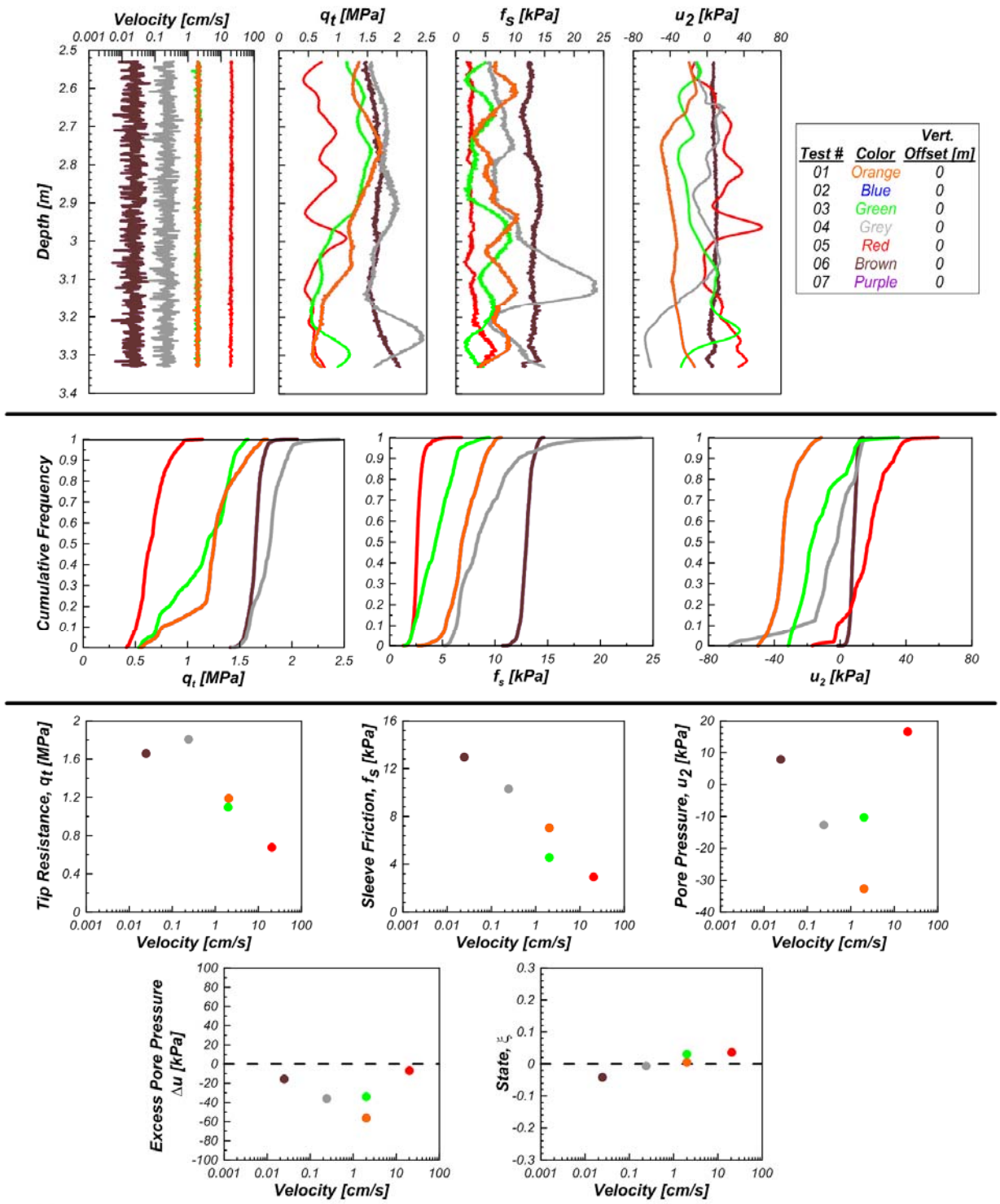

Soil Interactions Laboratory UCDAVIS	CPK	Variable Penetration Rate Interval Summary	Site	Kornbloom			Fig. 23
			Interval	1	Range [m]	2.53 - 3.33	

Figure 25 - Interval summary for Kornbloom depth range of 2.53 to 3.33 m.

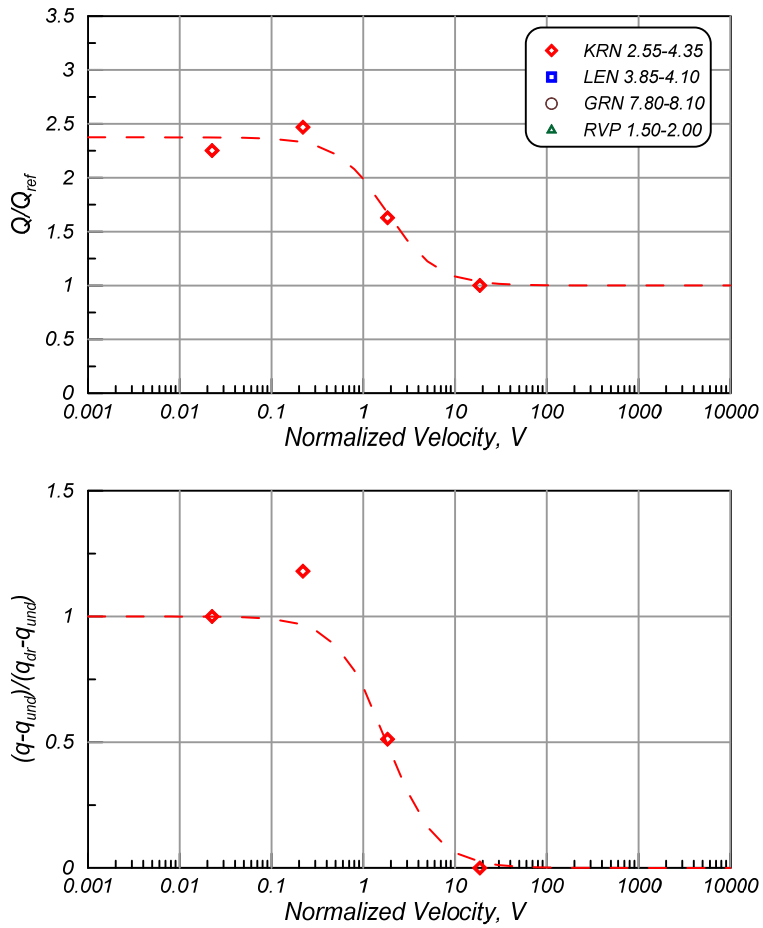

Figure 26 - Q/Q_{ref} behavior and drained to undrained normalization for Kornbloom Unit B.

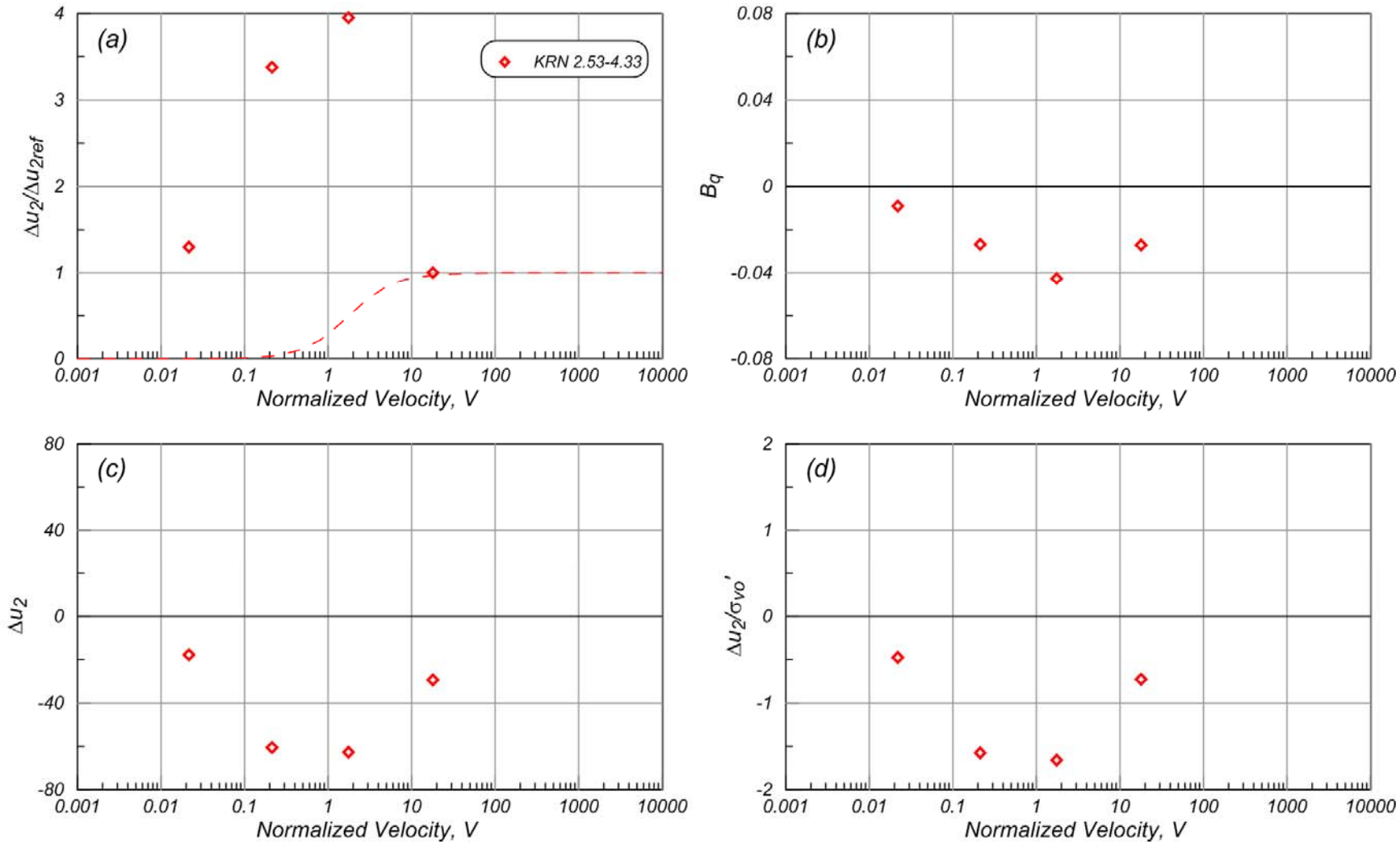

Figure 27 - Pore pressure behavior for Kornbloom Unit B.

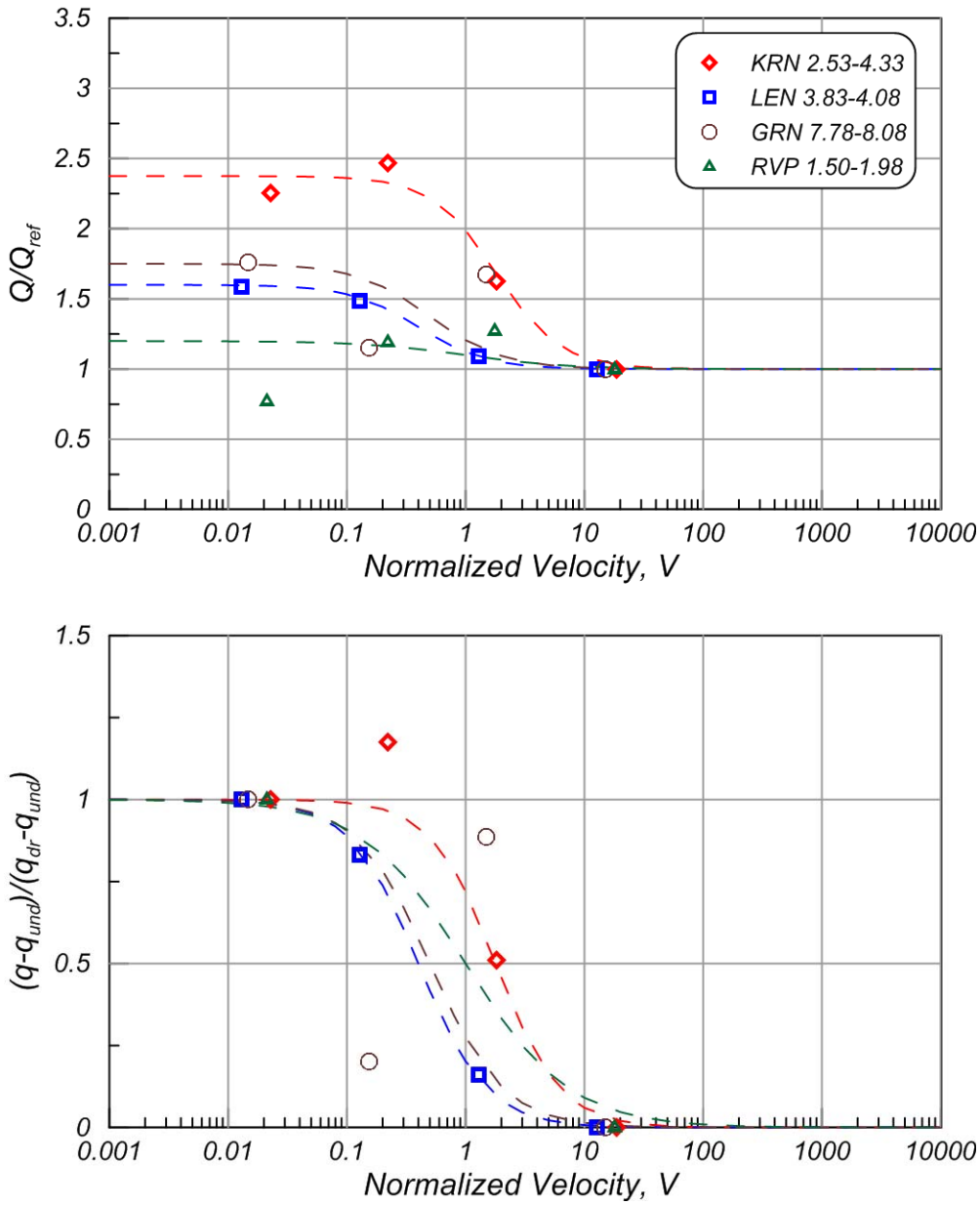

Figure 28 - Q/Q_{ref} behavior (top) and drained to undrained normalization (bottom) for the selected subintervals for each site.

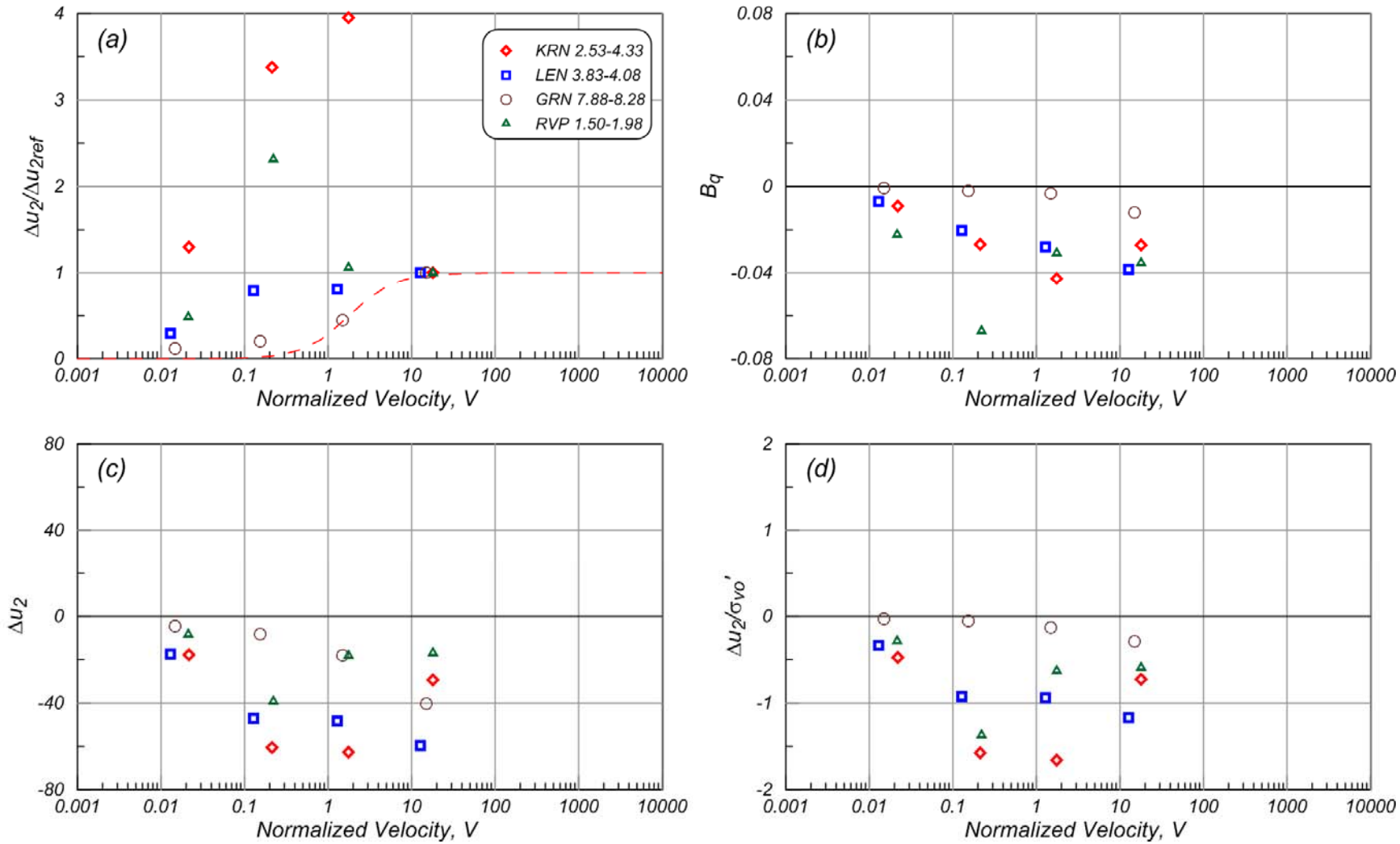

Figure 29 - Pore pressure behavior for all sites.

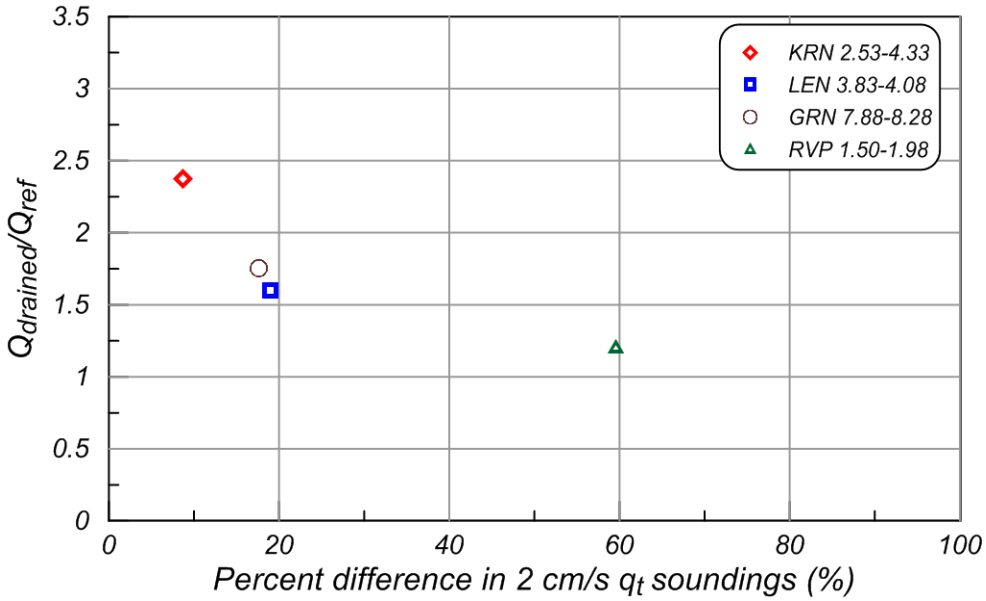

Figure 30 - $Q_{drained}/Q_{ref}$ shown versus percent difference between mean values of q_t for the selected subinterval for two different standard penetration rate soundings.

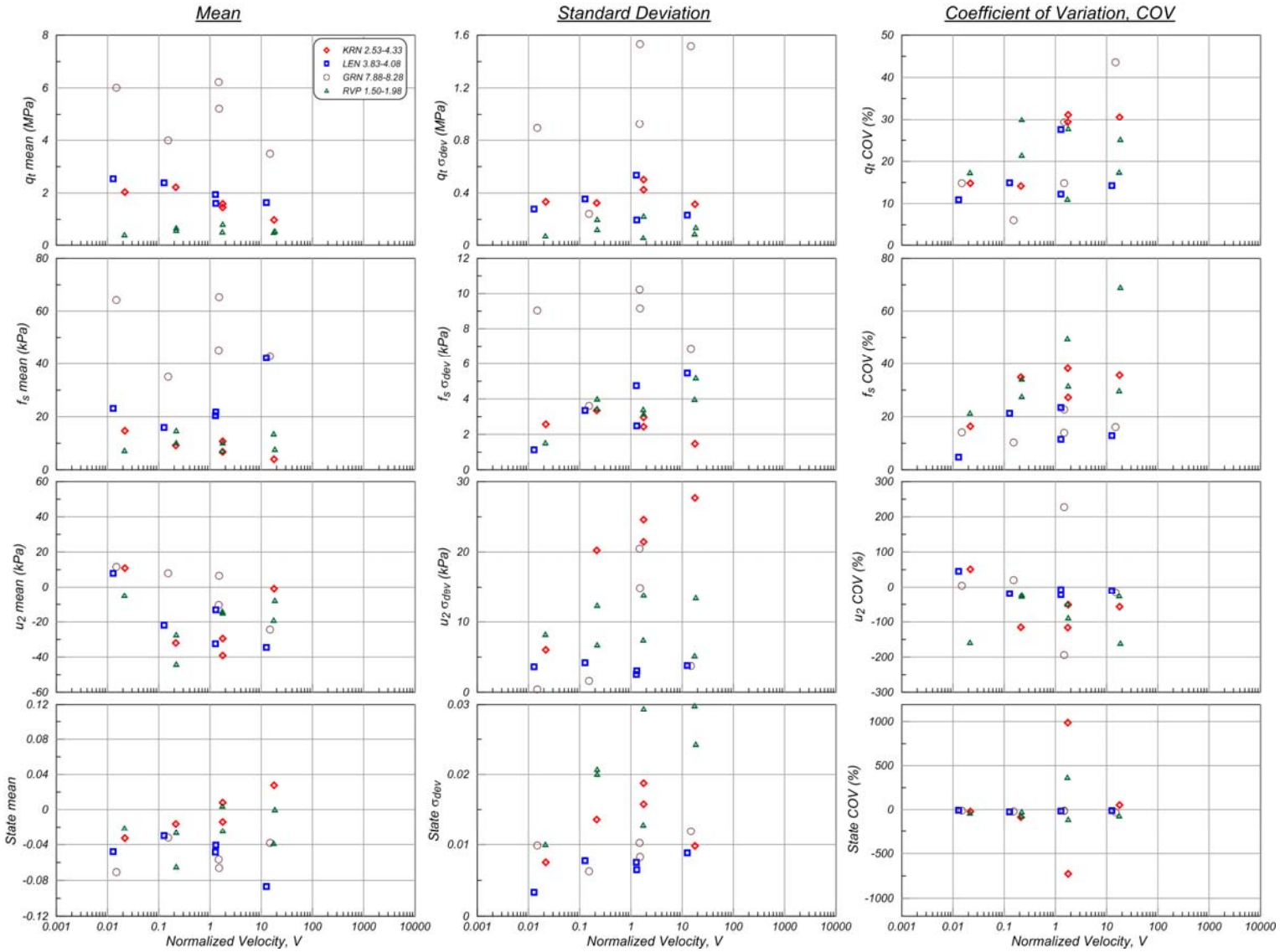

Figure 31 - Summary of mean, standard deviation and coefficient of variation (COV) values for each sensor measurement (q_t, f_s, u_2) and state estimation versus normalized velocity for selected subintervals for each site.

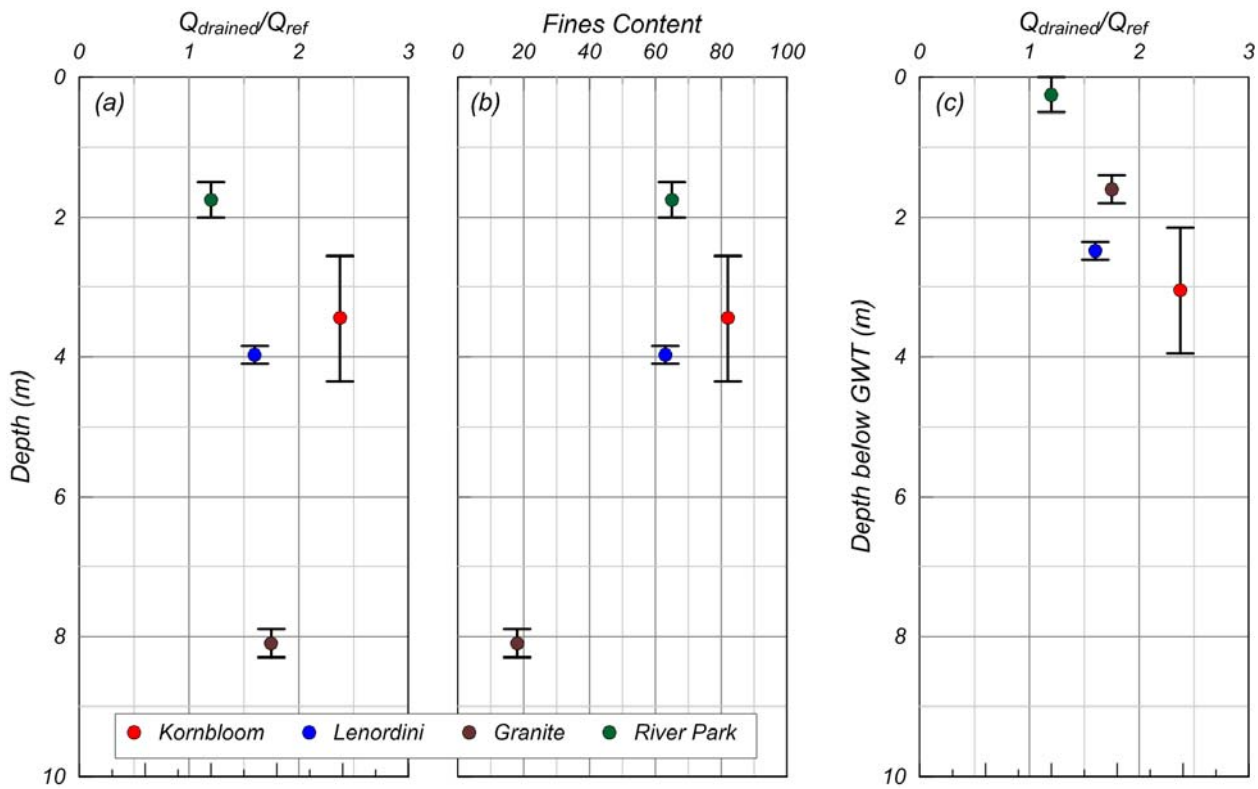

Figure 32 - Trends of (a) $Q_{drained}/Q_{ref}$ and (b) fines content versus depth and (c) $Q_{drained}/Q_{ref}$ versus depth below the ground water table. Symbols signify median depth, while the bars present signify the entire subinterval selected for analysis.

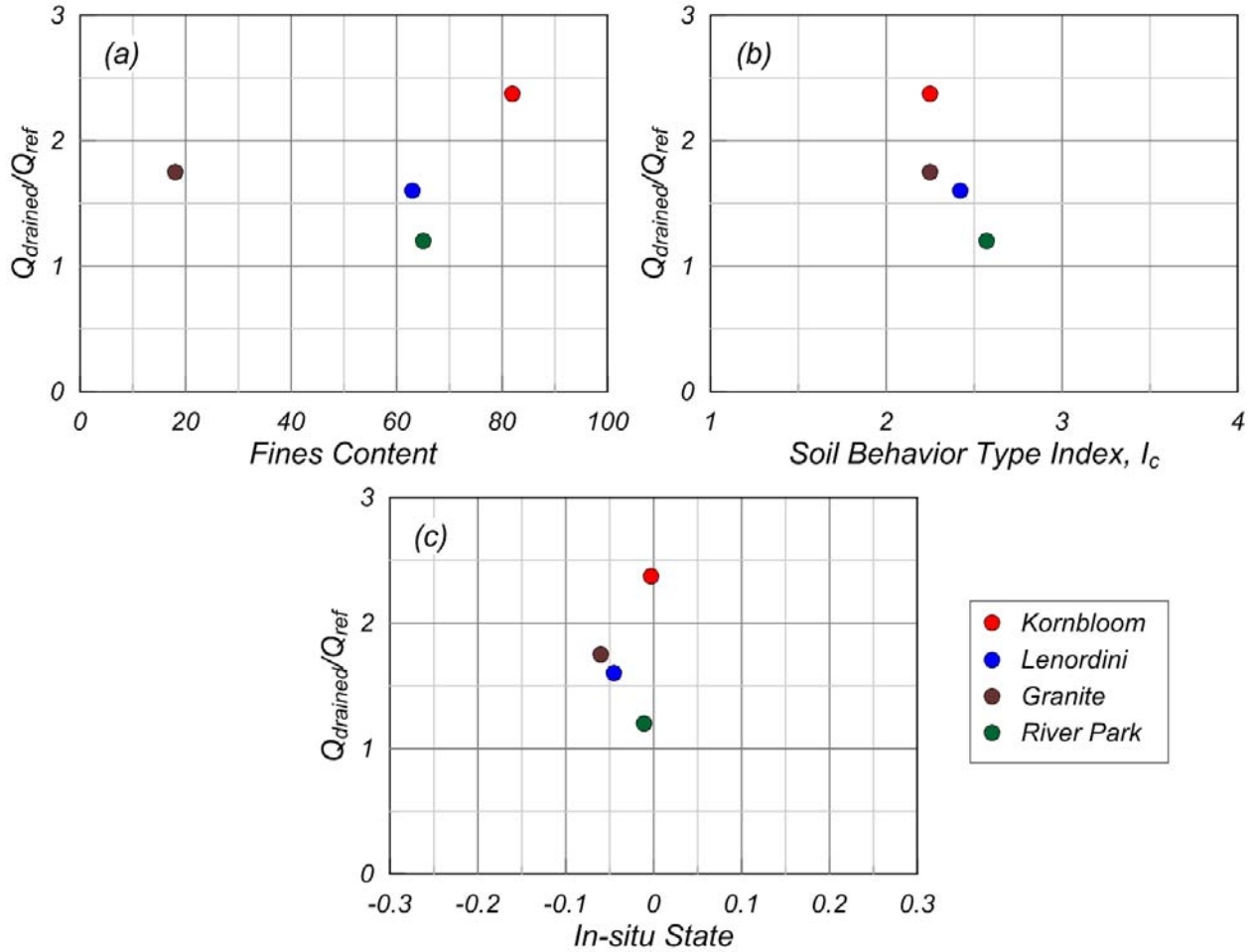

Figure 33 - Trends of $Q_{drained}/Q_{ref}$ vs. fines content, I_c, and in-situ state.

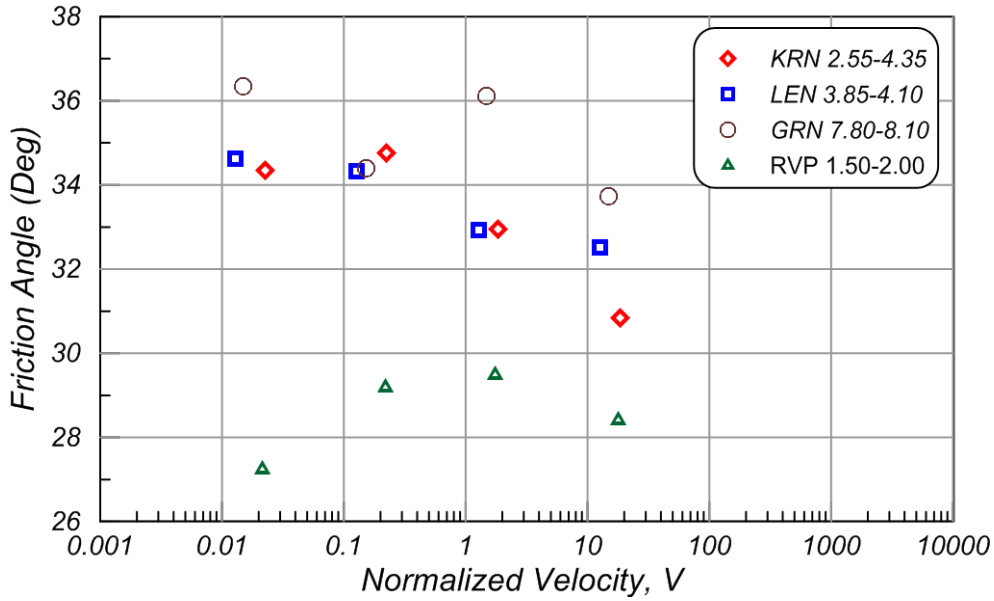

Figure 34 - Trends of friction angle estimates for different normalized velocities following the Mayne (2007) framework.

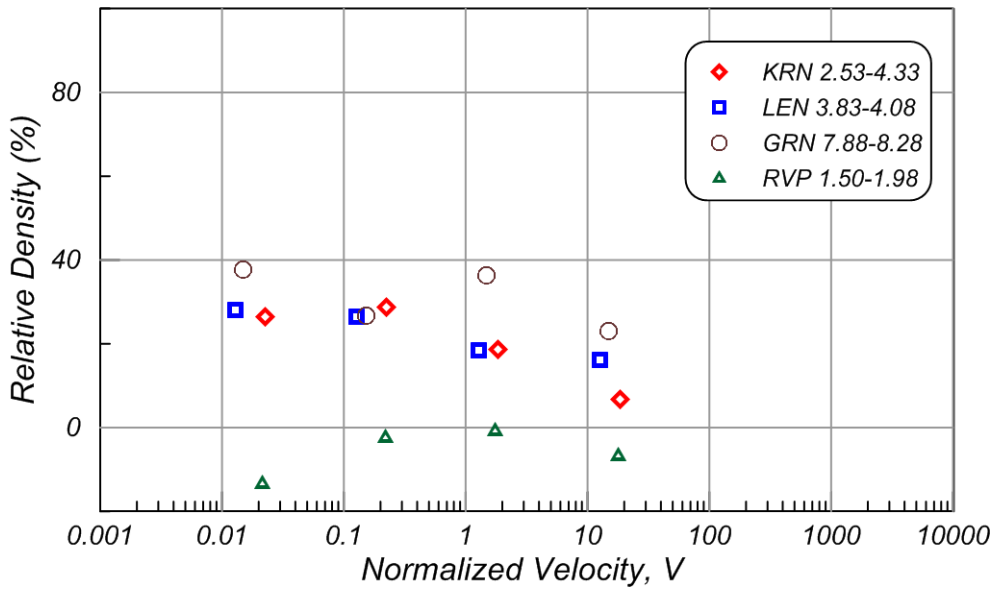

Figure 35 - Trends of relative density estimates for different normalized velocities following the Jamiolkowski et al. (2001) framework.

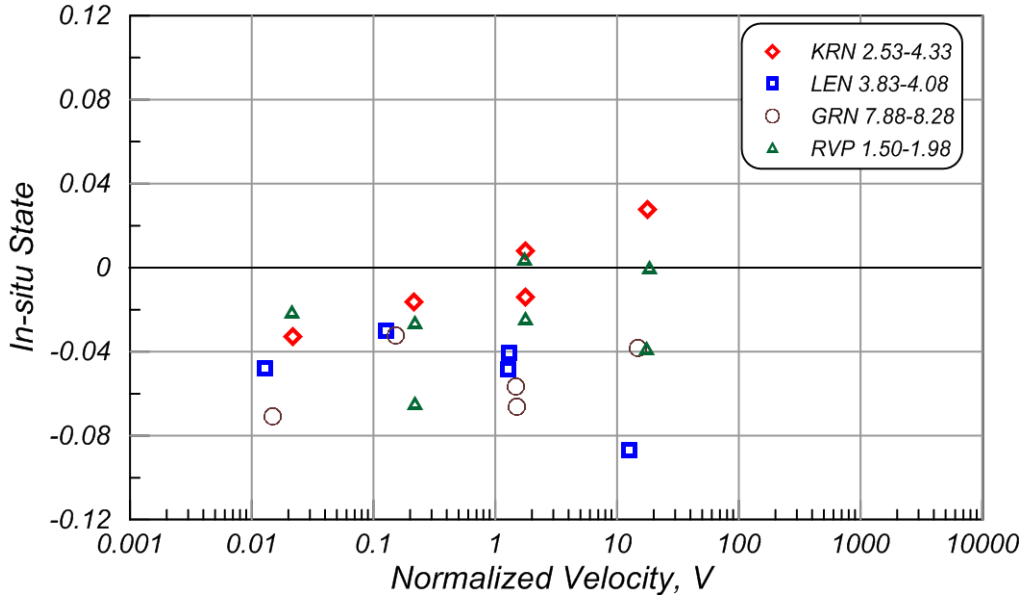

Figure 36 - Trends in state parameter estimates using Robertson (2010).

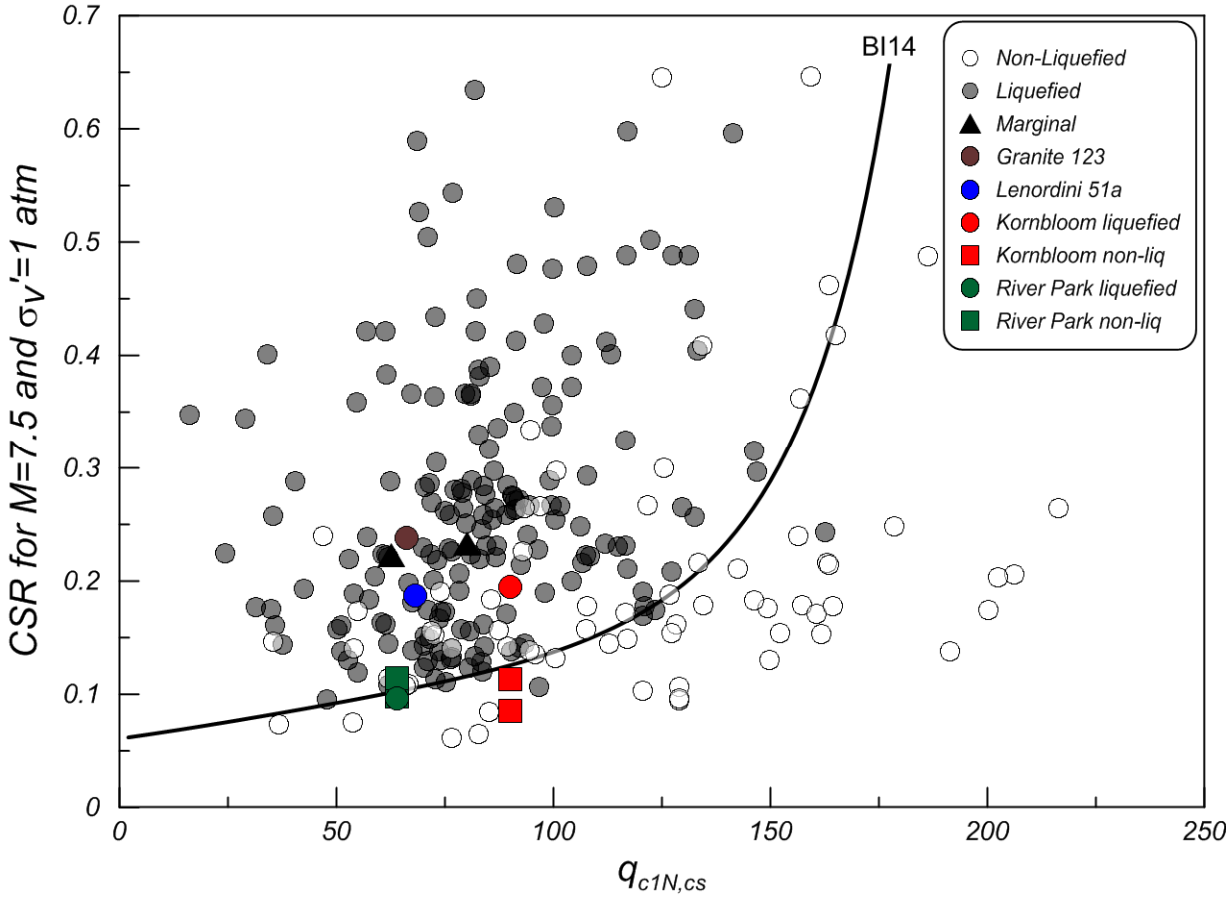

Figure 37 - Location of sites in Boulanger and Idriss (2014) triggering relationship. Note that River Park (green symbols) was not included in the original database.

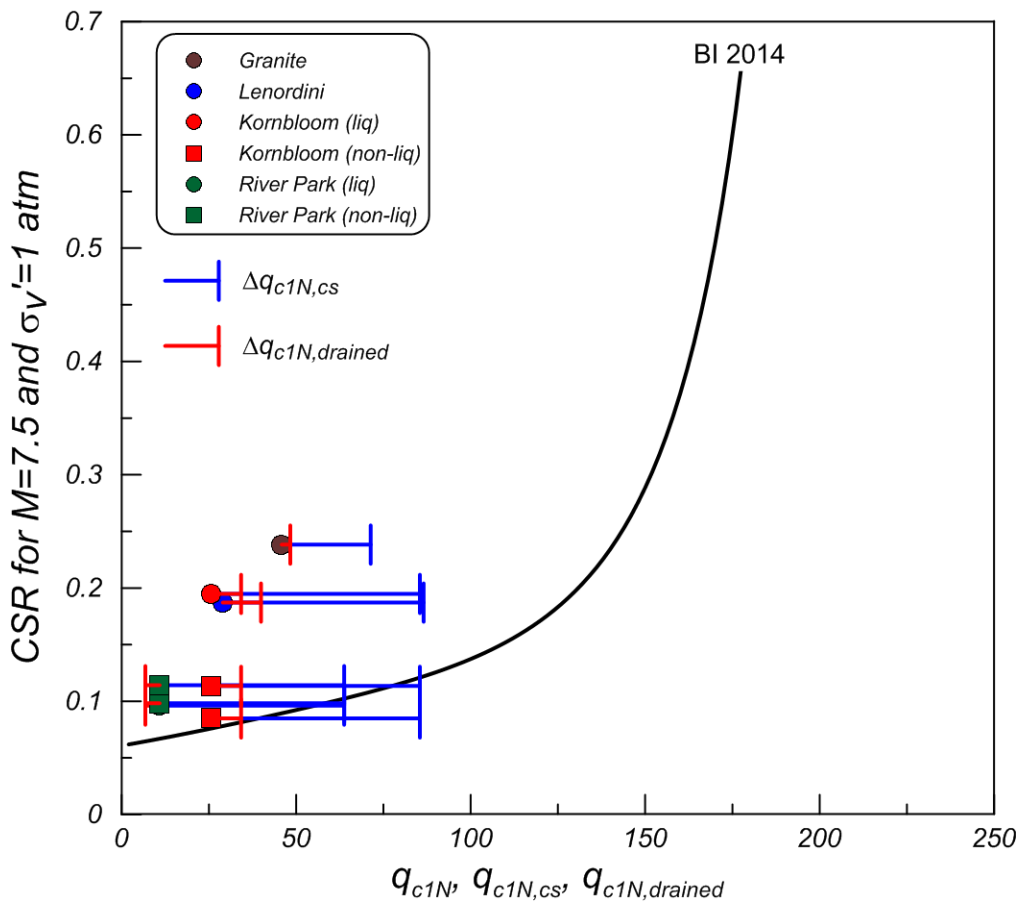

Figure 38 - Comparison between drained and clean sand corrections for selected subintervals. Symbols represent q_{c1N} values, horizontal blue lines represent Δq_{c1N} correction with vertical blue lines at q_{c1Ncs}, and horizontal red lines represent $\Delta q_{c1N,drained}$ correction with vertical red lines at $q_{c1N,drained}$.

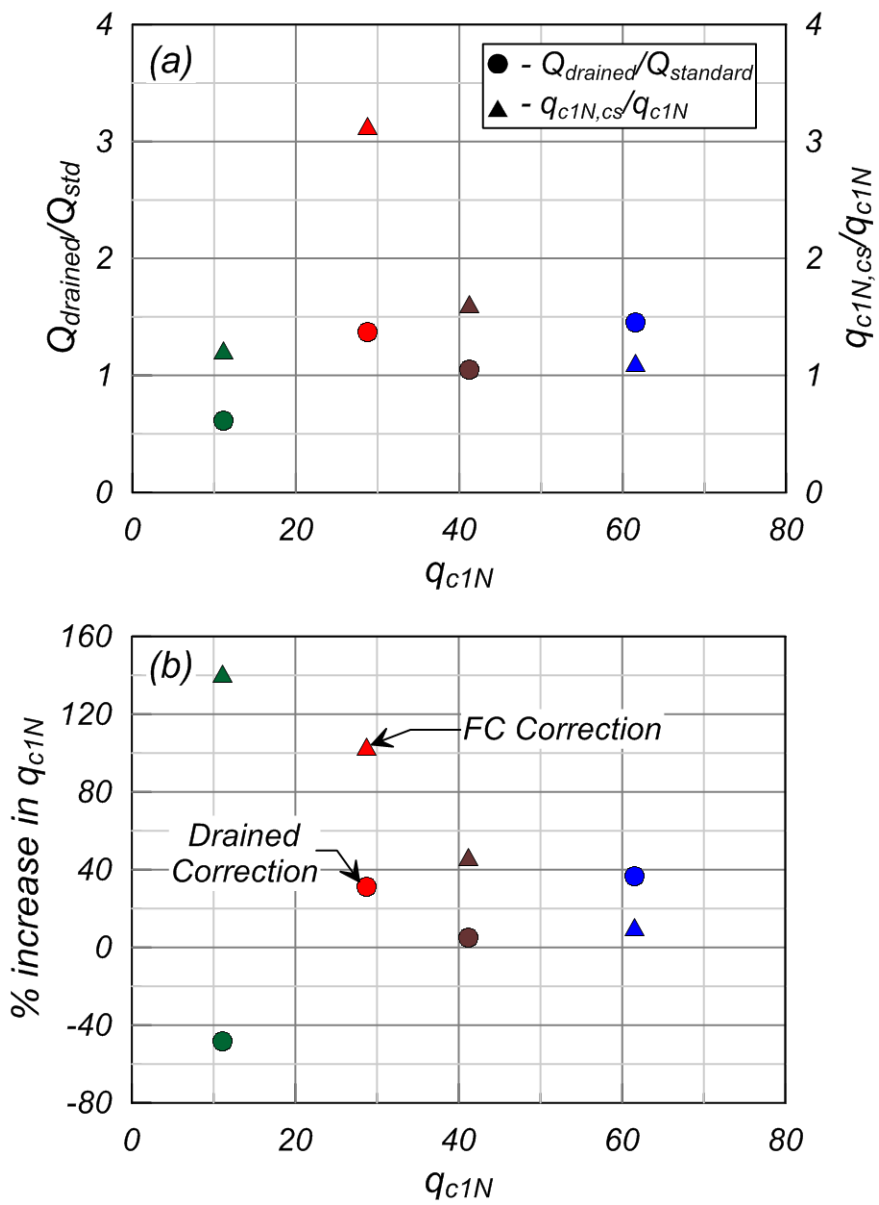

Figure 39 - Difference between Boulanger and Idriss (2014) correction and the $\Delta q_{c1N,drained}$ correction

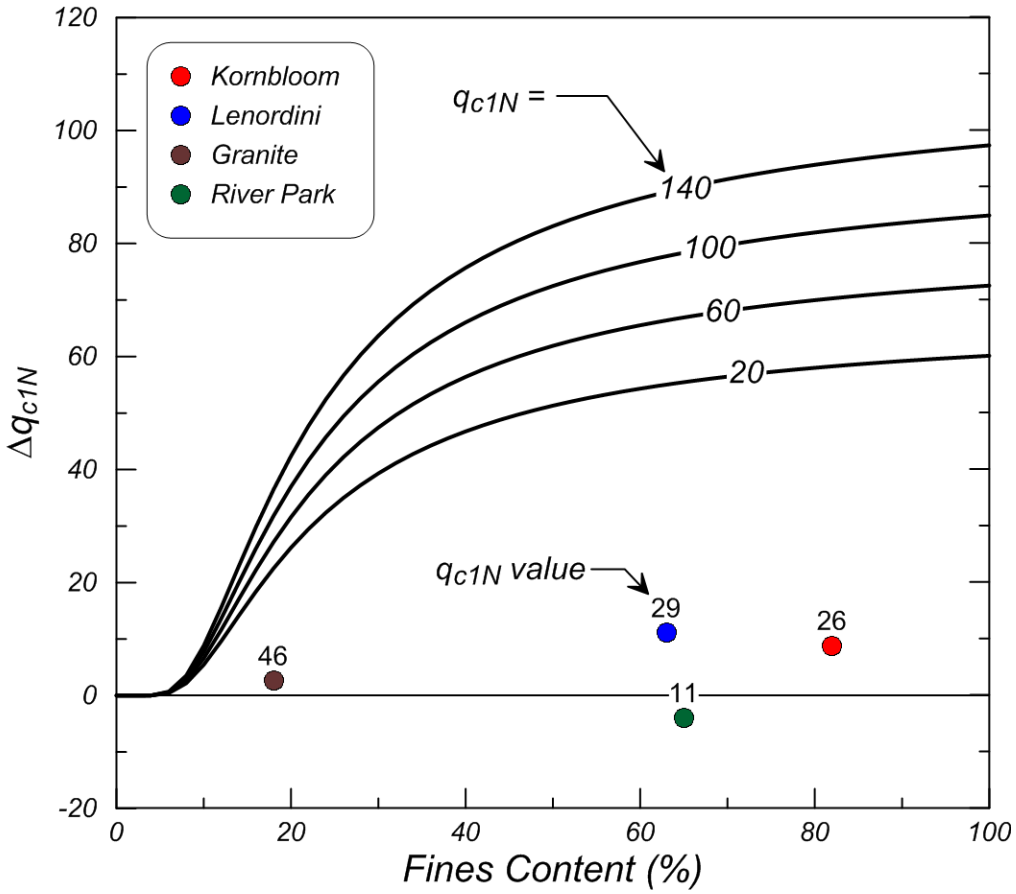

Figure 40 - Plot showing the empirical Δq_{c1N} correction proposed by Boulanger and Idriss (2014) where circular symbols represent $\Delta q_{c1N,drained}$ correction. Actual Δq_{c1N} can be inferred from qc1N values for each site.

APPENDIX A - GRANITE CONSTRUCTION SUPPLEMENTARY FIGURES

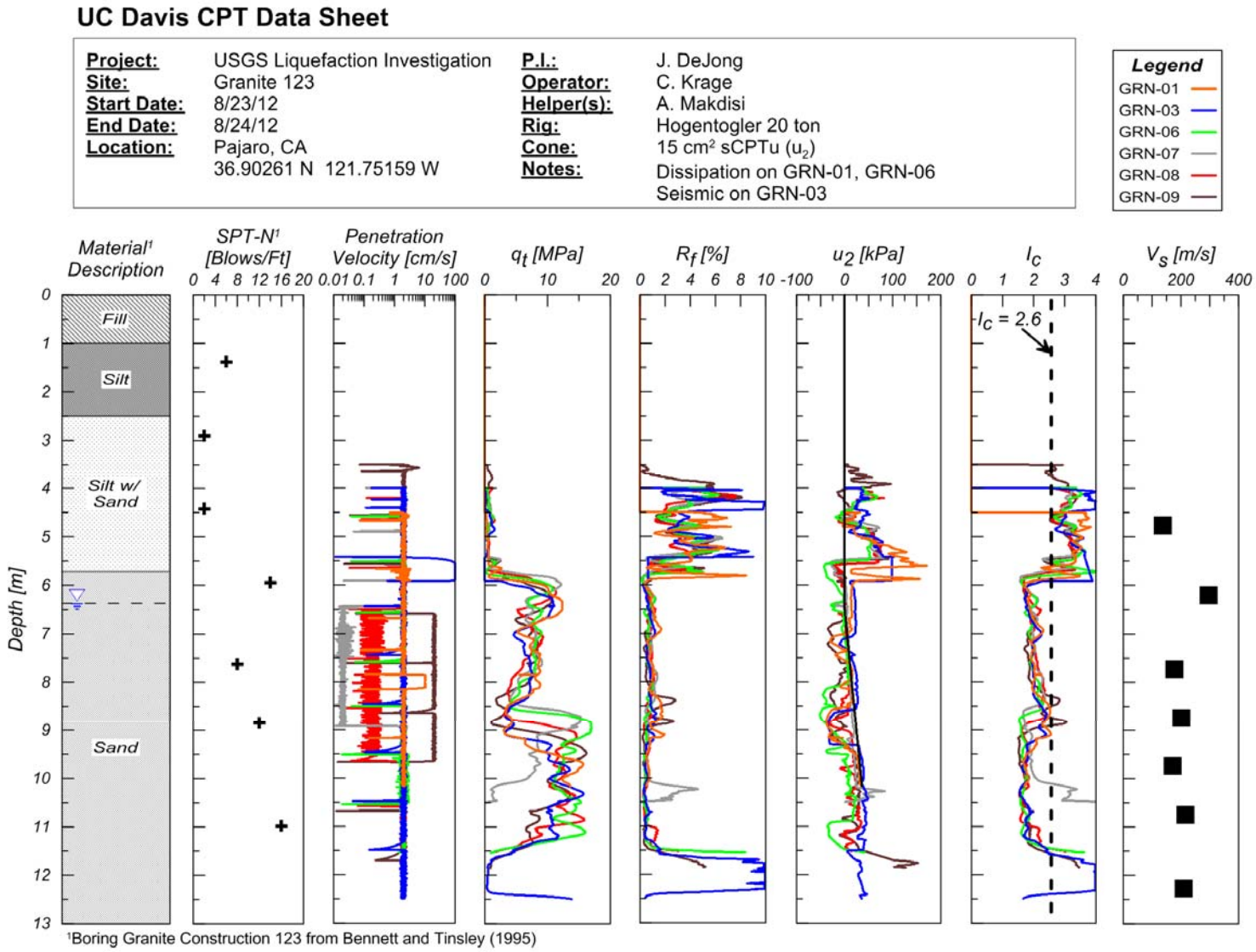

Figure A1 - Summary of variable penetration rate soundings at Granite.

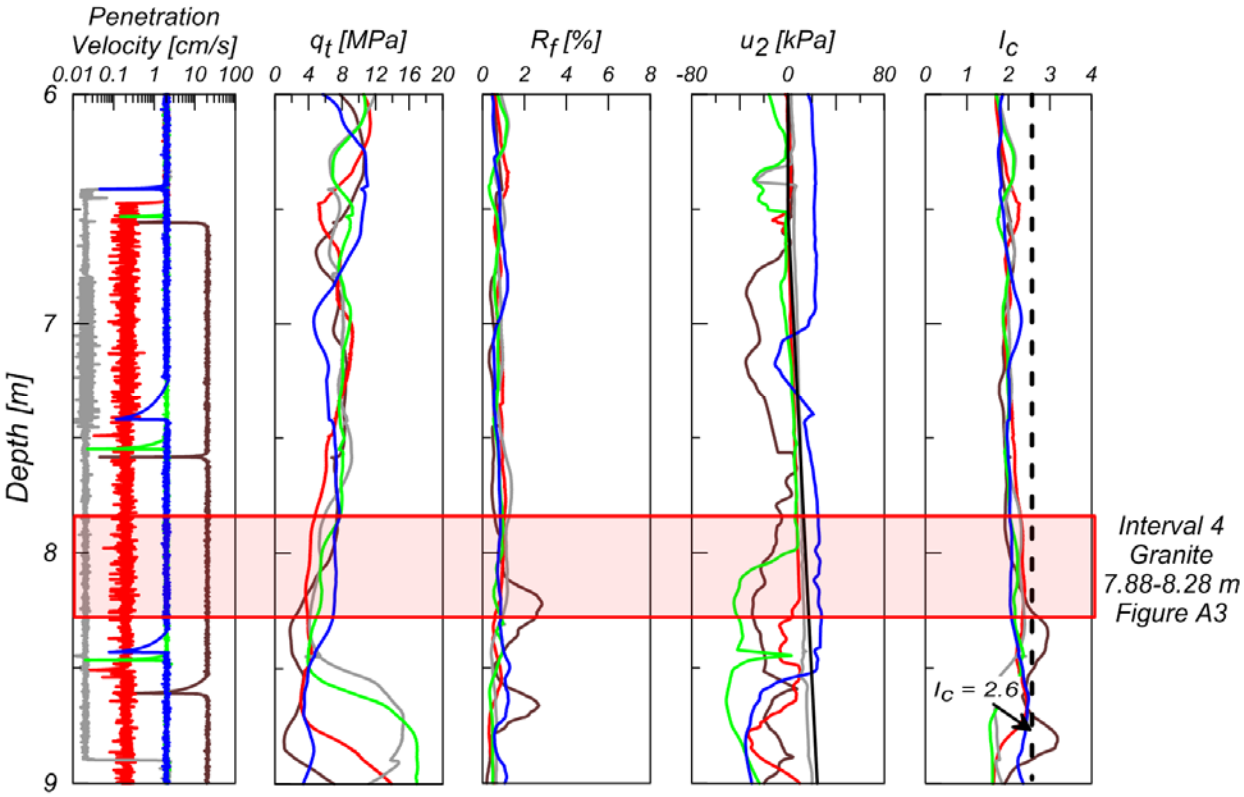

Figure A2 - Selected intervals for rate analysis for Granite.

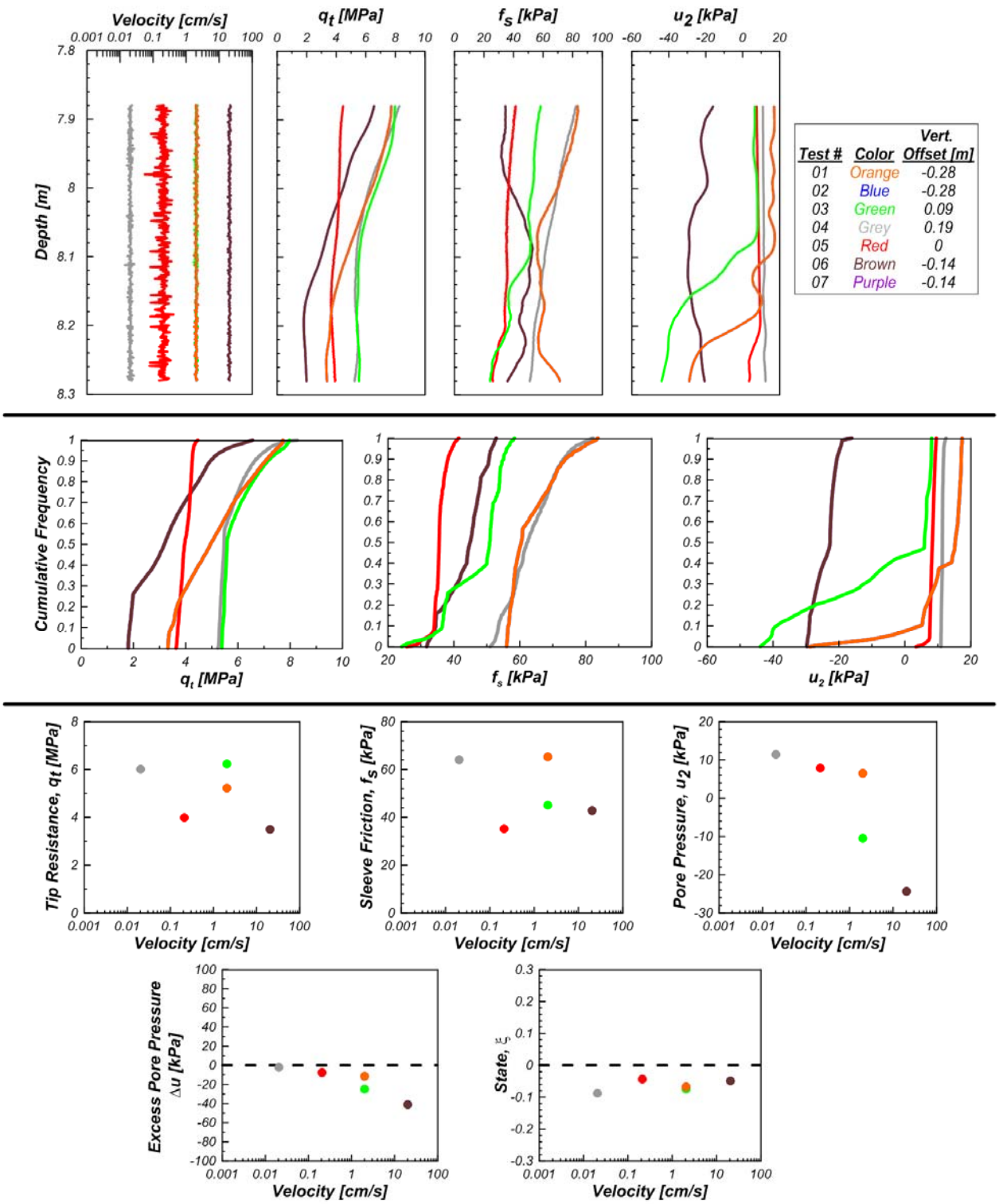

Soil Interactions Laboratory UCDAVIS	CPK	Variable Penetration Rate Interval Summary	Site	Granite			Fig. A3
			Interval	4	Range [m]	7.88 - 8.28	

Figure A3 - Interval summary for Granite depth range of 7.88 to 8.28 m

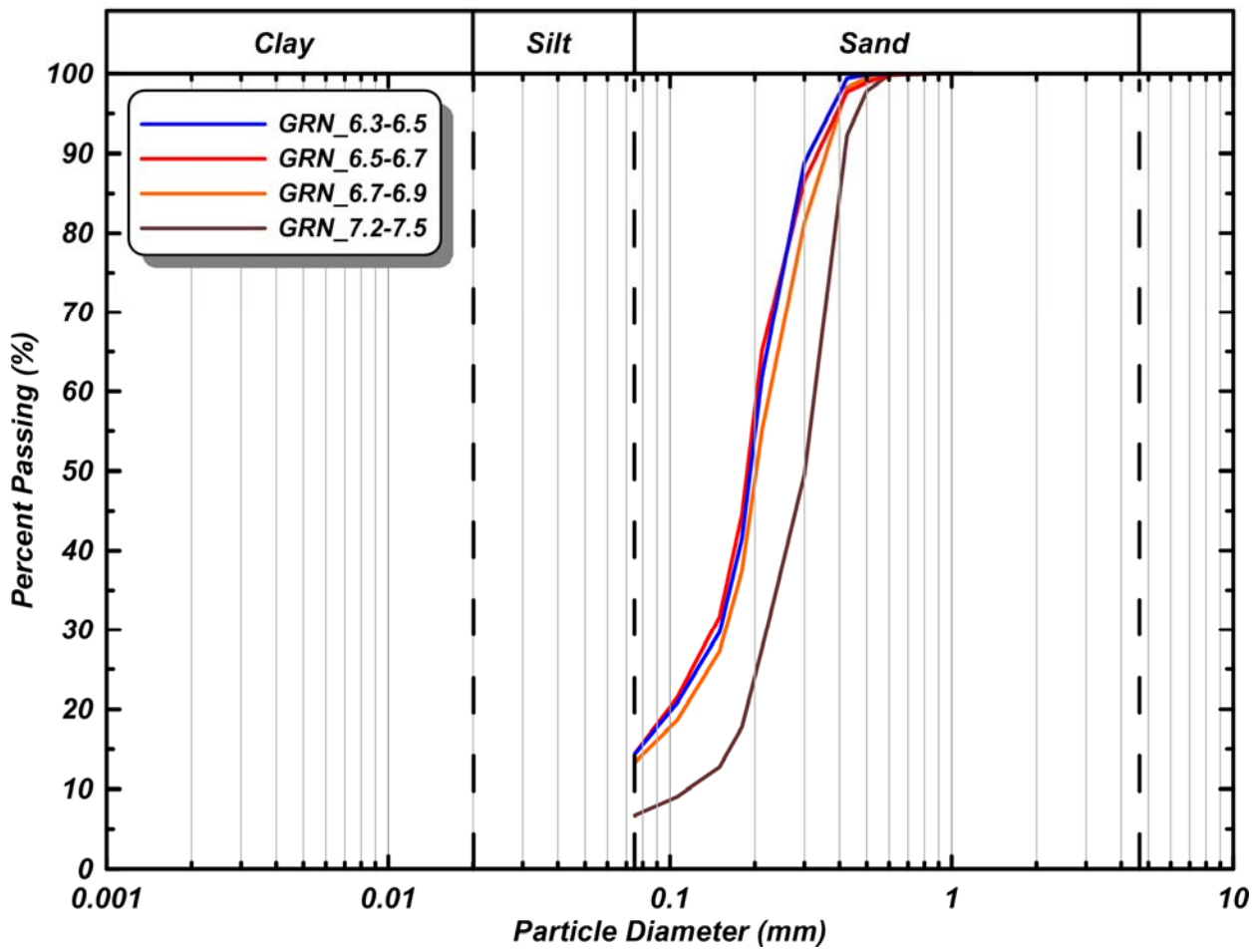

Figure A4 - Grain size distributions for the 4 Granite samples obtained in this study. Depth intervals are shown in the figure legend.

APPENDIX B - LENORDINI FARM SUPPLEMENTARY FIGURES

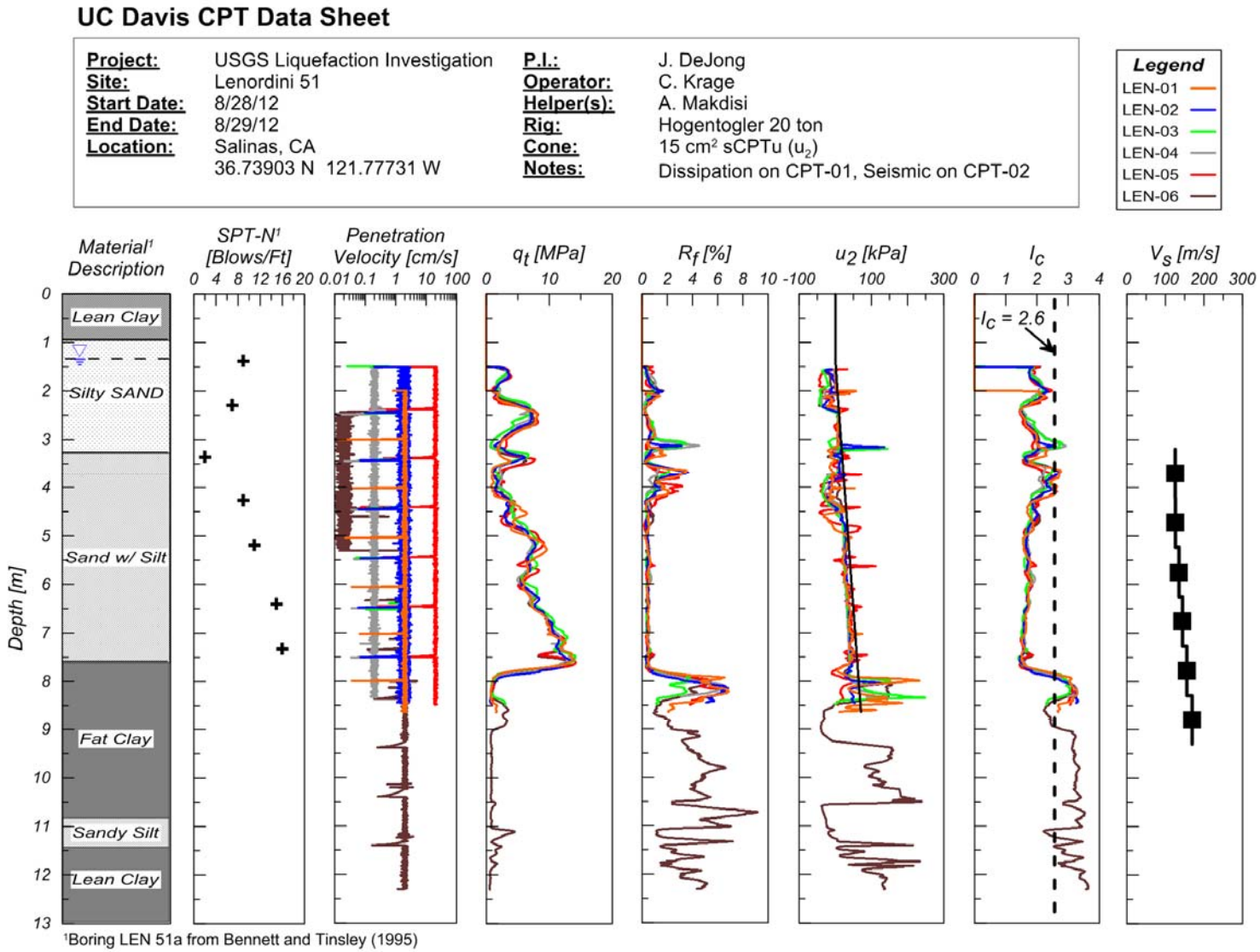

Figure B1- Summary of variable penetration rate tests at Lenordini.

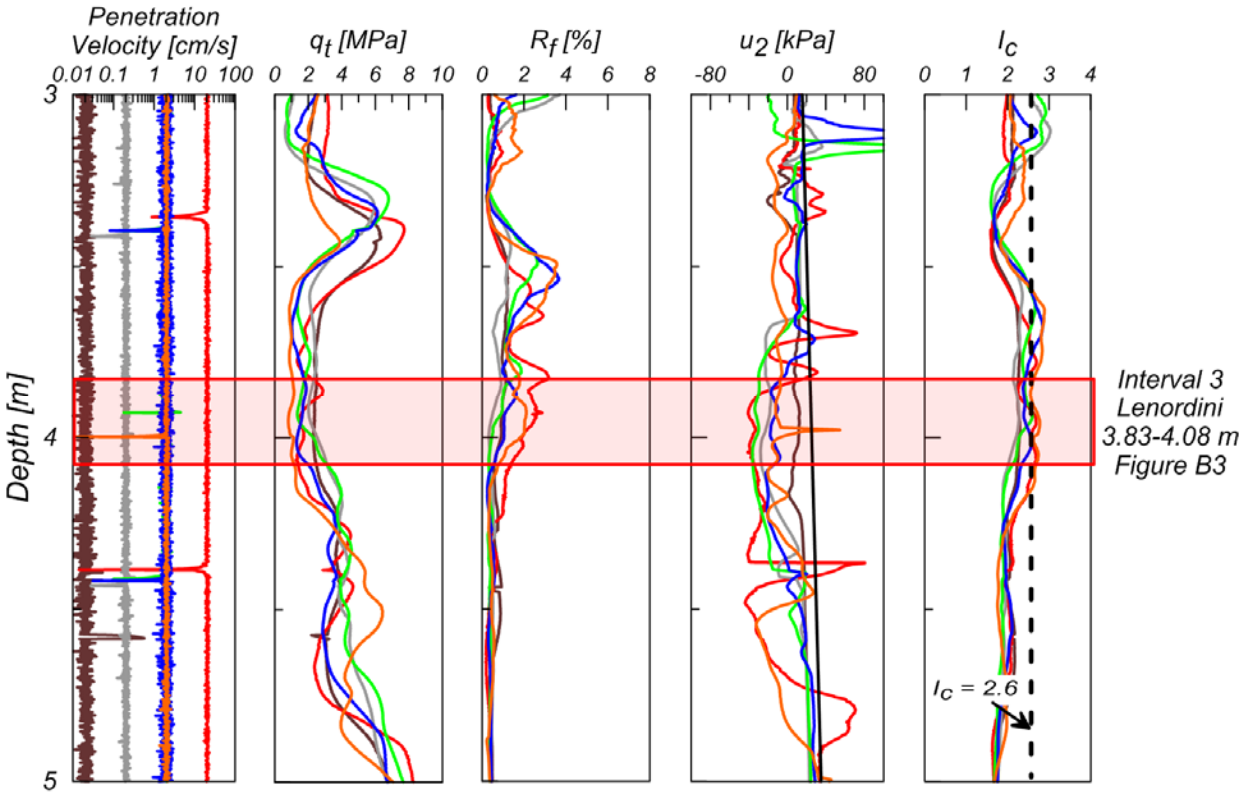

Figure B2 - Selected intervals for rate analysis at Lenordini.

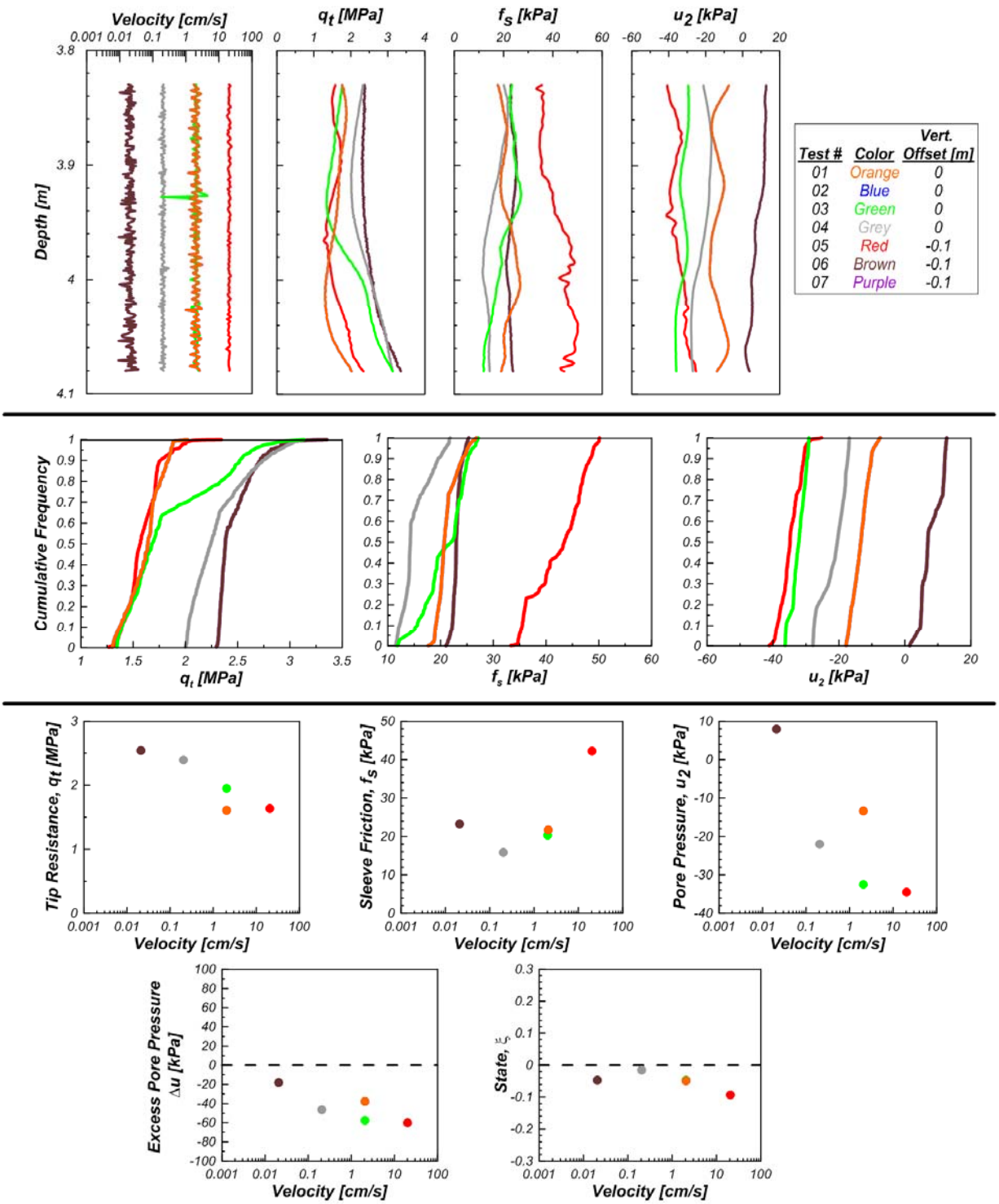

Soil Interactions Laboratory UCDAVIS	CPK	Variable Penetration Rate Interval Summary	Site	Lenordini			Fig. B3
			Interval	3	Range [m]	3.83 - 4.08	

Figure B3 - Interval summary for Lenordini depth range of 3.83 to 4.08 m

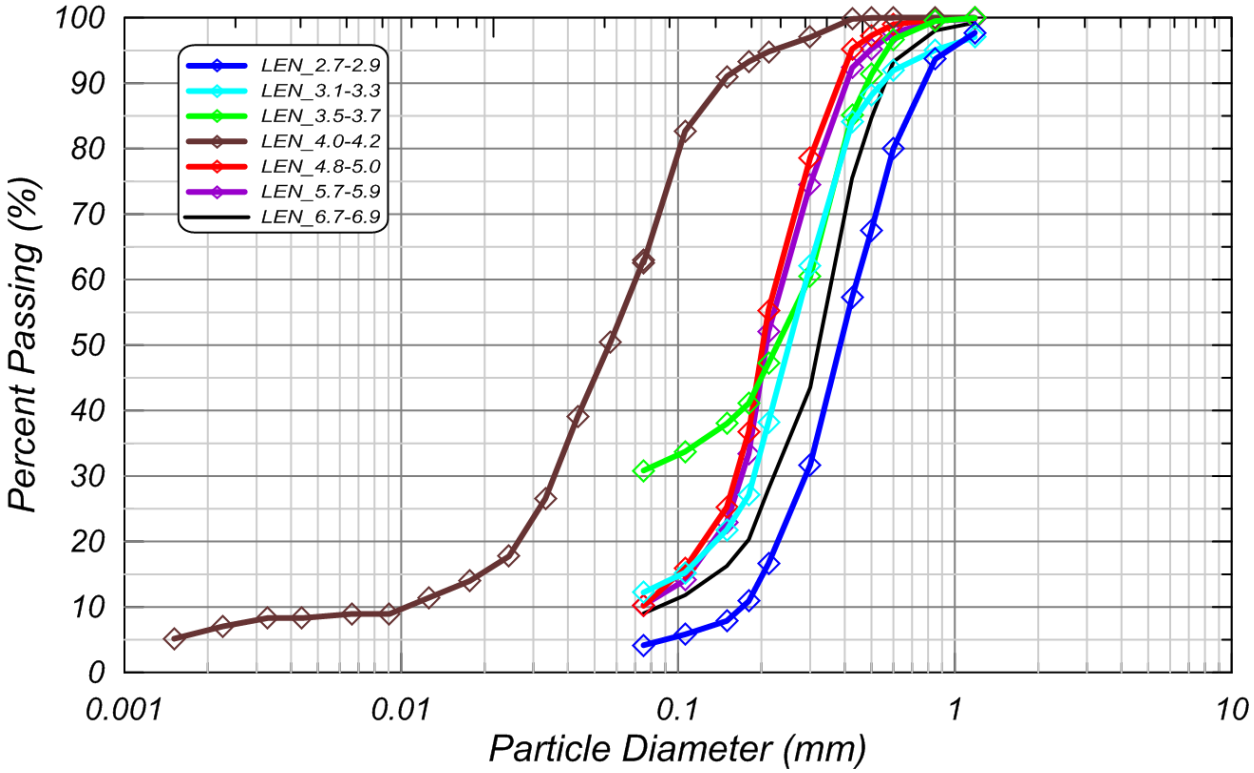

Figure B4 - Grain size distributions for the 7 Lenordini samples obtained in this study.

APPENDIX C - RIVER PARK SUPPLEMENTARY FIGURES

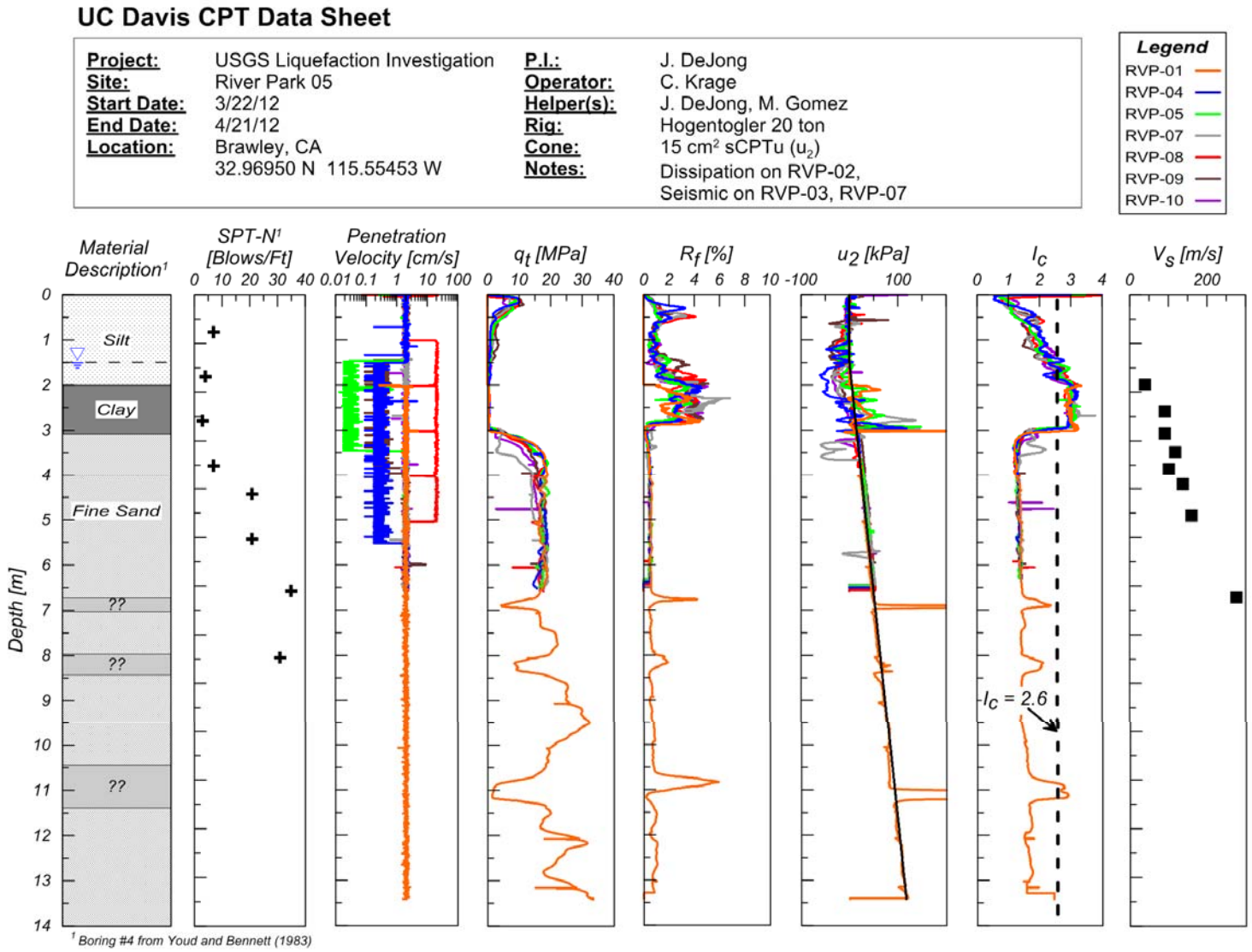

Figure C1 - Summary of variable penetration rate tests performed at River Park

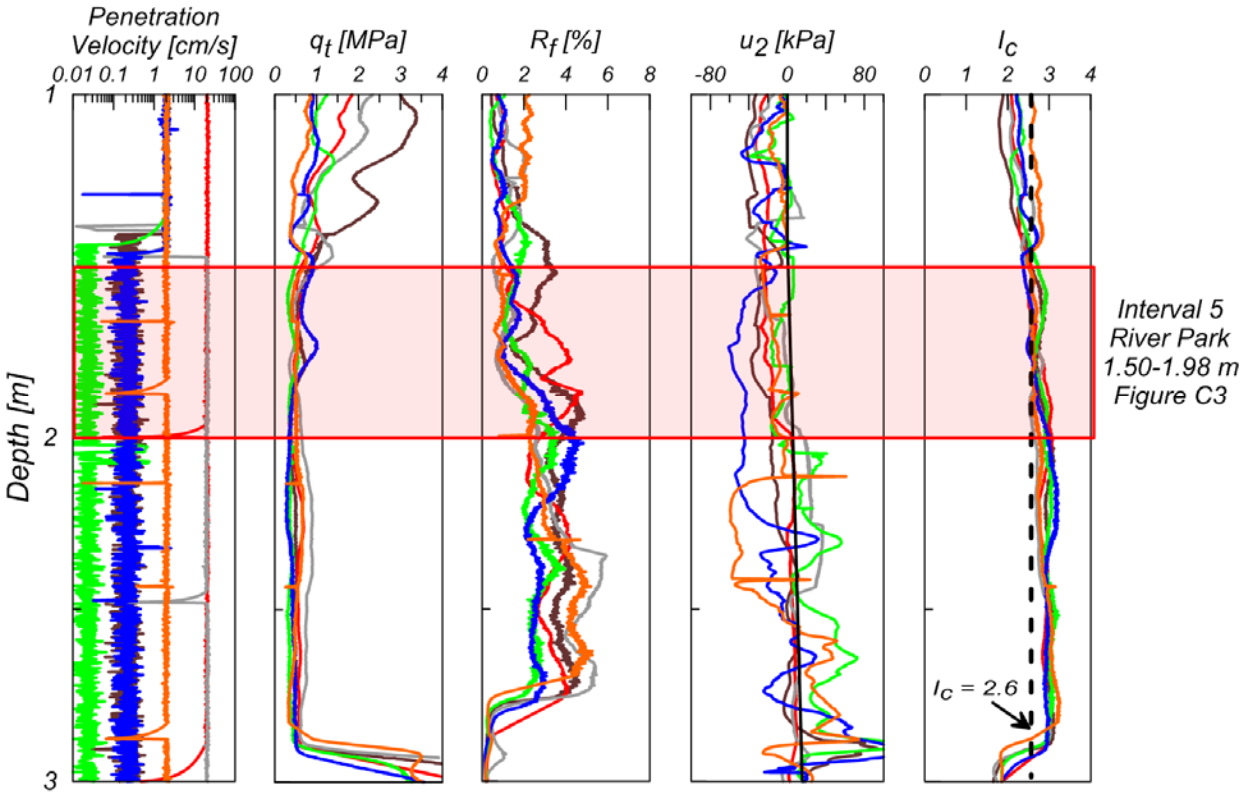

Figure C2 - Selected intervals for rate analysis at River Park.

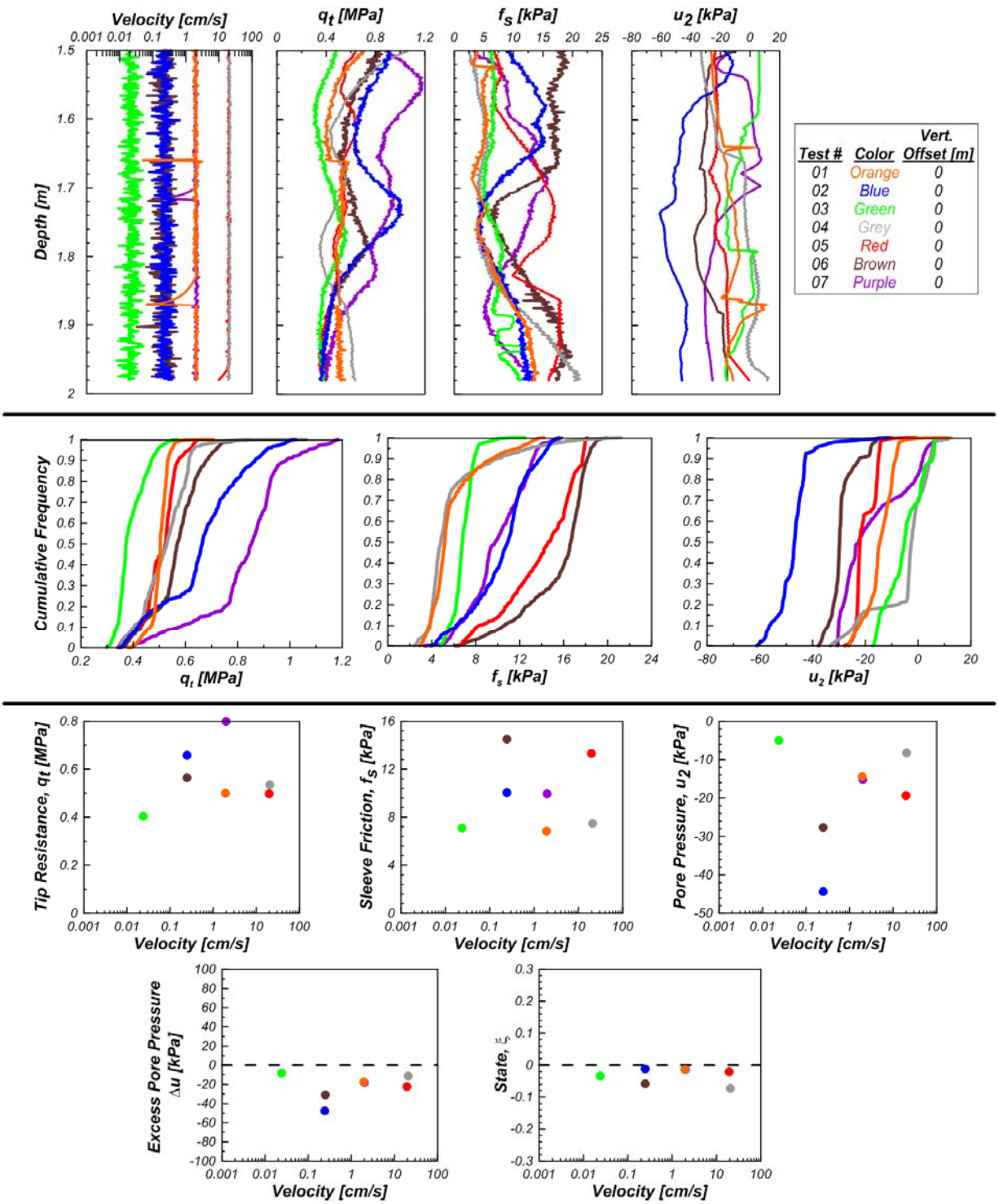

Soil Interactions Laboratory UCDAVIS	CPK	Variable Penetration Rate Interval Summary	Site	River_Park			Fig. C3
			Interval	5	Range [m]	1.5 - 1.98	

Figure C3 - Interval summary for River Park depth range of 1.5 to 1.98 m

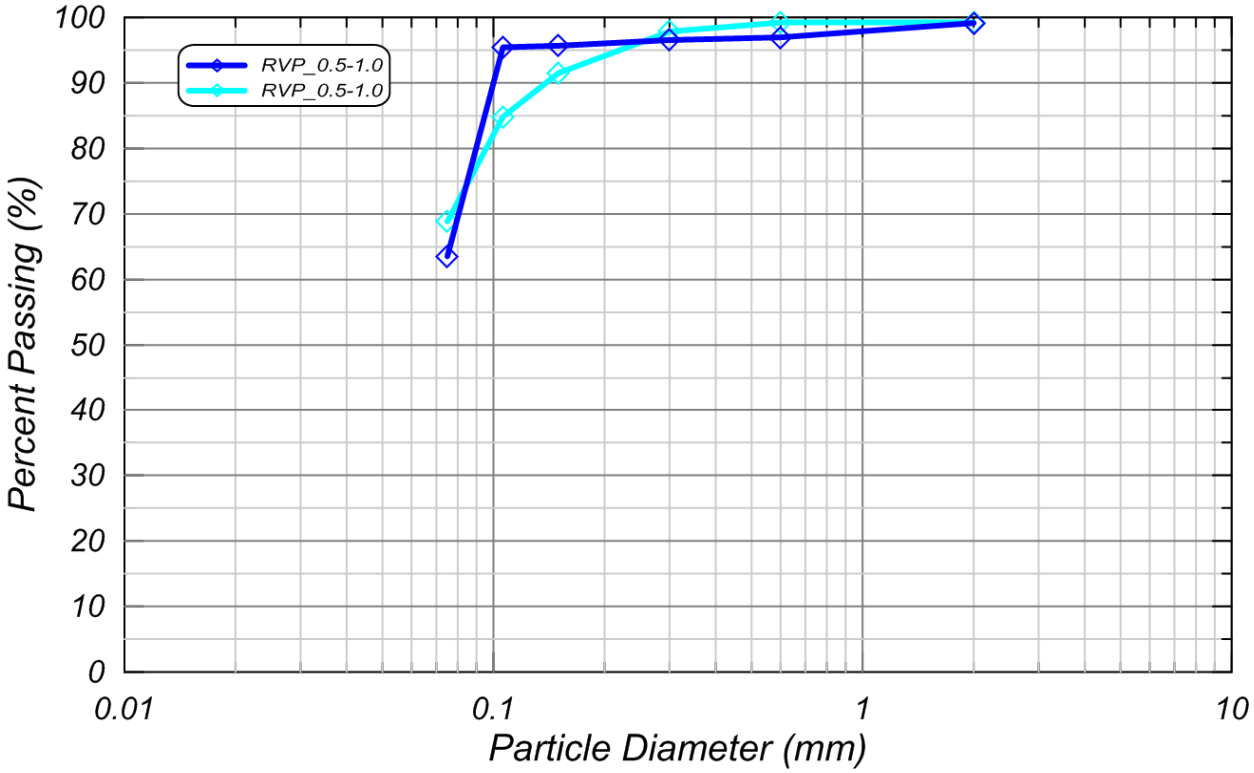

Figure C4 - Grain size distributions for 2 River Park samples obtained in this study.

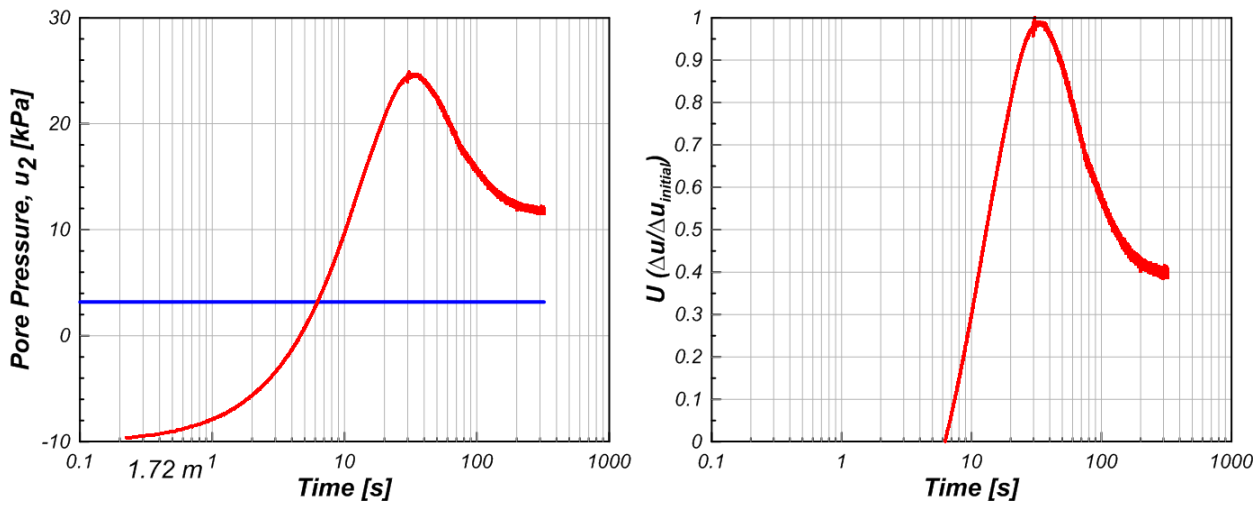

Figure C5 - Dissipation test performed at a depth of 1.72 m at River Park.

APPENDIX D - KORNBLOOM SUPPLEMENTARY FIGURES

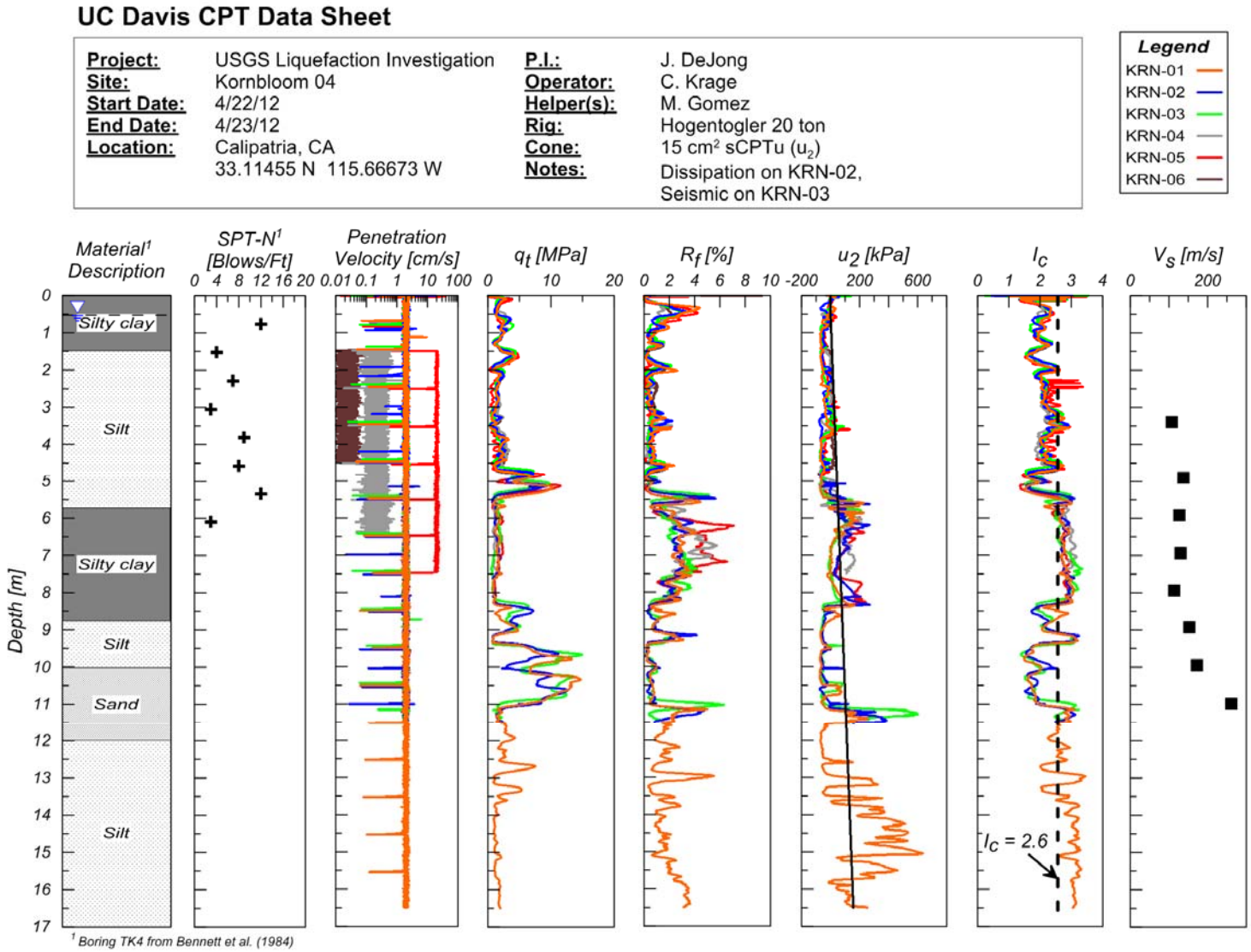

Figure D1 - Summary of variable penetration rate cone tests at Kornbloom

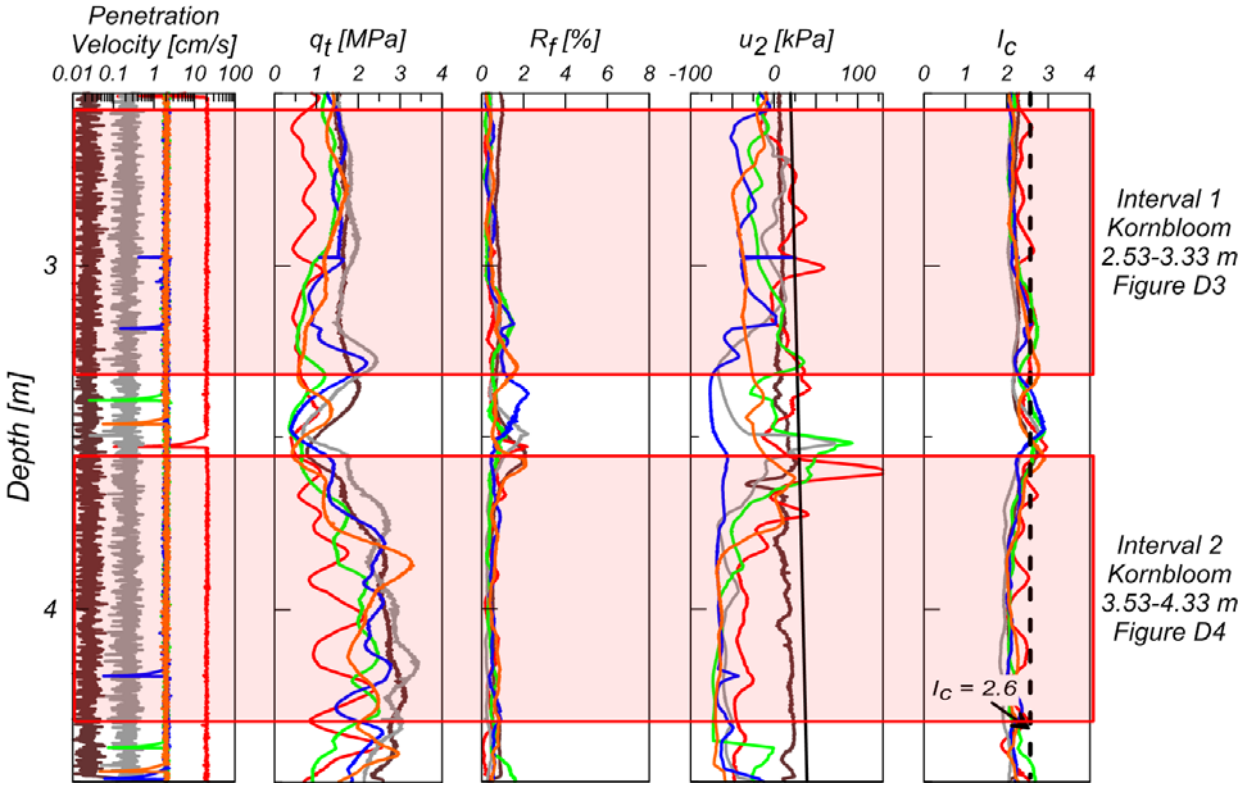

Figure D2 - Selected intervals for rate analysis within Kornbloom Unit B.

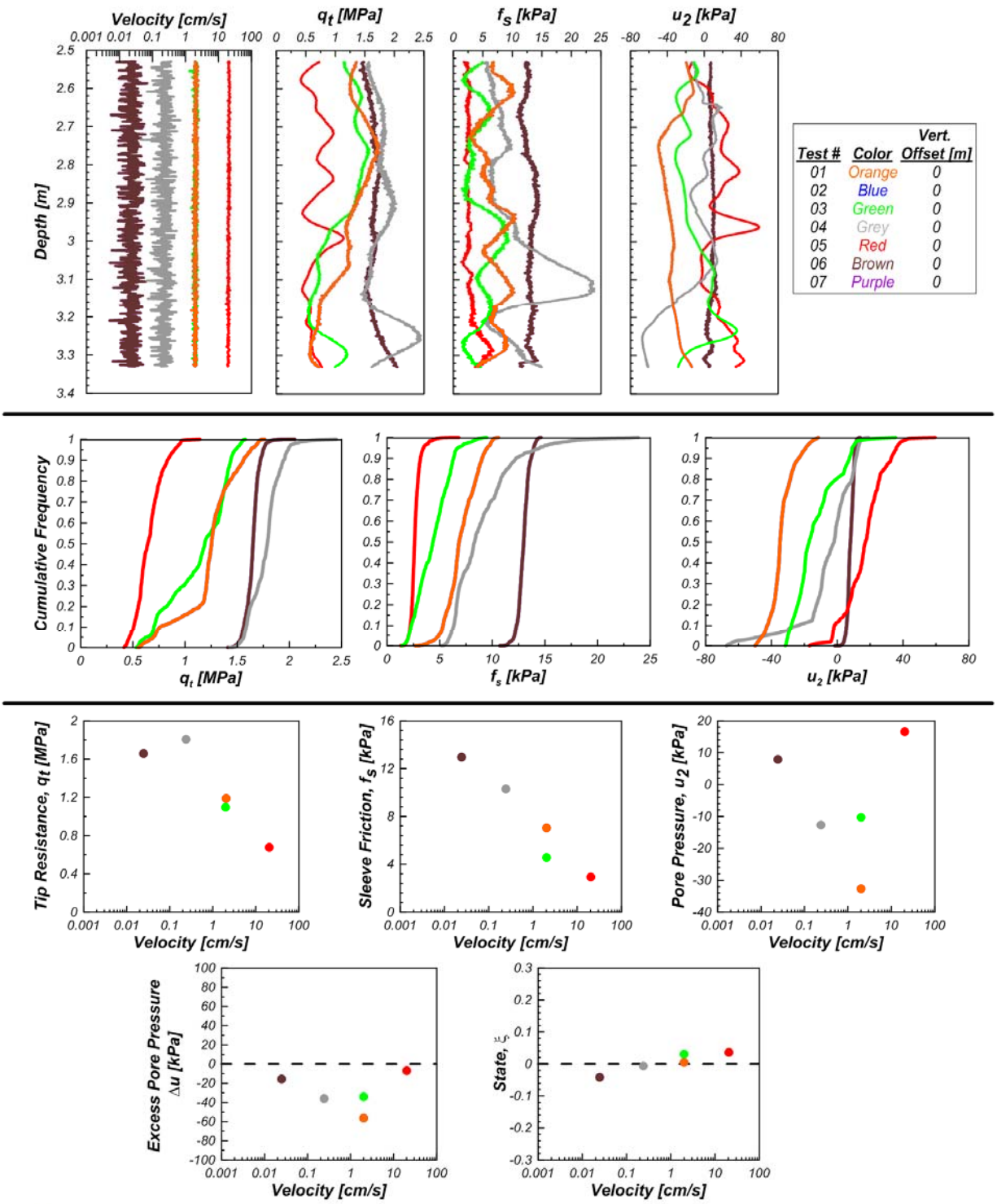

Soil Interactions Laboratory UCDAVIS	CPK	Variable Penetration Rate Interval Summary	Site	Kornbloom			Fig. D3
			Interval	1	Range [m]	2.53 - 3.33	

Figure D3 - Interval summary for Kornbloom depth range of 2.53 to 3.33 m.

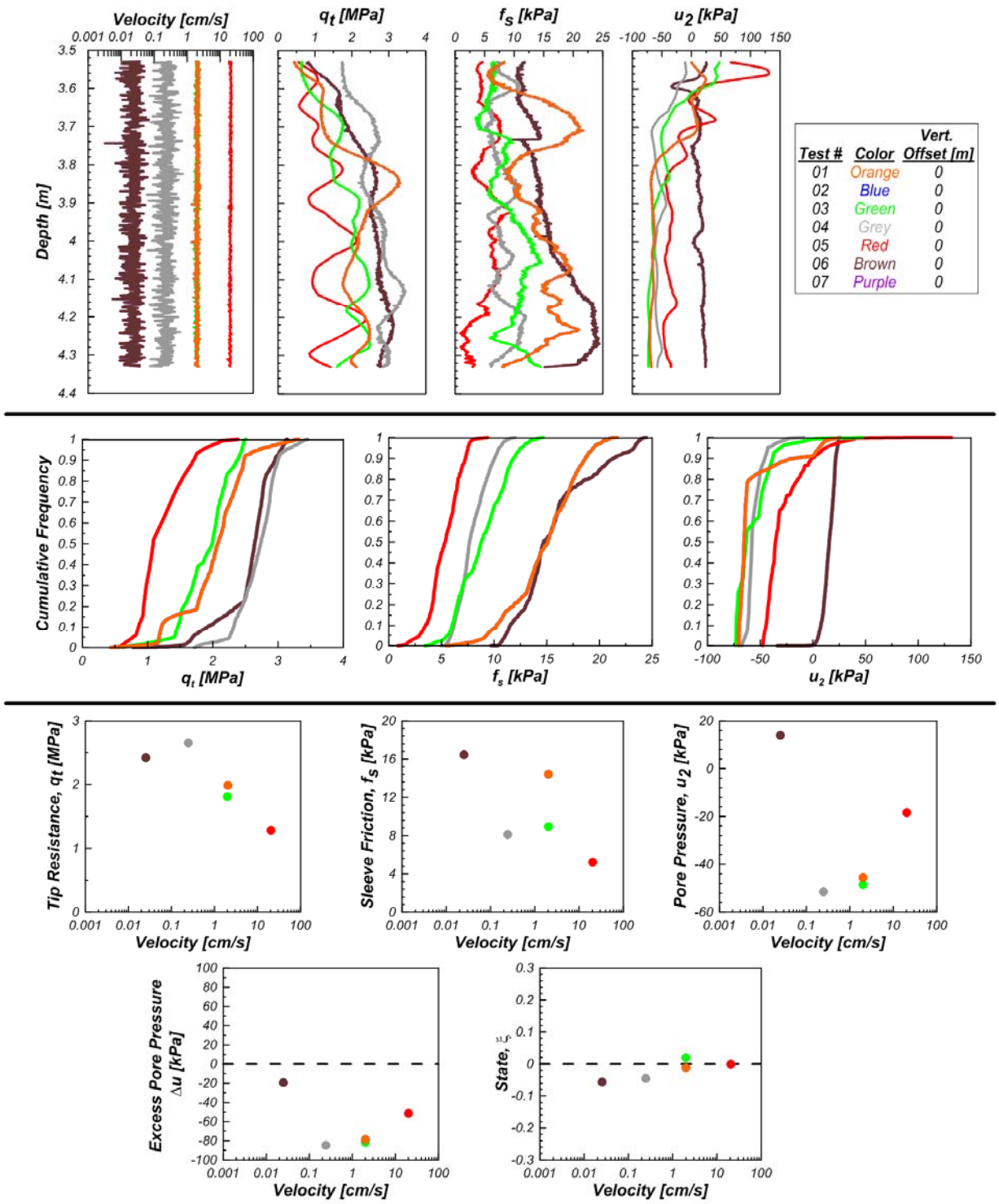

Soil Interactions Laboratory UCDAVIS	CPK	Variable Penetration Rate Interval Summary	Site	Kornbloom			Fig. D4
			Interval	2	Range [m]	3.53 - 4.33	

Figure D4 - Interval summary for Kornbloom depth range of 3.53 to 4.33 m.

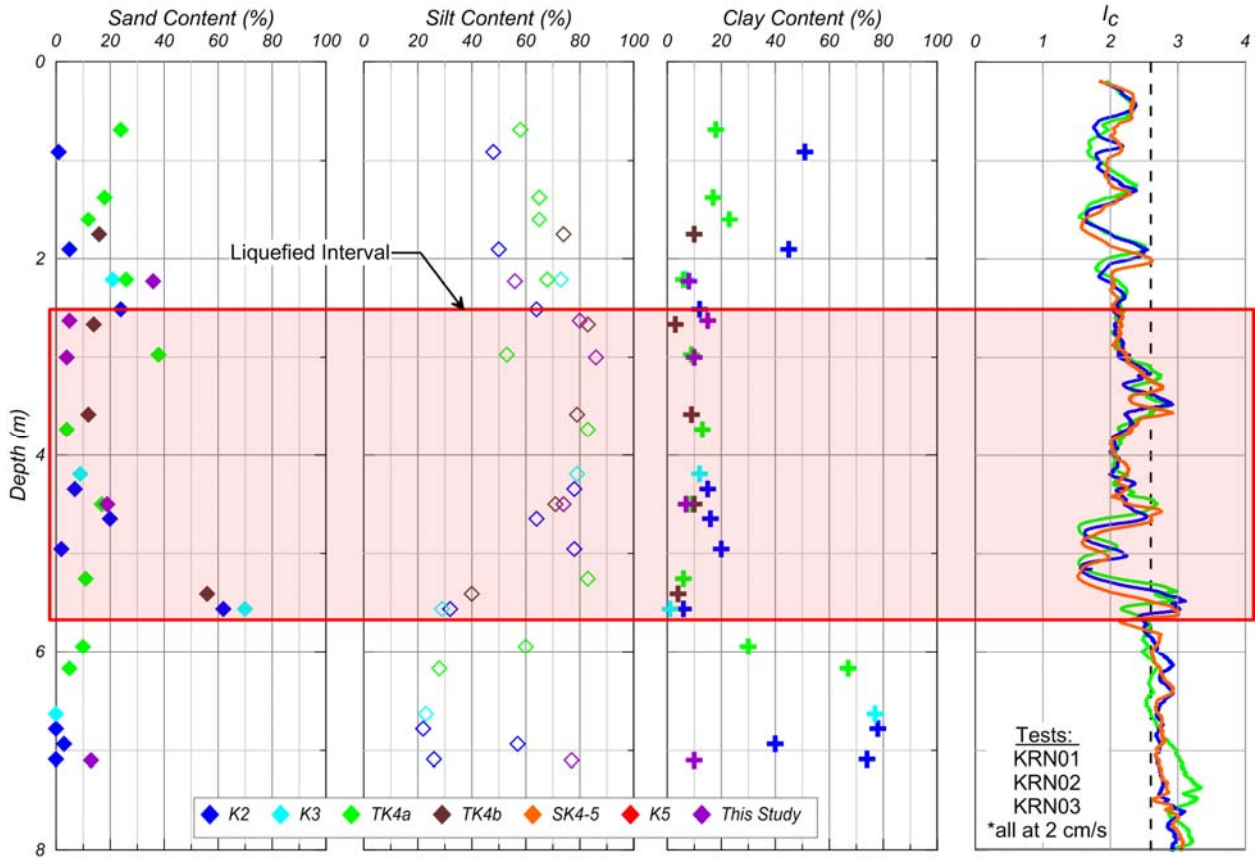

Figure D5 - Summary of samples obtained at the Kornbloom Site (data from Bennett et al. 1984 and this study).

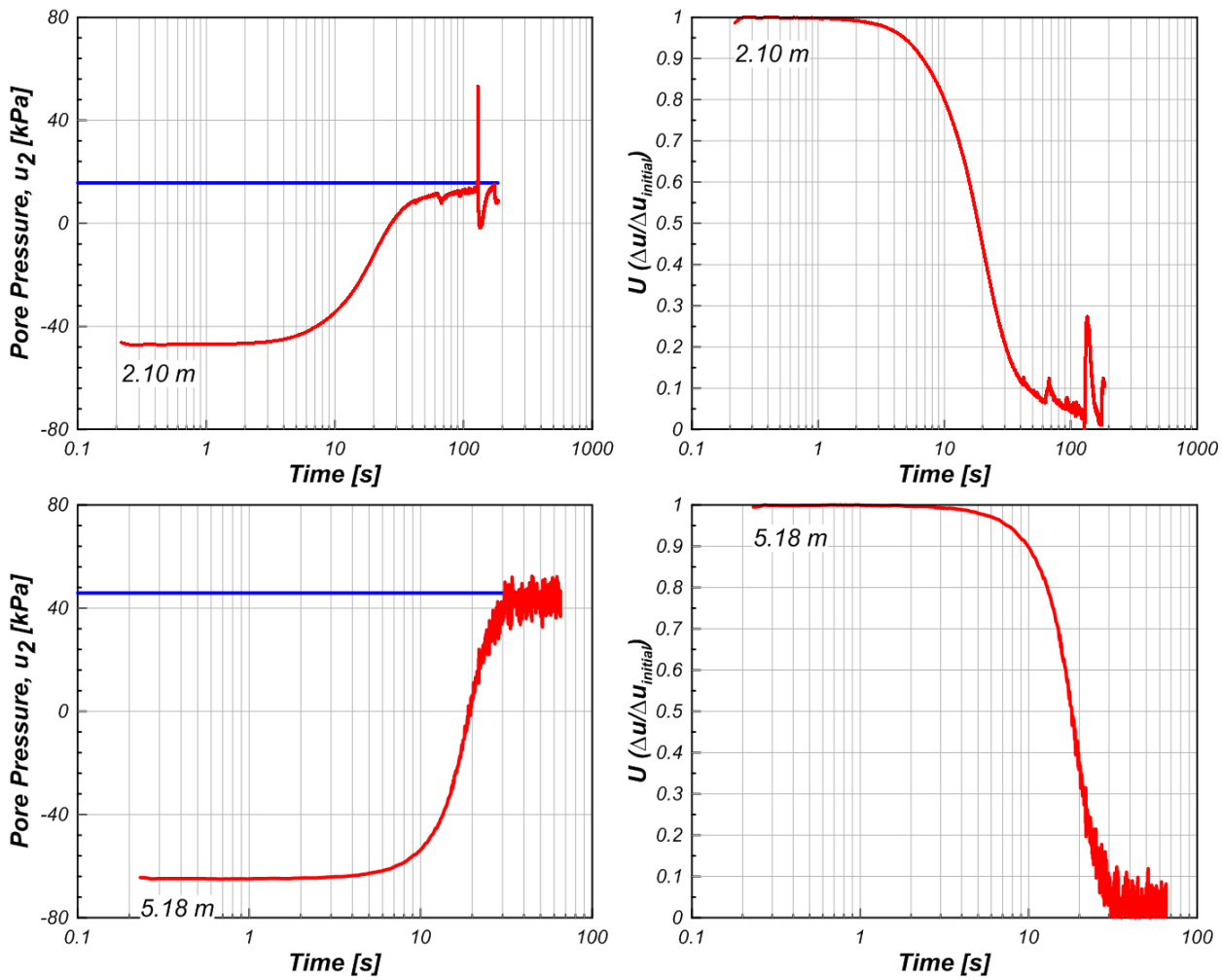

Figure D6 - Dissipation tests performed at depths of 2.10 m (top) and 5.18 m (bottom) at the Kornbloom site.